

# THERMOHYDRODYNAMIC ANALYSIS OF LUBRICATED PISTON RINGS OF INTERNAL COMBUSTION ENGINE

Submitted to Faculty of Technology, University of Delhi  
in fulfillment of the requirements for the award of the degree of

DOCTOR OF PHILOSOPHY

In  
Mechanical Engineering

By

RAMESH CHANDRA SINGH

Supervisors

Dr. S. Maji  
Professor  
Mech.Engg.Deptt.  
Delhi College of Engineering  
Delhi-110042

Dr. R. K. Pandey  
Associate Professor  
Mech.Engg.Deptt  
I. I.T. Delhi  
New Delhi-110016



Department of Mechanical Engineering  
Faculty of Technology, University of Delhi  
Delhi -110 007, INDIA

August, 2012

Dedicated

to

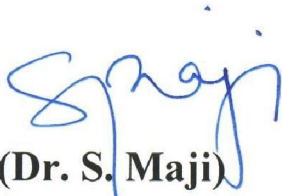
Bade Babuji (Late Shri Akshaibar Yadav)

And

Maternal Uncle (Late Shri Lalchand Prasad)

## **CERTIFICATE**

Certified that the thesis entitled “**Thermohydrodynamic Analysis of Lubricated Piston Rings of Internal Combustion Engine**” being submitted by **Mr. Ramesh Chandra Singh** [Enrollment Number - 59/2005] to Faculty of Technology, University of Delhi, in the fulfillment of the requirement for the award of the degree of Doctor of Philosophy from University of Delhi, is an authentic record of candidate’s own research work carried out by him under our guidance and supervision. It is also to certify that this research work being submitted herein has attained the standard required for a Ph D degree from the University of Delhi. Moreover, the results embodied in this thesis have not been submitted in part or full to any other University/Institute for award of any degree or diploma/certificate.



**(Dr. S. Maji)**  
Supervisor  
Professor, Mech.Engg.Deptt.  
Dept. of Mech. Engg.  
Delhi Technological University  
Delhi-110 042

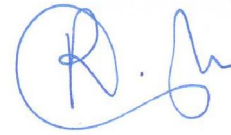


**(Dr. R. K. Pandey)**  
Supervisor  
Associate Professor  
Dept. of Mech. Engg.  
I.I.T. Delhi  
New Delhi-110 016

**(Dr. Raj Senani)**  
Head (Dept. of Mech. Engg.)  
Faculty of Technology,  
University of Delhi

## DECLARATION

It is hereby to declare that the Ph.D. dissertation entitled “Thermohydrodynamic Analysis of Lubricated Piston Rings of Internal Combustion Engine” which has been submitted to the Faculty of Technology (Department of Mechanical Engineering), University of Delhi, in fulfillment for the award of the Degree of Doctor of Philosophy, is an authentic record of my own work (Ramesh Chandra Singh, Enrollment Number - 59/2005). This research work has been carried out by me under the guidance of my supervisors Dr. S. Maji and Dr. R. K. Pandey. It is also to certify that the results embodied in this thesis have not been submitted in part or full to any other University/Institute for award of any degree or diploma/certificate.



(Ramesh Chandra Singh)  
Ph. D. Scholar  
(Enrollment Number - 59/2005)  
Dept. of Mech. Engg.  
Faculty of Technology  
University of Delhi.

## ACKNOWLEDGEMENTS

It is my immense pleasure to have this opportunity to express my gratitude and acknowledgement to my supervisors Dr. Sagar Maji, Professor, Department of Mechanical Engineering, Delhi Technological University (erstwhile Delhi College of Engineering) and Dr. Raj Kumar Pandey, Associate Professor, Department of Mechanical Engineering, IIT-Delhi, for their invaluable guidance and generous help provided in this endeavor. I acknowledge the valuable time imparted by my supervisors during completion of this task. I am very grateful to Dr. Naveen Kumar, Professor, Department of Mechanical Engineering, Delhi Technological University (erstwhile Delhi College of Engineering), without whose support the experimental part of this research work would have not been possible.


I am extremely thankful to Prof. Raj Senani, Dean, Faculty of Technology (FOT), University of Delhi, and Prof. P. B. Sharma, Vice Chancellor, Delhi Technonological University. They have been sources of inspiration for me in undertaking the challenges pertaining to research and development. I would be thankful to Prof. A. Trivedi, Formerly Dean, Faculty of Technology, University of Delhi. His suggestions/comments have been a driving force for propelling forward my research activities. It would be horribly incomplete, if I forget to express my gratitude towards Prof. B. Pathak (Head, Dept. of Mech. Engg.), Prof. S. K. Garg, Prof. R. S. Mishra, Prof. Samsher, Prof. D. S. Nagesh, Dr. B. B. Arora, Dr. Vipin, Dr. Reeta Wattal, Dr. A. K. Agrawal, Sh. V. K. Sethi and other faculty colleagues and staff members of department of mechanical engineering, Delhi Technological University, Delhi. They have been kind enough in supporting me towards pursuing this research work.

I would also express my gratitude to Dr. B. S. Chauhan, Mr. Rajesh Bohra, Mr. Lakhan, Mr. Rahul Mool, Mr. Bhupendra, Mr. Virendra, Mr. Kamal Nain,

Mr. Manmohan Singh and Mr. Ashok Kumar for their kind and timely support and co-operation rendered in the experimental works carried out in various laboratories of Department of Mechanical Engineering, Delhi Technological University, Delhi. Moreover, I would like to extend my sincere thanks to all the eminent people whose research works, findings, and analyses in this area inspired me to undertake this research topic.

I would be very thankful to Mr. H. H. Baa, Mr. Gopal Krishna, Mr. Narayanan and Mr. Neeraj and other staff of the Dean FOT office, University of Delhi, who kept me aware about the schedules and procedures to be followed as well as in imparting me important information time to time. Finally, my heartfelt gratitude to my colleague Mr. Rajiv Chaudhary and to all my well wishers, whose moral support and motivation made me to complete this long journey of dissertation.

Finally, I express my deep felt love and gratitude to my parents, wife (Sunita), daughter (Vidhatri), son (Vibudh), and all nears and dears for having patiently put up with me and constantly encouraging me throughout this work at the cost of their own sufferings.



(Ramesh Chandra Singh)

Date:

Place: New Delhi

## Abstract

Petroleum and automotive industries are facing tough time across the globe due to steep rise in petroleum based fuels' prices and ever increasing governments regulations related to improving the fuel economy and lower emissions from the fuel and lubricant system of IC engines. Therefore, worldwide substantial efforts in the design of reciprocating internal combustion (IC) engines are being made by the researchers for improving the fuel economy and reducing the exhaust emissions. Nowadays, great attention is being given on the reduction of friction at the various interfaces formed between the mating components of the IC engines. Effective lubrication at the interfaces of cylinder liner/piston rings, piston/piston rings, and piston skirt/cylinder liner play vital role in achieving high power efficiency, ensuring long operational life of the interfaces, limiting the consumptions of lubricating oil and fuel, providing a good dynamic sealing at various interfaces. Thus, efficient design of contacts formed between piston rings and counter surfaces in piston assembly is a great desirable task in the emerging scenario. It is worth mentioning here that dearth of studies can be seen in literature on the design and development of smart piston rings. Therefore, the main objective of this thesis is to study mathematically hydrodynamic lubrication of the interfaces formed between the cylinder liner and various surface profiles of the piston rings for reducing the frictional losses at the interfacial contacts. In the investigation reported herein, four single continuous surface profiles (Catenoidal, Cubic, Exponential, and Parabolic) on the face (surface in contact with cylinder liner) of piston rings have been considered for arriving on the best efficient face profile among these. These surface profiles for face of piston rings have been chosen in this investigation looking their potential performance as faces of pads in thrust bearing. The additional objective of this thesis is to perform the experiments on a commercial IC engine by manufacturing the best face profile (arrived based on

mathematical modeling) on all the compression piston rings for accessing the fuel saving and exhaust emissions.

Coupled solution of governing equations (Reynolds equation, Energy equation, Film thickness relation, and Rheological relation) has been achieved using finite difference method. Gauss-Seidel iterative method is employed in the solution of discretized equations. Using appropriate boundary conditions and convergence criterion, performance parameters of a single interface (cylinder liner and face of piston ring) have been thoroughly investigated. Based on the numerical study, it has been observed that exponential face profile of the piston ring yields lesser friction than other three profiles (Catenoidal, Cubic, and Polynomial). Thus, exponential face profile has been tried to fabricate on the faces of compression piston rings. However, due to manufacturing constraint an approximate exponential face profile only could be realized. Using approximate exponential face profile on compression piston rings, experiments have been carried out on a commercial diesel engine fueled with diesel and Jatropha based biodiesel (B100) at various loads. This exponential face profile of piston ring has considerable impact on engine's brake thermal efficiency (BTE), brake specific fuel consumption (BSFC), and mass flow rate, irrespective of fuels used. BTE of engine fueled with diesel increases 2 - 8% with exponential face profile design (III) of piston ring in comparison to standard (conventional) piston ring. BTE enhances 8 - 16% when engine is fueled with biodiesel using exponential face profile design (III) on piston rings. Corresponding to increase in BTE, the reduction in BSFC (biodiesel) is about 28 - 34%. Moreover, significant reductions in exhaust emissions are also recorded with exponential face profile on compression piston rings.

Moreover, friction reduction due to dimpling has been also explored. In this direction, some experiments have been conducted using a pin-on-disc machine. The



investigations carried out with micro-dimpling on generic tribo-contact give very significant reduction at interfacial friction. Thus, in future dimpling may be tried on face of piston rings for development of smart piston rings.

\*\*\*\*\*

# Contents

	Page No.
Certificate	i
Declaration	ii
Acknowledgement	iii
Abstract	v
Contents	viii
List of Figures	x
List of Tables	xiii
Nomenclature	xiv
Chapter 1 Introduction	01
1.1 Overview	01
1.2 Piston and Piston Rings	05
1.3 Scope of study	10
Chapter 2 Literature Review and Objective of Study	11
2.1 Mathematical modeling	13
2.2 Experimental Study	16
2.3 Surface texturing/ profiling	18
2.4 Conclusions of Literature review	18
2.5 Objective of Study	20
Chapter 3 Mathematical Model for Thermohydrodynamic Analysis of Lubricated Ring/Bore Interface	21
3.1 Mathematical model	21
3.1.1 Basic assumptions and considerations	22
3.1.2 Geometric description of domain	23
3.1.3 Reynolds equation for pressure	25
3.1.4 Energy equation for temperature	27
3.1.5 Viscosity temperature relationship	29
3.1.6 Miscellaneous relations	30
3.2 Computational procedure	30
3.3 Results and discussions	35
3.4 Conclusions	42
Chapter 4 Experimentation with an IC Engine using Exponential Face Profile of Piston Rings	43
4.1 Background	43
4.2 Fabrication of Exponential Face Profiles	44
4.3 Experimentation	46
4.4 Results and discussions	49
4.4.1 Brake Thermal Efficiency	50

4.4.2	Brake specific fuel consumption	53
4.4.3	Mass flow rate	54
4.4.4	Carbon Monoxide Emissions	56
4.4.5	CO <sub>2</sub> Emissions	58
4.4.6	NO <sub>x</sub> Emissions	59
4.4.7	Hydrocarbon Emissions	61
4.4.8	Smoke opacity	62
4.5	Conclusions	64
Chapter 5	Experimental Studies for Role of Surface Dimpling on the Performance of Lubricated Sliding Contact	67
5.1	Background	67
5.2	Fabrication of pin and dimples on discs	69
5.3	Experimentation	74
5.4	Results and discussions	76
5.5	Conclusions	82
Chapter 6	Conclusions and Suggestions for Future Study	83
6.1	Conclusions	83
6.1.1	Mathematical Model of Thermohydrodynamic Lubrication of Interface	83
6.1.2	Experiments with Exponential Face Profile of Piston Rings	84
6.1.3	Tribological Studies with Dimpled Surface	85
6.2	Suggestion for Future Study	85
References		86
Appendixes		95
Appendix I	Instruments for measurement of properties of fuels	95
Appendix II	Drawings of discs having different pitches	99

## List of figures

No	List of figures	Page No.
Fig. 1.1	Vital components of a typical IC engine	02
Fig. 1.2(a)	Chemical and mechanical energy losses in a typical IC engine; Break-ups of fuel's chemical energy	03
Fig. 1.2(b)	Chemical and mechanical energy losses in a typical IC engine; Break-ups of mechanical energy losses	03
Fig. 1.3	Photographic view of piston assembly	06
Fig. 1.4(a)	Face profiles and functions of piston rings; Face profiles of piston rings;	07
Fig. 1.4(b)	Face profiles and functions of piston rings; Functions of piston ring;	08
Fig. 1.5(a)	Movements of piston rings during operation; Transverse movement of piston ring	09
Fig. 1.5(b)	Movements of piston rings during operation; Primary (axial) movement of piston ring	09
Fig. 1.5(c)	Movements of piston rings during operation; Secondary motion (twisting) of piston ring	09
Fig. 3.1	Schematic diagram of geometry formed between a piston ring and cylinder liner	23
Fig. 3.2	Finite difference grid used in the computation	31
Fig. 3.3	Flowchart for computation	34
Fig. 3.4(a)	Geometries of faces on the piston rings; Catenoidal face profile	36
Fig. 3.4(b)	Geometries of faces on the piston rings; Cubic face profile	36
Fig. 3.4(c)	Geometries of faces on the piston rings; Exponential face profile	37
Fig. 3.4(d)	Geometries of faces on the piston rings; Parabolic profile	37
Fig. 3.5	Piston speed as a function of crank angle for 2000 rpm engine speed	38
Fig. 3.6	Combustion chamber pressure at moderate load	38
Fig. 3.7	Variation of film pressure at the interface in the axial direction	39
Fig. 3.8	Variation of friction force at the interface	39
Fig. 3.9	Comparison of pressure variations with the four face profiles of ring	40
Fig. 3.10	Comparison of minimum film thickness variations with the four face profiles of ring	41

Fig. 3.11	Comparison of friction force variations with the four face profiles of ring	41
Fig. 3.12	Comparison of power loss variations with the four face profiles of ring	42
Fig. 4.1	Photographic view of fixture with a clamped piston ring	45
Fig. 4.2	Schematic diagrams of standard (conventional) and three new face profiles of piston rings	47
Fig. 4.3	Photographic view of test engine	48
Fig. 4.4	Engine's loading system	48
Fig. 4.5	Variation of brake thermal efficiency with load using diesel fuel	52
Fig. 4.6	Variation of brake thermal efficiency with load using biodiesel fuel	52
Fig. 4.7	Variation of brake specific fuel consumption with load	53
Fig. 4.8	Variation of brake specific fuel consumption with load	54
Fig. 4.9	Variation of mass flow rate of diesel with load	55
Fig. 4.10	Variation of mass flow rate of biodiesel with load	55
Fig. 4.11	Variation of carbon mono oxide with engine load using diesel fuel	57
Fig. 4.12	Variation of carbon monoxide with engine load using biodiesel fuel	57
Fig. 4.13	Variation of CO <sub>2</sub> with engine load using diesel fuel	58
Fig. 4.14	Variation of CO <sub>2</sub> with engine load using biodiesel fuel	58
Fig. 4.15	Variation of NO <sub>x</sub> with engine load using diesel fuel	59
Fig. 4.16	Variation of NO <sub>x</sub> with engine load using biodiesel fuel	59
Fig. 4.17	Variation of Hydrocarbon with engine load using diesel fuel	61
Fig. 4.18	Variation of Hydrocarbon with engine load using biodiesel fuel	61
Fig. 4.19	Variation of smoke opacity with engine load using diesel fuel	62
Fig. 4.20	Variation of smoke opacity with engine load using biodiesel fuel	63
Fig. 5.1(a)	Details of pin used in the experiments; Dimension of the pin	70
Fig. 5.1(b)	Details of pin used in the experiments; Photographic view of pin	70

Fig. 5.2	Schematic diagram of pin-on disc tribometer	71
Fig. 5.3	Schematic diagrams of dimples on the disc	72
Fig. 5.4	Orthographic views of the disc	73
Fig. 5.5	Photographic view of a dimpled disc plate (C-50)	74
Fig. 5.6	Photographic views of the dimpled discs after conducting the experiments	75
Fig. 5.7	Coefficient of friction variation with pitches of the dimples, [Load= 118 N, Speed=500 rpm, Test duration = 40 minutes]	76
Fig. 5.8	Variation of coefficient of friction with speed (Mixed regime, [Load= 120 N, Test duration = 40 minutes, Pitch= 1mm]	77
Fig. 5.9	Variation of wear (mass loss of pin) with speed (Mixed regime), [Load= 120 N, Test duration = 40 minutes, Pitch= 1mm]	78
Fig. 5.10	Variation of coefficient of friction with load (Mixed regime), [Speed=1000 rpm, Test duration = 40 minutes, Pitch= 1mm]	78
Fig. 5.11	Variation of wear with load (Mixed regime); [Speed=1000 rpm, Test duration = 40 minutes, Pitch= 1mm]	79
Fig. 5.12	Variation of coefficient of friction with speed (Fully flooded); [Load= 120 N, Test duration = 40 minutes, Pitch= 1mm]	80
Fig. 5.13	Variation of wear with speed (Fully flooded); Load= 120 N, Test duration = 40 minutes, Pitch= 1mm]	80
Fig. 5.14	Variation of coefficient of friction with load (Fully flooded); [Speed=1000 rpm, Test duration = 40 minutes, Pitch= 1mm]	81
Fig. 5.15	Variation of wear with load (Fully flooded); [Speed=1000 rpm, Test duration = 40 minutes, Pitch= 1mm]	82
Fig. A1	U-Tube Oscillating True Density meter	95
Fig. A2	Kinematic viscometer	96
Fig. A3	A Pensky Martens apparatus used for determination of flash point	97
Fig. A4	Calorimeter	97
Fig. A5(a)	Smoke meter	98
Fig. A5(b).	Gas analyzer	98
Fig. B1	Dimpled disc with pitch=1 mm, 420 micron	99
Fig. B2	Dimpled disc with pitch=2 mm, 420 micron	100
Fig. B3	Dimpled disc with pitch=3 mm , 420 micron	101
Fig. B4	Dimpled disc with pitch=4 mm, 420 micron	102

## List of tables

---

No	List of tables	Page No.
Table 3.1	Input data of engine; [Source: Jeng (1992)]	35
Table 4.1	Technical specifications of test engine	49
Table 4.2	Properties of diesel and Jatropha based biodiesel	50
Table 5.1	Some specific parameters for tribometer	74
Table 5.2	Properties of lubricating oil (20W40)	75

# Nomenclature

---

$\sigma_c$	Combine roughness
$\phi_x$	Flow factor
$\phi_s$	Shear factor
$\eta$	Viscosity of lubricating oil
$\omega$	Angular velocity
$\theta$	Angular displacement
$\eta_0$	Initial viscosity
$\beta$	Viscosity temperature index
$\delta_1$ & $\delta_2$	Random roughness amplitude of the two surface measured from their mean level
%	Percent
$\rho$	Density
$\mu$	Coefficient of friction
ASTM	American Society for Testing and Materials
AVL-437	AVL-437 Smoke Meter
B100	Pure Biodiesel
BMEP	Break Mean Effective Pressure
BSEC	Brake Specific Energy Consumption
BTE	Brake Thermal Efficiency
Cc	Cubic centimeter
CI	Compression Ignition
CO	Carbon Monoxide
CO <sub>2</sub>	Carbon Dioxide
C <sub>p</sub>	Specific heat at constant pressure
cSt	Centi Stoke
CV	Calorific Value
H	Nominal film thickness



HC	Hydrocarbon
$h_{\text{film}}$	Thickness of the film
$h_m$	Minimum oil film thickness
HP	Horse Power
$h_T$	Local film thickness
$h_x$	Additional oil film thickness over $h_m$
IC	Internal Combustion
kW	Kilo Watt
kW-h	Kilo Watt Hour
Mm	Millimeter
NO <sub>x</sub>	Oxides of Nitrogen
O <sub>2</sub>	Oxygen
°C	Degree Celsius
P	Pressure
Ppm	Parts per million
P-	Pressure – Crank Angle
Rpm	Revolutions Per Minute
T	Tonnes, temperature/ initial temperature
T <sub>0</sub>	Initial temperature
THD	Thermohydrodynamic
u and w	Velocities in x and z directions
U <sub>2</sub> and U <sub>1</sub>	Velocity of piston
UBHC	Unburnt Hydrocarbon
vs.	Versus

# Chapter 1

## Introduction

---

This chapter mainly presents an overview pertaining to tribological aspects for improving the performance of IC engine. At the end of this chapter, scope for the study is also provided.

### 1.1 Overview

Internal combustion engine (IC) as shown schematically in Fig. 1.1 is the most important mechanical invention done by human beings, which has played great role in the industrialization of the globe after world war-II. But, now due to fast depletion of conventional fuel resources and increasing environmental issues, there is worldwide relentless pressure on the researchers to develop ever more fuel efficient and compact IC engines having reduced environmental issues. In the last couple of decades, there have been many studies on the frictional evaluations at the various interfaces in IC engines in order to identify the crucial interfaces of the engine components for minimizing the interfacial frictional losses associated with it.

It is worth mentioning here that major portion of fuel energy (i.e. chemical energy) goes as waste in the form of heat. Even, significant portion of chemical energy liberated during the combustion of precious fuel is

consumed in the frictional resistance present at the various interfaces of the moving engine components. Fig. 1.2a illustrates percentage of chemical energy taken away by various modes in a typical IC engine. It can be seen that the portion of chemical energy consumed in friction during mechanical motions in a typical IC engine is considerably large. Moreover, Fig. 1.2b also provides break ups of frictional losses in a typical IC engine. Due to considerably large frictional losses in piston assembly, this system contributes in more fuel and lubricating oil consumptions and in this way it happens to be a potential source of hydrocarbons and particulate emissions.

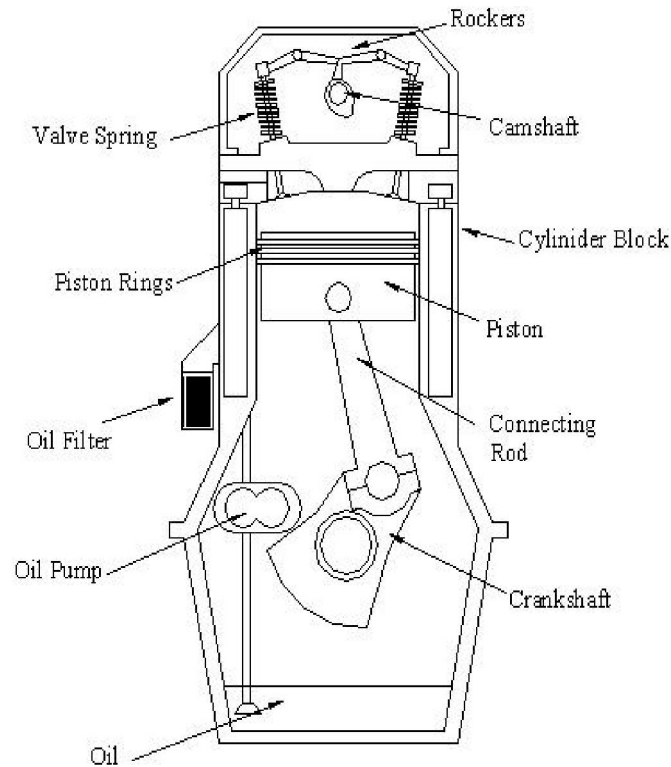
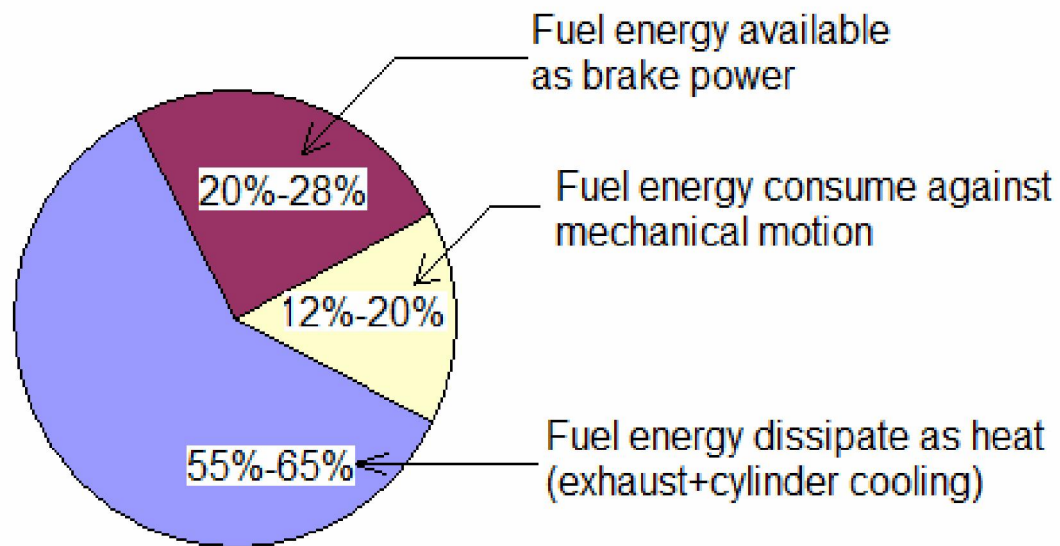
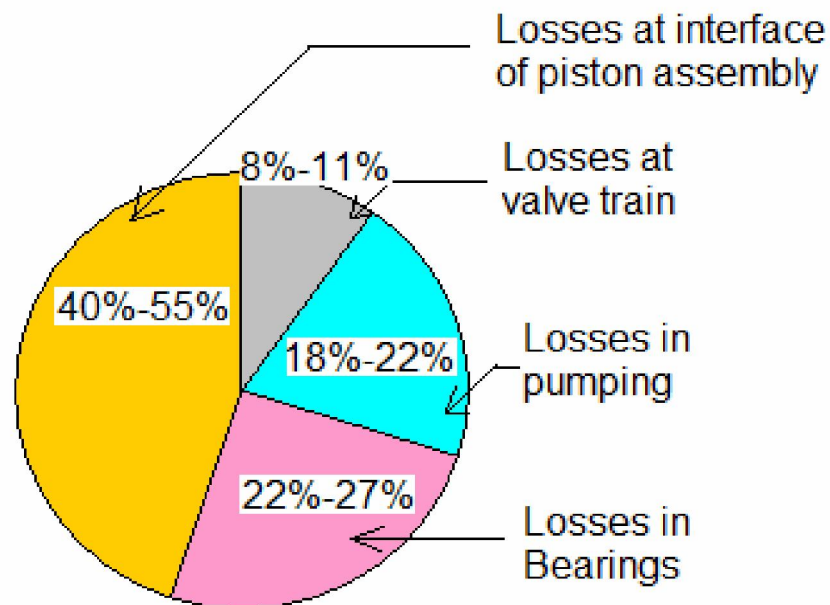


Fig. 1.1 Vital components of a typical IC engine [1]



(a) Break-ups of fuel's chemical energy



(b) Break-ups of mechanical energy losses

Fig. 1.2 Chemical and mechanical energy losses in a typical IC engine [1]

Reductions of fuel consumption and emission in an internal combustion engine are largely a function of improved lubrication. Therefore, advanced concepts are now being explored to reduce the friction at various interfaces in an IC engine. The development of smart IC engines and their proper use are of great importance for the national economy, individual and environment. Energy efficient IC engines can save billions of dollars in the case of an industrialized nation. It is worth to mention here that improvements in the tribological performance of interfaces in IC engines can lead to the following benefits:

- Reduced fuel consumption
- Increased engine power output
- Reduced oil consumption
- A reduction in harmful exhaust emissions
- Improved durability, reliability and engine life
- Reduced maintenance requirements and longer service intervals

With large numbers of IC engines in use across the globe, even a fraction of improvements in engine efficiency and emission level can have a major influence on the world fuel economy and the environment in a long term.

## 1.2 Piston and Piston Rings

It will be appropriate to say that heart of the reciprocating internal combustion engine is the piston assembly. Figure 1.3 presents photographic view of piston assembly. Piston and piston rings form a critical unit in transforming the fuel energy into useful kinetic energy. The piston ring pack includes the piston rings, which is a series of compression rings and oil ring. The primary role of the compression piston ring is to maintain an effective gas seal between the combustion chamber and the crankcase. The piston rings of the piston assembly, which form a labyrinth seal, achieve this function by closely conforming to their grooves in the piston and interfacing to the cylinder wall. The additional role of the piston rings is to transfer heat from the piston into the cylinder wall and limit the amount of lubricating oil that is transported from the crankcase to the combustion chamber. This flow path is perhaps the largest contributor to engine oil consumption and leads to increase in harmful exhaust gas emissions as the lubricating oil mixes and reacts with the other contents present in combustion chamber.



Fig. 1.3 Photographic view of piston assembly [2]

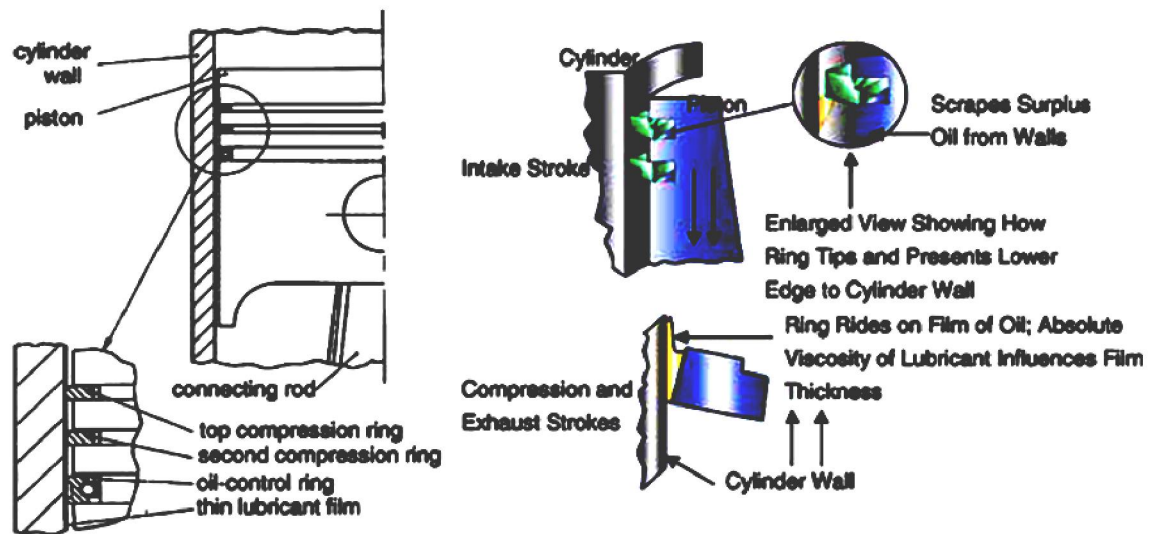
Figures 1.4(a) and 1.4(b) illustrate face profiles and functions of piston rings in an IC engine. Two top piston rings are compression rings. The pressure generated during the combustion pushes the piston rings radially outward, which causes engagement of the entire piston ring face with the cylinder wall. This process helps in gas sealing. The second compression ring, which is known as a scraper ring is designed to assist in the limiting of the upward oil flow in addition to providing a secondary gas

sealing. Figure 1.4 (b) illustrates surplus oil scraping from the cylinder wall by the second compression piston ring. For scraping function, the second compression ring is provided a tapered-faced profile. The bottom piston ring in the piston assembly is known as oil control ring, which has two running faces (or lands) and a spring element to enhance the radial load. The role of this ring is to limit the amount of oil transported from the crankcase to the combustion chamber.



(a) Face profiles of piston rings

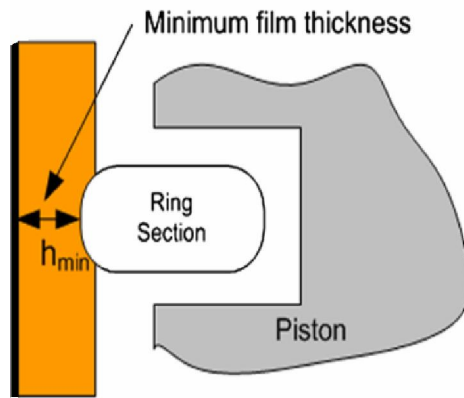




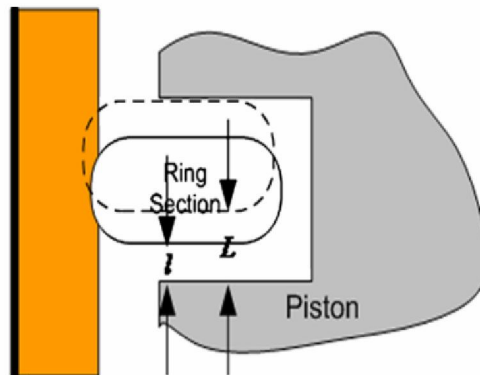
(b) Functions of piston ring

Fig. 1.4 Face profiles and functions of piston rings [1, 3]

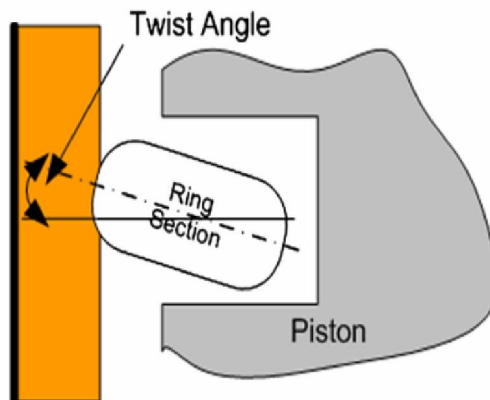
The piston ring is the most complicated tribological component in the internal combustion engine to analyze because of large variations of load, speed, temperature and lubricant availability. In one single stroke of the piston, the piston ring interface with the cylinder liner wall may experience boundary, mixed and full fluid film lubrication. During the engine cycle the piston itself exhibits a complex motion i.e. transverse motion, axial motion, and secondary motion; as illustrated in Figs. 1.5(a), 1.5(b), and 1.5(c). Such motions result in hydrodynamic/mixed lubrication at the various interfaces in piston assembly. In presence of poor lubrication at the piston skirt and cylinder wall, noise generation may take place due to piston slap.



(a) Transverse movement of piston ring



(b) Primary (axial) movement of piston ring



(c) Secondary motion (twisting) of piston ring

Fig. 1.5 Movements of piston rings during operation [4]

### 1.3 Scope of Study

It is widely understood that surface profiling and surface topography of mating solids have remarkable influence on tribological behaviors in both dry and lubricated sliding conditions. Though the influences of the micro and nano scale topography are more complex but, at the same time it offers interesting possibilities for friction reduction. The most promising results related to friction reduction may come out with some novel surface profiles in presence and absence of surface texturing. Therefore, in light of stringent federal legislations pertaining to better fuel economy and reduced emissions, there are needs to revisit lubrication and tribological contact design aspects in IC engine for friction reduction. Improving performance of piston assembly from tribological aspects (reducing friction) will have immense influence on fuel saving and controlling the emissions.

\*\*\*\*\*

## Chapter 2

### Literature Review and Objectives of Study

---

This chapter mainly incorporates the literature review related to tribological studies in the area of piston rings and cylinder/bore interfaces. However, some papers dealing with performance and emissions studies of IC engines (based on different fuels) are also reported herein. Literature review has been mainly grouped in three categories namely: (1) Mathematical modeling; (2) Experimental study; and (3) Surface texturing/profiling. Based on the literature review, research gaps have been highlighted. Moreover, at the end of this chapter, objectives of the study are provided.

Some of the review papers related to engine tribology are presented by various researchers [1, 5-10] under different titles highlighting the important issues in the area. Taylor [6] has highlighted the importance of the tribological design of the major frictional components of the automotive internal combustion engine. The author has emphasized issues of efficiency, durability, and emissions of IC engines. Moreover, he has mentioned that field of engine tribology represents a rich and varied environment for researchers and practitioners with potentially significant influence upon wealth creation and quality of life. Richardson [7] has nicely discussed in the

form of review paper the power cylinder friction for diesel engines. The author has reported that the power cylinder friction constitutes a significant portion of the total mechanical friction of engine. Suggestion was given for friction reduction with lower viscosity lubricating oil by the author. Through a review paper on maximizing the fuel efficiency of engine oils, Korcek et al. [9] have discussed about the role of tribology. The authors have mentioned that the development of engine oils with substantially improved fuel efficiency is an excellent example of the application of tribology to solving an important practical problem. Many facets of tribology have been and still are being used to deliver better oils to the market. Trends in tribological materials and engine technology have been presented by Becker [10]. This paper has presented some tribological considerations for reducing engine friction. The author has stressed upon that to promote effective environmental protection, automotive engineers, material engineers and tribologists need to cooperate with each other to solve the difficult aspects of engine tribology.

Recently a review paper is published related to global energy consumption due to friction in passenger cars by Holmberg et al. [11]. The authors have presented calculations on the global fuel energy consumption used to overcome friction in passenger cars in terms of friction in the engine, transmission, tires, and brakes. They have mentioned that one third of the

fuel energy is used to overcome friction in the engine. In total, about 21.5% of the fuel energy is used to move the car. The authors have presented information that worldwide about 208000 million liters of fuel (gasoline and diesel) was used in 2009 to overcome friction in passenger cars. Thus, reduction in frictional losses will have a threefold improvement in fuel economy, as it will reduce both the exhaust and cooling losses also at the same ratio. These authors have written about potential mechanisms to reduce friction in passenger cars are to use advanced coatings and surface texturing on engine and transmission components, low viscosity and low shear lubricants with novel additives. From the contents of the overview papers [1, 5-11], it is apparent that lubrication aspects of a typical engine system play vital role in controlling the performance and emissions of an IC engine. Thus, thorough literature review is presented in sections to appear.

## 2.1 Mathematical modeling

Many researchers [12-39] have presented mathematical modeling related to their problems in the area of piston ring lubrication. Some of the papers' contents have been described in detail. Nautiyal et al. [13] have presented a theoretical model related to friction and wear processes in piston rings. The authors have reported the factors mainly responsible for wear as surface temperature, peak combustion pressure, and total energy on wearing

surfaces etc. Piston ring friction in internal combustion engines are studied by Wakuri et al. [16]. The authors have reported that the oil film of a compression ring is remarkably reduced over the complete cycle. They have noticed that oil starvation has a remarkable effect on the friction force. As a means of reducing the friction loss, the authors have suggested to effectively decrease the number of piston rings.

Blair et al. [19] have studied reduction of piston ring friction and improvement of wear, scuffing and corrosion resistance of piston rings, as well as reduction of the lubricating oil consumption. The author has mentioned that reduction of piston ring tension and using two ring packages are effective in reducing piston ring friction. It has been mentioned that an increase in lubricating oil consumption by reducing piston ring tension or using two ring packages can be minimized by properly modifying piston ring design.

A novel analytical approach for piston ring lubrication solution is presented by Sawicki and Yu [29] taking proper account of mass conservation in the cavitation region. The author has used a system of five non-linear equations to calculate oil film thickness, friction force, power loss, and oil flow rate. Method presented by author is easily implemented in a computer program and can be used as a platform for future study. Meng et al. [34] have investigated the influence of oil film inertia forces on thermo-

elasto-hydrodynamic lubrication performances of a piston skirt. The numerical studies presented by them show that oil film inertia forces can result in increments in film pressure and temperature, hydrodynamic friction force and load capacity, deformation, and transverse displacement of piston skirt. Charles et al. [36] have derived a dimensionless Reynolds equation based on a double Newtonian rheology. The authors have analyzed the influence of the double Newtonian rheology on friction and load carrying capacity in a model of piston ring cylinder wall contact. They have reported that the friction coefficient changes with increasing shear rate as the contact goes through the non-Newtonian transition.

Junhong et al. [37] have investigated the mechanism of ring-liner lubrication in the vicinity of the top and bottom dead centers of an internal combustion engine. The authors have found that the cavitation which is located at the trailing edge of the contact before reversal, briefly survives after reversal as a confined bubble at the leading edge. Qasim et al [38] have studied low viscosity shear heating in piston skirts elastohydrodynamic in the low initial engine start up speeds. Shear heating effects have been incorporated in 2-D hydrodynamic and EHL model by solving 2-D heat equation. The authors have calculated elastohydrodynamic pressures using inverse solution scheme. They have found that increase in temperature varies with speed, viscosity, and film thickness. A geometric multigrid scheme for



the solution of the Reynolds equation in the piston-cylinder interface of an axial piston machine is presented by Pelosi et al. [39].

## 2.2 Experimental study

Several experimental studies [40-69] have been conducted by the researchers either from tribological perspective or from engine's performance evaluations using alternative fuels/ biodegradable lubricants. For the last many decades, researchers have given major emphasis on energy and finding its substitutes like i) sustainable renewable alternative source of energy, ii) alternative fuel iii) blending fuel to fossil diesel which are limited and depleting on earth. In country like India, diesel engines have proved its utility in industries, agriculture, transportation and rural electrification. It has been observed by the active researchers that the vegetable oils can be used in diesel as a blend for internal combustion engine. Studies [51-69] report that presently biofuels and eco-friendly lubricants are being explored as a sustainable energy source to substitute diesel. For biodiesel fuels, large scale research activities are being carried out across the world considering technical, environmental, social and economical issues. In addition to exploration of renewable fuels, researchers are also putting great efforts in the development of more fuel efficient and environmental friendly compact

internal combustion (IC) engines. In this direction, mechanical losses at various interfaces in engines are being studied and minimized for improving the fuel economy and reducing the exhaust emissions irrespective of fuels being employed in the engines.

Friction losses at various interfaces in IC engines play vital role in determining the engine's fuel economy and exhaust emissions. About 30 to 50 percent of the friction losses in IC engines occur at the interfaces of the piston-cylinder, piston ring-cylinder, and piston-piston ring [1-12, 40-50]. About 60 to 80 percent of these friction losses happen at the piston rings and cylinder liner interfaces. It is essential to mention here that even small reduction in friction at the piston ring-cylinder liner interface may contribute in significant fuel saving and reduction in emissions [1]. Piston rings-cylinder liner and piston rings-piston interfaces have a major influence on IC engines' fuel consumptions, blow-by, and wear. Very hostile environments (high temperature and high gas pressure) in the vicinity of the top compression piston ring of IC engines demand effective lubrication of the interface between the top compression piston ring and cylinder liner. Thus, the design of the top compression piston ring has a significant impact on the lubricating oil consumption in addition to engines' overall performance.

## 2.3 Surface texturing/profiling

Surface texturing technology has recently been explored in the tribology area as a method for improving friction and lubrication. Many researchers [70-87] have tried surface texturing in their respective tribological studies and have reported positive outcome in majority of the situations. Etsion and co-authors [70-72, 77, 78] have presented a novel texturing idea to reduce the friction force between the tribo-contacts. The tribo-element faces are textured with micro-pores, which act as micro-hydrodynamic bearings to improve the lubrication. In 2005, Etsion [87] reviewed various forms of surface texturing in general and the laser surface texturing in particular from tribological performance perspective. Fundamental research works utilizing various texturing techniques are also reported by the author. The benefits of surface texturing and its optimization in forms and dimensions under various operating conditions are amply highlighted and discussed in paper [87].

## 2.4 Conclusions of literature review

Literature review presented above in this chapter reveals the following main information:

- Very limited theoretical studies have been carried out by the researchers with different face profiles of the piston rings.

- Mathematical modeling incorporating the thermal aspects in piston ring lubrication area is rare.
- Experimental studies on IC engines using new face profiles (Catenoidal, cubic, parabolic etc.) of piston ring could not be seen.
- Efforts are being made by the researchers to test IC engines for its performance using bio/alternative fuels.
- Attempts are being done to reduce the friction at various interfaces in IC engines.
- Roles of surface texturing are being explored to reduce the friction at various conformal and non-conformal contacts.
- Limited experimental studies could be noticed with surface textured piston rings. But these studies have been conducted using very fine dimple sizes (5 to 10  $\mu\text{m}$ ).
- Surface dimpling of large size done by chemical etching has not been tried on the faces of the piston rings.
- Sliding studies in mixed lubrication regime with large size (200 – 400  $\mu\text{m}$ ) surface dimpling have not been seen using pin-on-disc tribometer for various operating parameters.

## 2.5 Objectives of study

Based on the conclusions drawn from the literature review presented in chapter-2, the following objectives of the study are set forth:

1. Thermohydrodynamic analysis of fully flooded lubricated interfaces formed between the single continuous surface profiles (Catenoidal, Cubic, Exponential, and Parabolic) of piston ring and cylinder/bore surface.
2. Performance and emission evaluations of an IC engine by fabricating energy efficient surface profile (arrived based on the analyses carried out at point-1 of objective of study) on the faces of piston rings.
3. Assessing the roles of large size surface dimpling on the tribological performance of sliding contacts for incorporating the texturing concept on the faces of piston ring profile for improved performance.

Chapters 3, 4, and 5 incorporate the studies pertaining to above objectives.

\*\*\*\*\*

## Chapter 3

### Mathematical Model for Thermohydrodynamic Analysis of Lubricated Ring/Bore Interface

---

This chapter describes the mathematical model employed for the evaluation of performance parameters at the lubricated interface formed between the four face profiles (Catenoidal, Cubic, Exponential, and Polynomial) of piston ring and counter stationary plain surface (which simulates a cylinder bore surface). The effects of these four single continuous surface profiles (as face profile of top compression of piston ring) on the performance parameters have been numerically investigated and discussed. Contents of this chapter have been broadly divided into four sections: (1) Mathematical model for thermal analysis of lubricated piston ring-cylinder liner interface; (2) Computational procedure; (3) Numerical results with discussions for the input data of an IC engine; and (4) Conclusions.

#### 3.1 Mathematical model

This section presents relevant governing equations for the mathematical simulations of lubricated interfaces formed between the piston ring and cylinder bore surface.

### 3.1.1 Basic assumptions and considerations

In real situations, piston rings and cylinder liner interfaces experience very complex nature of motions due to piston dynamics. Thus, a mathematical simulation of actual movements at the piston ring/liner interface is really a tough task. In order to simplify the model, the following assumptions and considerations have been done:

1. Oil inhomogeneity along the circumferential direction of piston ring is neglected.
2. There is only primary motion i.e. piston ring does not tilt and twist in its groove. It moves radially and axially under normal loading.
3. Piston ring contact with cylinder liner is steady.
4. Influence of heat conduction inhomogeneities due to joint in piston ring is neglected.
5. Fully flooded lubrication has been considered.
6. Metal to metal contact at the top dead centre and bottom dead centre positions are neglected.
7. Newtonian lubricant rheology and laminar flow are considered.
8. Both body and inertia forces are neglected.
9. There is no slip at the boundaries of the domain.

### 3.1.2 Geometric description of domain

The piston ring essentially behaves as a reciprocating slider bearing subjected to cyclic variations in velocity and pressure (or load). The physical domain (lubricated interface formed between piston ring and cylinder liner) which has been analyzed mathematically in this thesis is illustrated in Fig.

3.1.

The film thickness between the cylinder wall and the piston ring is expressed as follows (refer Fig. 3.1):

$$h(x,t) = h_{\min}(t) + h_x \quad (3.1)$$

Where,  $h_{\min}(t)$  is minimum film thickness and it varies with time (or crank angle).

$h_x$  is film thickness corresponding to the geometry of piston ring face profile.

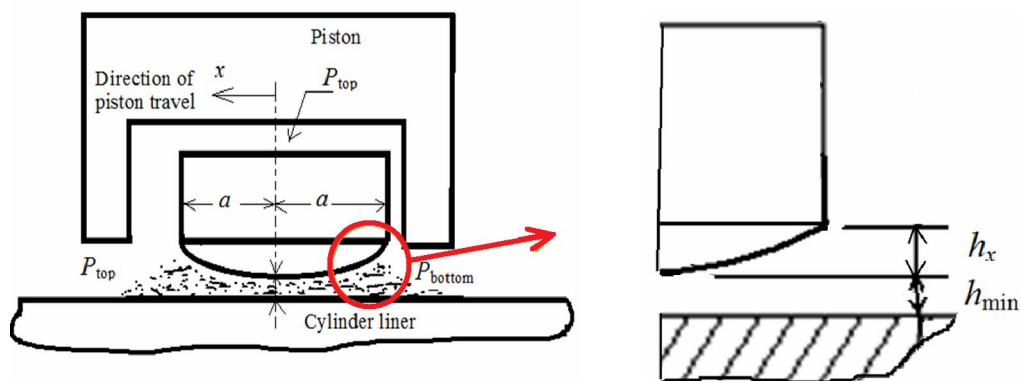


Fig. 3.1 Schematic diagram of geometry formed between a piston ring and cylinder liner



In this study, four single continuous surface profiles (Catenoidal, Cubic, Exponential, and Parabolic) on the face of piston ring have been considered. Expressions for the film thickness ( $h_x$ ) due to these face geometries are written as below:

Catenoidal profile:

$$h_x(x) = (a^2 / 2\delta_0) \left\{ -1 + \cosh \left( \frac{2\delta_0}{a^2} x \right) \right\} \quad (3.2)$$

Cubic profile:

$$h_x(x) = (\delta_0 / 2) \left\{ (x/a)^3 + (x/a) \right\} \quad (3.3)$$

Exponential profile:

$$h_x(x) = -1 + \exp \left( \frac{\ln(\delta_0 + 1)}{a} x \right) \quad (3.4)$$

Parabolic profile:

$$h_x(x) = \delta_0 (x/a)^2 \quad (3.5)$$

In above equations (3.2) to (3.5), ' $\delta_0$ ' and ' $a$ ' are crown height and piston ring half width, respectively.

### 3.1.3 Reynolds equation for pressure

The hydrodynamic pressures are computed in the domain by solving the one dimensional Reynolds equation derived from the Navier-Stokes equation by assuming the classical hypotheses of lubrication theory i.e. the surfaces are smooth and the magnitude of the thickness of the lubricating film is small compared to other dimensions at the contact surface. For an isothermal and incompressible lubricant, the one-dimensional transient Reynolds equation is written as:

$$\frac{\partial}{\partial x} \left( \frac{h^3}{\eta} \frac{\partial p}{\partial x} \right) = 6U \frac{\partial h}{\partial x} + 12 \frac{\partial h}{\partial t} \quad (3.6)$$

Where,  $p$  is the hydrodynamic pressure,  $\eta$  is the lubricant dynamic viscosity,  $U$  is the sliding velocity of the piston ring surface.

Considering the viscosity of lubricating oil as constant, eqn. (3.6) is written as:

$$\frac{\partial}{\partial x} \left( h^3 \frac{\partial p}{\partial x} \right) = 6U\eta \frac{\partial h}{\partial x} + 12\eta \frac{\partial h}{\partial t} \quad (3.7)$$

The crank's angular velocity is expressed as:

$$\begin{aligned} \omega &= \frac{\partial \theta}{\partial t} \\ \rightarrow \partial t &= \frac{\partial \theta}{\omega} \end{aligned} \quad (3.8)$$

Using eqns. (3.7) and (3.8), the Reynolds equation of transient case is achieved as:

$$\frac{\partial}{\partial x} \left( h^3 \frac{\partial p}{\partial x} \right) = 6U\eta \frac{\partial h}{\partial x} + 12\omega\eta \frac{\partial h}{\partial \theta}$$

Or

$$h^3 \frac{\partial^2 p}{\partial x^2} + \frac{\partial p}{\partial x} \left( 3h^2 \frac{\partial h}{\partial x} \right) = 6U\eta \frac{\partial h}{\partial x} + 12\omega\eta \frac{\partial h}{\partial \theta} \quad (3.9)$$

When the piston is in down stroke, the inlet boundary condition at the leading edge of the ring is:

$$p(+a, t) = p_{\text{top}} \quad (3.10a)$$

And the exit boundary condition at the trailing edge is:

$$p(-a, t) = p_{\text{bottom}} \quad (3.10b)$$

Where,  $p_{\text{Bottom}}$  and  $p_{\text{Top}}$  are the pressures at trailing and leading edges of the ring, respectively.

Swift-Steiber (or Reynolds) boundary conditions are implemented in the solution of Reynolds equation, which are as follows:

- Pressure gradient ( $\partial p / \partial x$ ) at the cavitation boundaries is zero.
- Pressure within the cavitation regions is constant and equal to the vapor/gas pressure ( $p_{cav} = 0$ ) of the lubricant.

Solution of governing equation is carried out employing iterative methods. Finite Difference Scheme (FDS) with Successive Over-Relaxation (SOR) procedure is used in computation. In this method, the cavitation boundaries are automatically found setting to zero all the pressures going down below to  $p_{cav}$ . Although this model does not satisfy mass conservation of the lubricant flow throughout the cavitation boundaries, but it is popular due to convenience in its implementation in the solution. Moreover, it does not introduce much error in the numerical results too. It is worth mentioning here that even today several researchers use this boundary condition in their models.

#### 3.1.4 Energy equation for temperature

To account for the viscosity variation with temperature, the energy equation must be invoked. The temperature rise in oil film is determined by using

transient energy equation with heat generated from viscous dissipation (or shear heating). Considering non-inertial laminar lubricating films without dilatational viscosity, the energy equation for the lubrication of piston ring interface is written as:

$$\rho_f C_{pf} \left( \frac{\partial T}{\partial t} + u \frac{\partial T}{\partial x} \right) = k_f \frac{\partial^2 T}{\partial z^2} + \eta \left( \frac{\partial u}{\partial z} \right)^2 \quad (3.11)$$

In eqn. (3.11), the terms due to conduction  $\left( \frac{\partial}{\partial x} \left\{ k_f \frac{\partial T}{\partial x} \right\} + \frac{\partial}{\partial y} \left\{ k_f \frac{\partial T}{\partial y} \right\} \right)$  and convection  $\left( \rho_f C_{pf} u \frac{\partial T}{\partial z} + \rho_f C_{pf} v \frac{\partial T}{\partial z} \right)$  are omitted. The magnitudes of these terms are usually very small in comparison to the convection along the film and conduction across the film.

In energy equation, the temperature varies in both the x and z directions. The x-direction is the direction of motion of the piston and the z direction is associated with film thickness across the cylinder wall. This numerical model bears the assumption that the lubricant properties other than viscosity remain constant and that the adiabatic compression work in the fluid is negligible. Furthermore, due to the axisymmetric nature of the problem, temperature variation in the circumferential direction is ignored.

The boundary conditions for energy equation are:

$$T(-a, z) = T_0 \quad (3.12a)$$

$$\frac{\partial T}{\partial x}(+a, z) = 0 \quad (3.12b)$$

$$T(x, 0) = T_0 \quad (3.12c)$$

$$\frac{\partial T}{\partial x}(x, h) = 0 \quad (3.12d)$$

Equation (3.12a) specifies a uniform temperature at the leading edge corresponding to the lubricant inlet temperature. At the trailing edge the temperature gradient in the flow direction is zero as given by eqn. (3.12b). Equation (3.12c) specifies temperature of the cylinder wall which is equal to the inlet temperature of lubricating oil. At the oil-ring interface ( $z = h$ ) an adiabatic boundary condition is applied through eqn. (3.12d). This condition simplifies the problem significantly while it provides a conservative estimate of the performance parameters.

Oil film mean temperature is estimated using following relation:

$$T_m = \frac{1}{h} \int_0^h T(x) dx \quad (3.13)$$

### 3.1.5 Viscosity-temperature relationship

The temperature dependency of lubricating oil's viscosity is estimated using the following relation:

$$\eta = \eta_0 e^{-\gamma(T-T_0)} \quad (3.14)$$

### 3.1.6 Miscellaneous relations

The relation used for the computation of shear stress is given as follows:

$$\tau = \frac{h}{2} \frac{\partial p}{\partial x} + \frac{\eta U}{h} \quad (3.15)$$

Load carrying capacity (per unit circumferential length) is written as:

$$W = \int_{-a}^{+a} p \, dx \quad (3.16)$$

Friction force (per unit circumferential length) is written as:

$$F = \int_{-a}^{+a} \tau \, dx \quad (3.17)$$

Power loss is computed as:

$$\text{Power loss} = F \cdot u \quad (3.18)$$

## 3.2 Computational procedure

Coupled solution of governing eqns. (3.1) to (3.14) is achieved using Finite difference Scheme method (FDS). First order forward difference is used for discretization of time containing terms of governing equations, however, the second order central difference scheme is used to discretize the space related terms. Finite difference grid employed in computation is shown in Fig. 3.2.

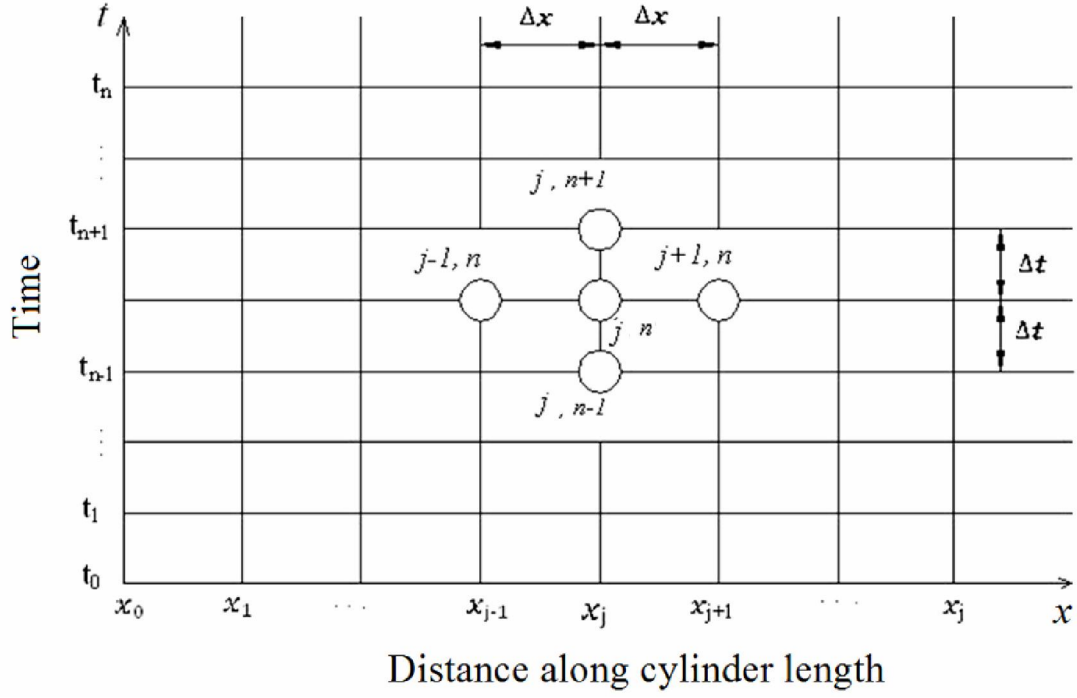


Fig. 3.2 Finite difference grid used in the computation

Discretization of Reynolds equation:

$$\left( \frac{\partial p}{\partial x} \right)_j = \frac{p_{j+1}^n - p_{j-1}^n}{2\Delta x} \quad (3.19a)$$

$$\left( \frac{\partial^2 p}{\partial x^2} \right)_j = \frac{p_{j+1}^n - 2p_j^n + p_{j-1}^n}{(\Delta x)^2} \quad (3.19b)$$

$$\left( \frac{\partial h}{\partial \theta} \right)_j = \frac{h_j^{n+1} - h_j^n}{\Delta \theta} \quad (3.19c)$$

$$\left( \frac{\partial h}{\partial x} \right)_j = \frac{h_{j+1}^n - h_{j-1}^n}{2\Delta x} \quad (3.19d)$$

$$\eta_j = \eta_0 e^{-\gamma [T_j^n - T_0]} \quad (3.19e)$$



Substituting eqns. (3.19a) to (3.19e) in eqn. (3.9), the following discretized Reynolds equation is achieved:

$$\begin{aligned}
& (h_j^3)^n \left( \frac{p_{j+1}^n - 2p_j^n + p_{j-1}^n}{(\Delta x)^2} \right) + \\
& \left( \frac{p_{j+1}^n - p_{j-1}^n}{2\Delta x} \right) 3(h_j)^n \left( \frac{h_{j+1}^n - h_{j-1}^n}{2\Delta x} \right) \\
& = 6U\eta_j \left( \frac{h_{j+1}^n - h_{j-1}^n}{2\Delta x} \right) + 12\omega\eta_j \left( \frac{h_j^{n+1} - h_j^n}{\Delta\theta} \right)
\end{aligned} \tag{3.20}$$

Discretization of Energy equation:

The finite difference form of terms of the energy equation is written as:

$$\rho_f C_{pf} \frac{\partial T}{\partial t} = \rho_f C_{pf} \left( \frac{T_j^{n+1} - T_j^n}{\Delta t} \right) \tag{3.21a}$$

$$\rho_f C_{pf} u \frac{\partial T}{\partial x} = \rho_f C_{pf} u_j^n \left( \frac{T_{j+1}^n - T_{j-1}^n}{2\Delta x} \right) \tag{3.21b}$$

$$k_f \frac{\partial^2 T}{\partial z^2} = k_f \left( \frac{T_{j,k}^n - 2T_{j,k}^n + T_{j,k}^n}{(\Delta z)^2} \right) \tag{3.21c}$$

$$\eta = \eta_0 e^{-\gamma[T_{j,k} - T_0]} \tag{3.21d}$$

$$\eta \left( \frac{\partial u}{\partial z} \right)^2 = \eta_{j,k}^n \left( \frac{u_{j+1,k}^n - u_{j-1,k}^n}{2\Delta z} \right)^2 \tag{3.21e}$$

Terms expressed by eqn. (3.21c) disappears due to average temperature across the film thickness.

Substituting eqns. (3.21a) to (3.21e) in eqn. (3.11), the following discretized energy equation is achieved:

$$\begin{aligned} & \rho_f C_f \left( \frac{T_{j,k}^{n+1} - T_{j,k}^n}{\Delta t} \right) + \rho_f C_{p_f} u_{j,k}^n \left( \frac{T_{j+1,k}^n - T_{j-1,k}^n}{2\Delta x} \right) \\ & = k_f \left( \frac{T_{j,k+1}^n - 2T_{j,k}^n + T_{j,k-1}^n}{(\Delta z)^2} \right) + \eta_{j,k}^n \left( \frac{u_{j+1,k}^n - u_{j-1,k}^n}{2\Delta z} \right)^2 \end{aligned} \quad (3.22)$$

The flow chart of the computation is given in Fig.3.3. In order to achieve converged solution, the following convergence criterions are used:

For pressure:

$$\frac{\sum |(p_j)_N - (p_j)_{N-1}|}{\sum |(p_j)_N|} \leq 10^{-5} \quad (3.23)$$

For temperature:

$$\frac{\sum |(T_{j,k})_N - (T_{j,k})_{N-1}|}{\sum |(T_{j,k})_N|} \leq 10^{-5} \quad (3.24)$$

Where, N represents number of iterations and j & k denote number of nodes.

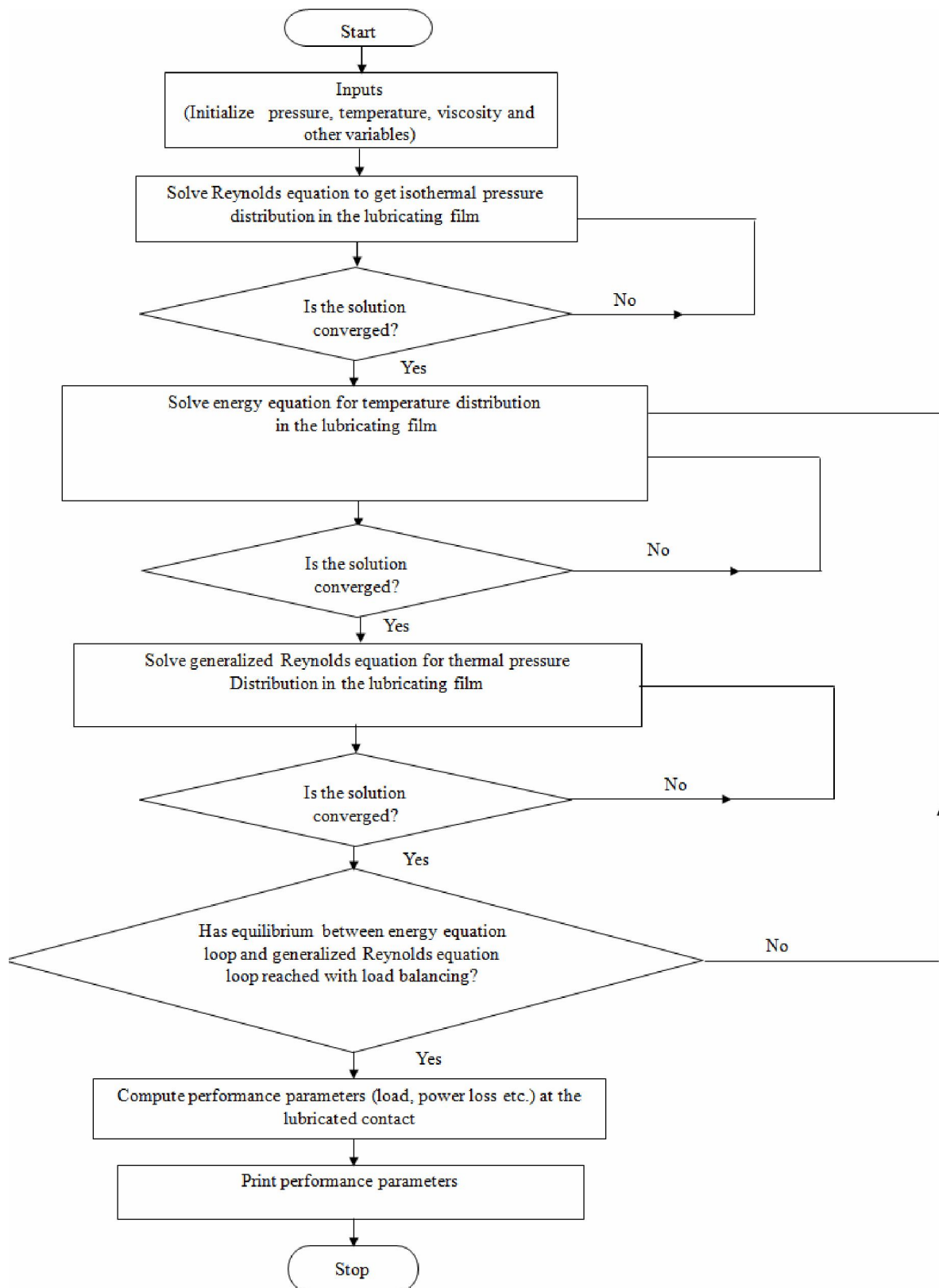


Fig. 3.3 Flowchart for computation

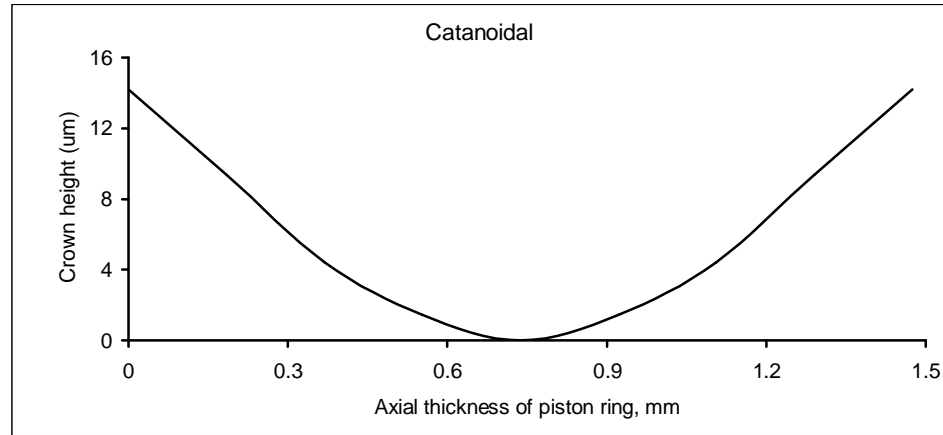
### 3.3 Results and discussions

Numerical results pertaining to Thermohydrodynamic lubrication analyses of the interfaces formed between the face of piston rings and cylinder/bore liner are presented herein using the mathematical model outlined in the previous sections. Input data used in this investigation is listed in Table 3.1. This input data corresponds to a typical automotive engine used by Jeng (1992). It is essential to mention here that unless otherwise specified, the parameters values listed in Table 3.1 are used for the calculations.

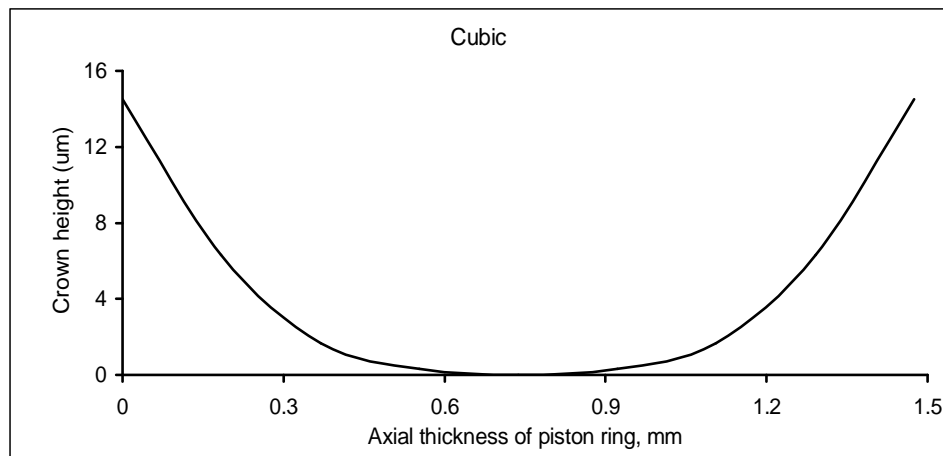
Table 3.1 Input data of engine  
[Source: Jeng (1992)]

S. No.	Parameter	Value
1	Engine speed (rpm)	2000
2.	Cylinder bore (mm)	88.9
3.	Bore radius (mm)	44.45
4.	Crank radius (mm)	40
5.	Connecting rod length (mm)	141.9
6.	Piston ring width (mm)	1.475
7.	Piston ring thickness (mm)	3.8
8.	Piston ring's material Young's modulus (GPa)	70
9.	Piston ring crown height ( $\mu\text{m}$ )	14.9
10.	Lubricant viscosity (Pa-s)	0.007
11.	Temperature viscosity coefficient ( $\text{K}^{-1}$ )	0.0214
12.	Ambient temperature ( $^{\circ}\text{C}$ )	35
13.	Lubricant thermal conductivity (W/m-K)	0.12
14.	Specific heat (J/kg-K)	2000

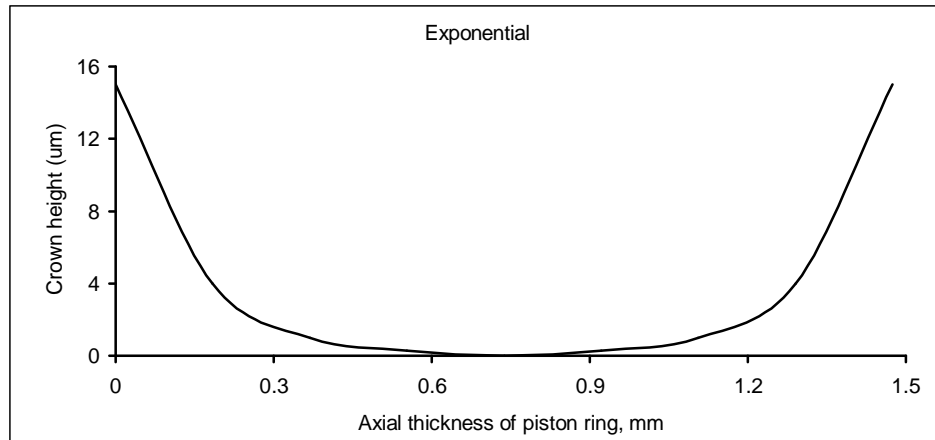
Figures 3.4 (a) - 3.4 (d) demonstrate face profiles of piston ring considered in this numerical study. These face profiles have been drawn using the eqns. (3.2) to (3.5) and input data of Table 3.1.



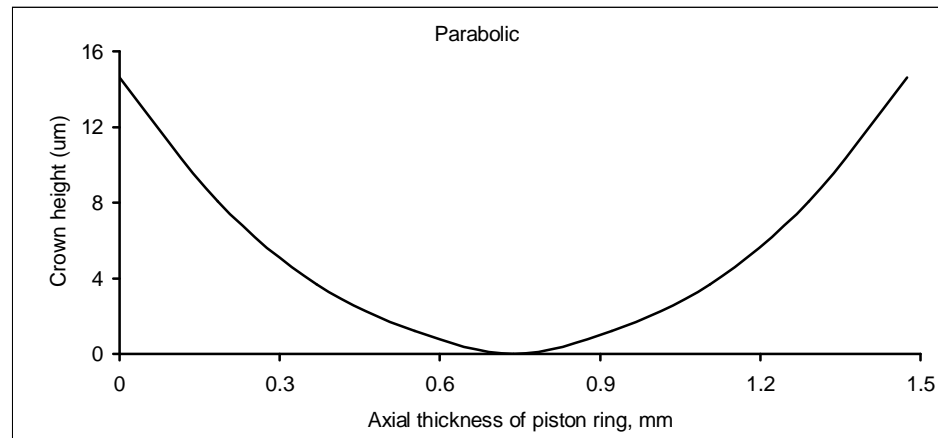
(a) Catenoidal face profile



(b) Cubic face profile



(c) Exponential face profile



(d) Parabolic profile

Fig. 3.4 Geometries of faces on the piston rings

Figure 3.5 illustrates a plot of the piston speed as a function of crank angle for an engine speed of 2000 rpm. The combustion chamber pressure is used as the pressure at the top of the first compression ring and half of that pressure is used as the pressure at bottom of the ring. Figure 3.6 shows a typical gas pressure distribution in the combustion chamber at a moderate

load. In Figs. 3.5 and 3.6, zero crank angle is defined from top dead centre of the stroke.

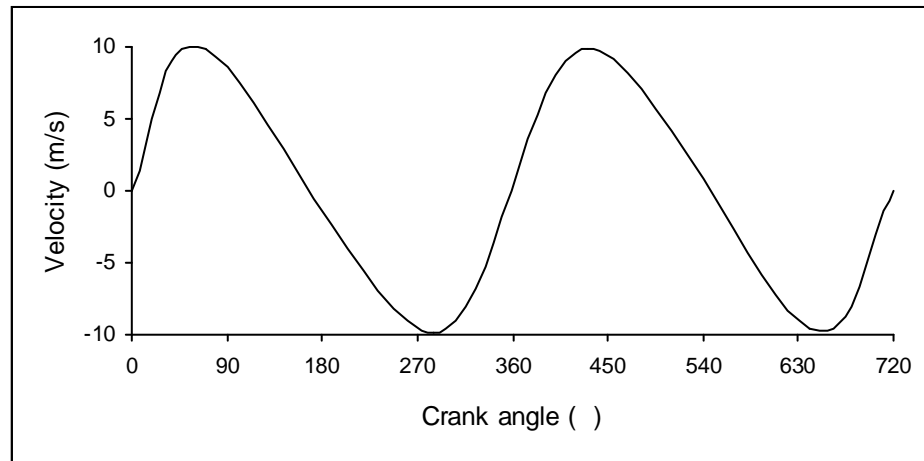


Fig. 3.5 Piston speed as a function of crank angle for 2000 rpm engine speed

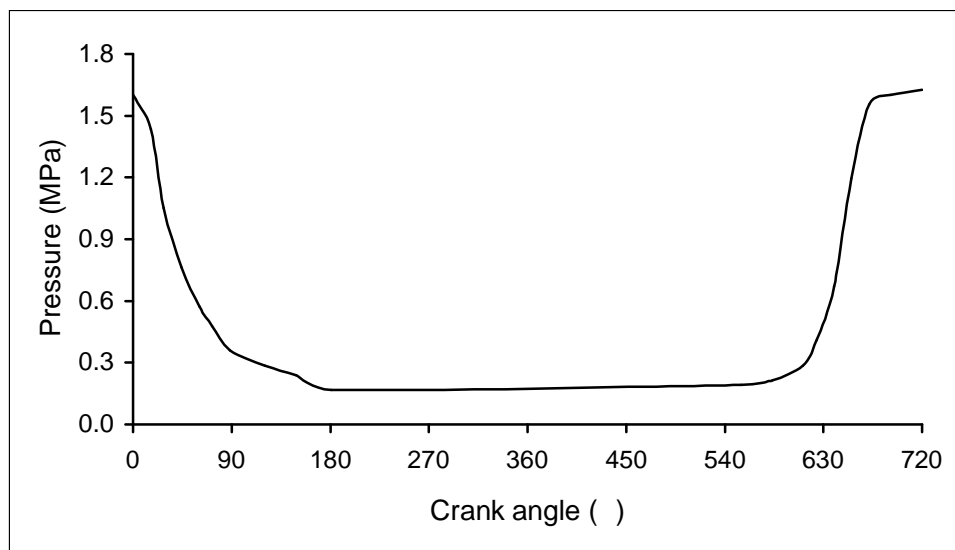


Fig. 3.6 Combustion chamber pressure at moderate load

### Validation of the proposed model

In order to have confidence in the proposed numerical model, the results achieved by the proposed mathematical model is compared with the

results of Jeng (1992). From the Figs.3.7 and 3.8, a reasonably good correlation can be seen between both the results. This develops a reasonable confidence in the model adopted here in.

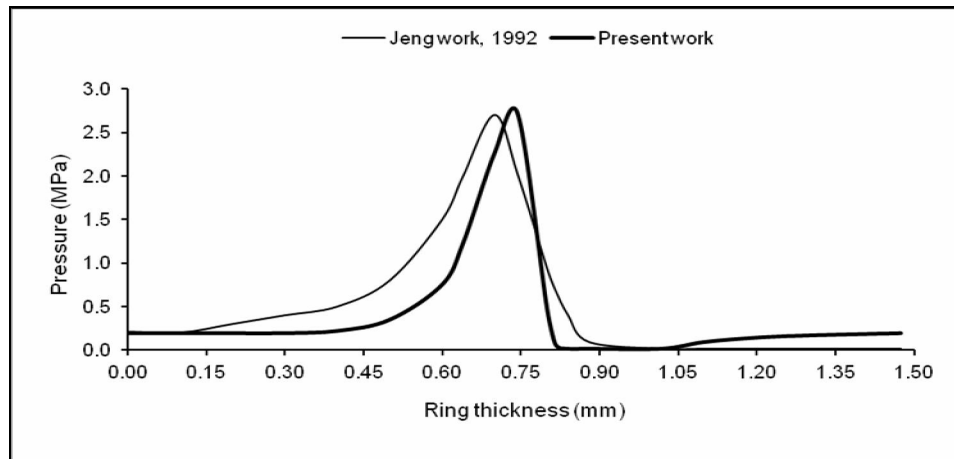


Fig. 3.7 Variation of film pressure at the interface in the axial direction

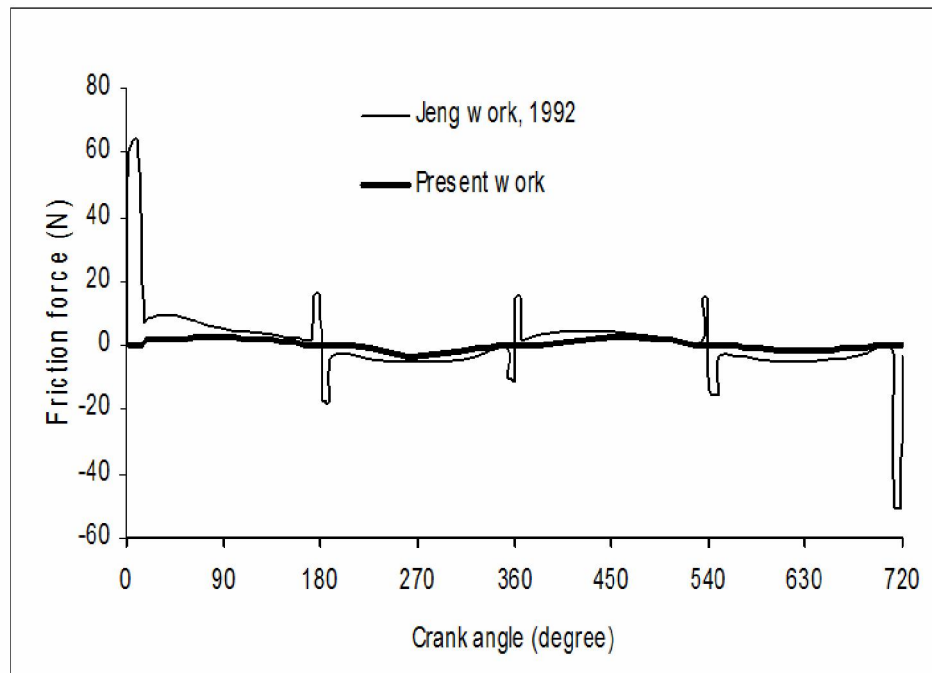


Fig. 3.8 Variation of friction force at the interface



Figure 3.9 presents pressure distributions at the interface with catenoidal, cubic, exponential, and parabolic face profiles on the piston rings. Large magnitude of film pressure in small contact area is seen with parabolic face profile. However, uniform film pressure distribution at the lubricated interface can be seen with exponential face profile. This type of pressure distribution is good from dynamics and tribological point of views. From Fig. 3.10, it can be seen that the minimum film thickness for a whole cycle occurs at top and lower dead centers. With exponential face profile of piston ring, minimum film thickness comes out much less than other three profiles (catenoidal, cubic, and parabolic). Minimum film thickness is beneficial from stability point of view during the piston dynamics. It is worth to mention here that less shearing of lubricating oil leads to less heat generation.

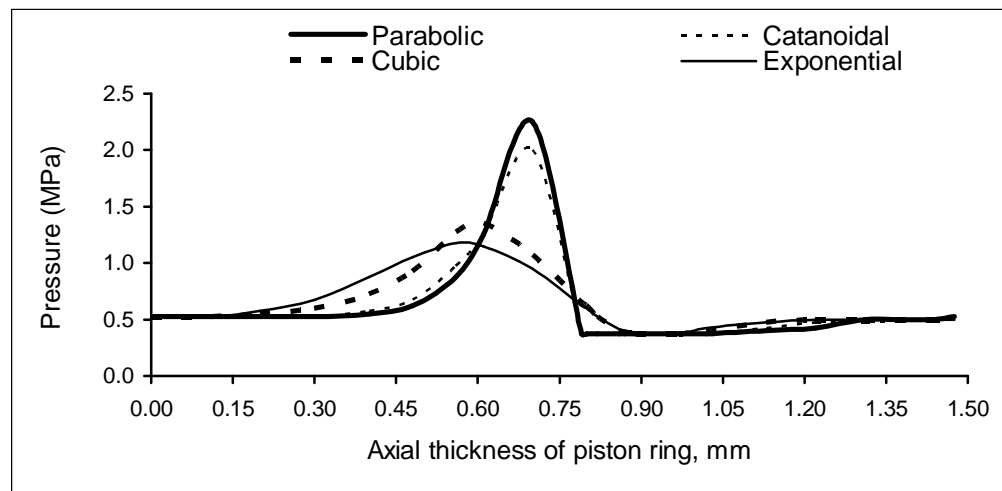


Fig. 3.9 Comparison of pressure variations with the four face profiles of ring

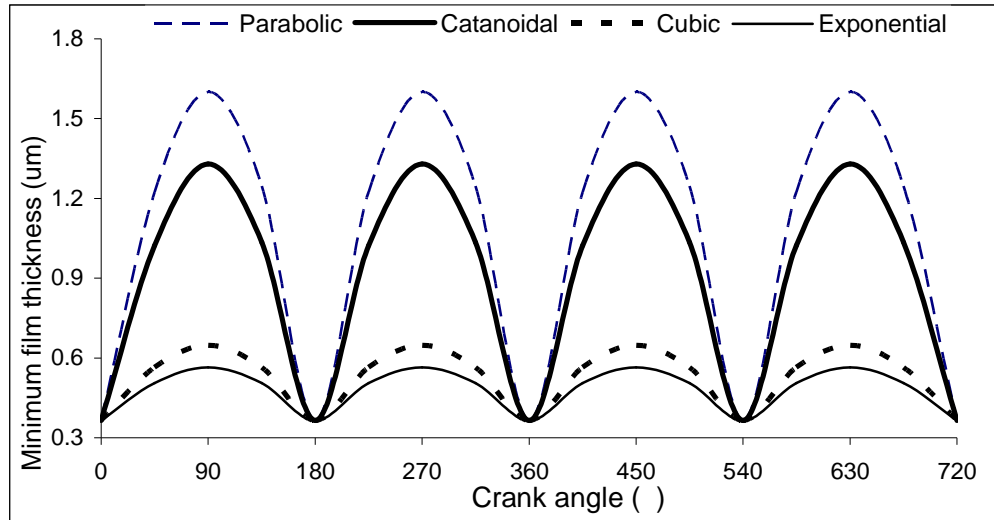


Fig. 3.10 Comparison of minimum film thickness variations with the four face profiles of ring

Figures 3.11 and 3.12 illustrate variation of friction force and power loss for a cycle. From Fig. 3.12, it can be seen that due to better wedging action power loss is about 50% less with exponential face profile in comparison to parabolic face profile, which is normally used on faces of piston rings in IC engines. Thus, results with exponential face profile is encouraging.

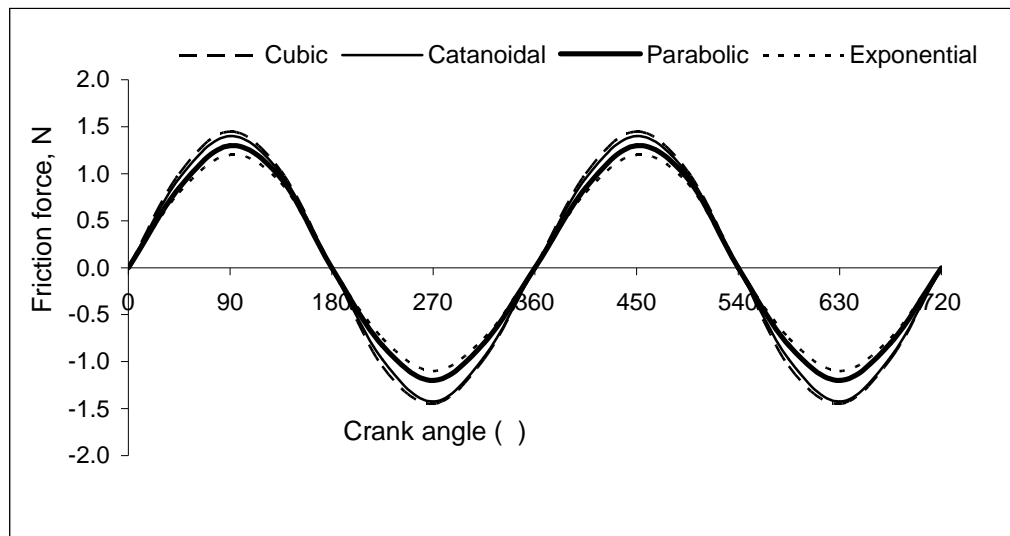


Fig. 3.11 Comparison of friction force variations with the four face profiles of ring

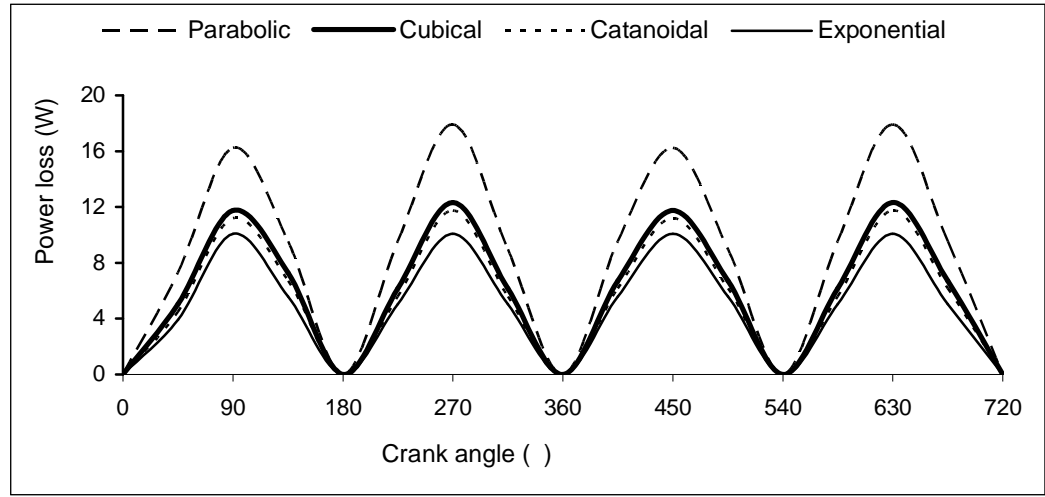


Fig. 3.12 Comparison of power loss variations with the four face profiles of ring

### 3.4 Conclusions

A thermal model of hydrodynamic lubrication at the ring/bore interface has been formulated for numerically assessing the roles of four (Catenoidal, cubic, exponential, and parabolic) single continuous face profiles of piston ring for evaluating the performance of lubricated interface. Based on the numerical investigations, it is observed that exponential face profile on piston ring is proving much energy efficient in comparison to other face profiles considered in this investigation. Thus, it is planned to fabricate this profile on piston rings of an IC engine for conducting the experiments for checking the fuel saving and emissions.

\*\*\*\*\*

## Chapter 4

### Experimentation with an IC Engine using Exponential Face Profile of Piston Rings

---

This chapter covers fabrication of designs (I, II and III) face profile piston rings which have been arrived by energy efficient exponential face profile based on the mathematical modeling reported in previous chapter-3, and limitations of manufacturing. Experiments have been conducted with diesel and Jatropa based biodiesel (B100) at various loads that varying up to 100 percent on commercial IC engine. The performance and emissions behaviors of a diesel engine have been investigated and compared using standard (conventional) and three new face profile designs of piston rings.

#### 4.1 Background

Fossil fuels are major sources of non-renewable energy, which are depleting rapidly due to their exhaustive uses in industrial, transportation, agriculture and domestic sectors. Biodiesel is one of the major sources of sustainable renewable energy and lots of works were carried out in this field that can be used in above mentioned sectors. There is also need to design the engine parts especially piston ring and interacting surfaces for better efficiency and to meet the international intrinsic environment conditions.

Based on the literature review, works have done on the synthesis of alternative fuels and their evaluations (performances/emissions) or tribological studies of the components of IC engine for the cases in which engines are run with conventional fuels and conventional piston rings. The experiments have been carried on IC engines using diesel and biodiesel (B100) as fuel and following have been taken as objective.

(1) Comparison of performance parameters and emissions of a commercial diesel engine fueled with diesel and Jatropha based biodiesel (B100).

(2) Performance assessment of the diesel engine with both the fuels using standard (conventional) and three different face profile designs (I, II and III) of the piston rings.

#### 4.2 Fabrication of Exponential Face Profiles

As already highlighted, piston rings of three different face profile designs (I, II and III) have been arrived based on the mathematical modelling chapter 3 of hydrodynamically lubricated interface formed between the piston ring and cylinder liner. While arriving at these designs (I, II and III), manufacturing issues have been also considered. A fixture as shown in Fig. 1 is developed to hold the piston rings for micro machining the face profiles. In this fixture, a circular groove (OD = 102 mm, ID = 94

mm, and depth = 1.5 mm) is fabricated for properly holding the piston ring during machining. It is worth mentioning here that the standard (conventional) piston ring's outer diameter is 102 mm and thickness is 3 mm. Clamped piston ring in fixture can be seen in Fig.1. Rigidly locking device to piston ring to be modified have been made using nut and bolt.

Conventional and new face profiles of piston rings are illustrated in Fig. 2. It is essential to mention here that the piston and cylinder assembly of the test engine has four piston rings (three compression rings and one oil scraper ring). In each design (I, II and III), the oil scraper ring attached at the end from top dead center on piston have the similar structure whereas, the from other rest three compression rings in a piston ring package two have the same type of face profiles.



Fig. 4.1 Photographic view of fixture with a clamped piston ring

### 4.3 Experimentation

Experiments have been carried out on a single cylinder, four-stroke, and water-cooled commercial diesel engine. Photographs of the test engine and loading system are shown in Figs. 4.3 & 4.4 respectively. Detailed technical specifications of the test engine are provided in Table 4.1. The engine has coupled to an electrical dynamometer for measuring engine load. A fuel-measuring unit and stopwatch have been employed for the measurement of fuel consumption and time elapsed during the experiments, respectively. Time elapsed for consumption of 30cc has been taken for the performance calculation of the test engine. The parameters measured are fuel consumption, speed (rpm) and power output. The engine has been run for each set of rings, at no load condition for one hour. Thereafter, the test engine has been loaded gradually keeping the speed within permissible limits while recording the readings pertaining to different parameters. Engine performance tests have been carried out using a standard (conventional) face profile for the piston rings.

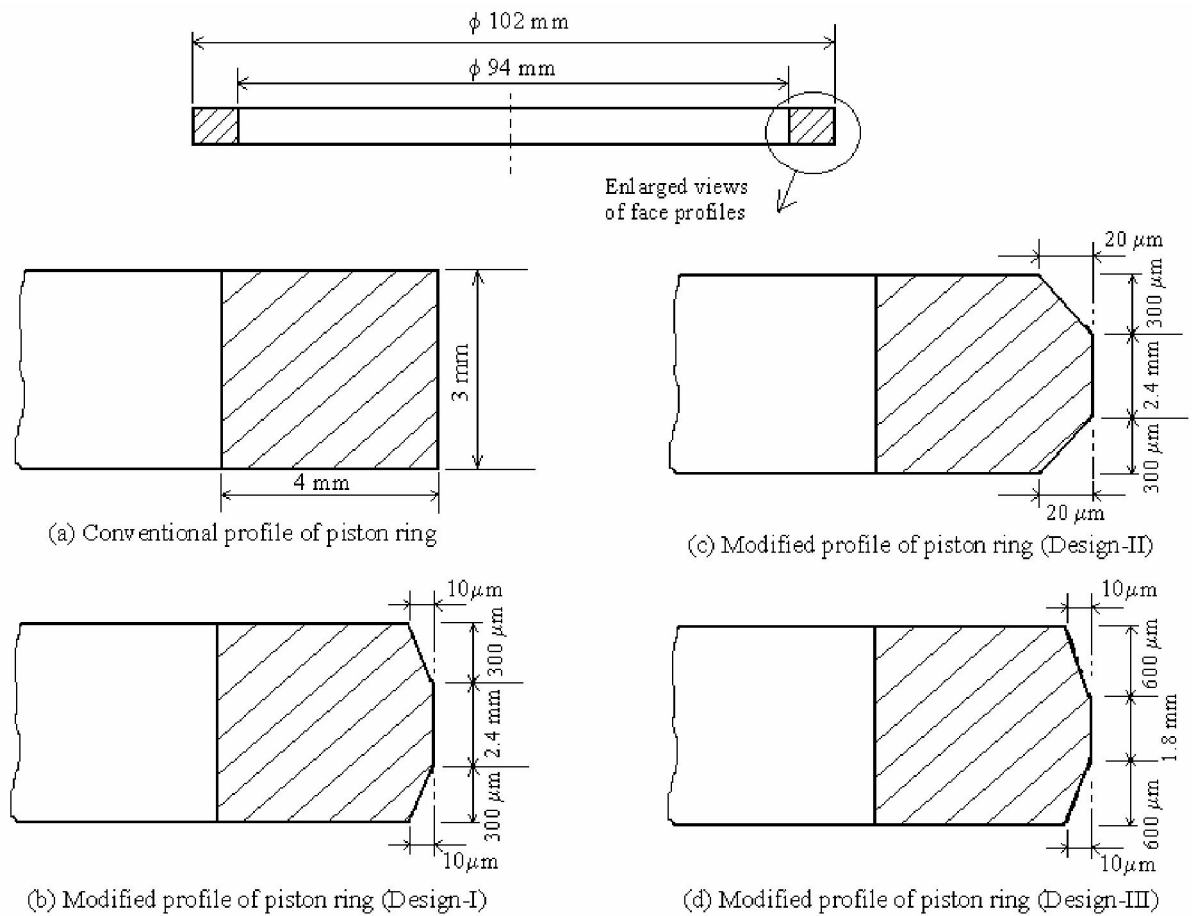


Fig. 4.2 Schematic diagrams of standard (conventional) and three new face profiles of piston rings

Fuels used in these experiments were commercial diesel and jatropha based biodiesel. Both diesel and biodiesel fuels have been used for generating the base line data for performance and emissions comparison. Some of the important properties of diesel and biodiesel are given in (Table 4.2) and the instruments used are described in Appendix-1. Thereafter, performance parameters readings have been recorded with new face profile



designs (I, II and III) of piston rings using both diesel and biodiesel fuels.

The new face profiles of piston rings can be seen in Fig.4.2.

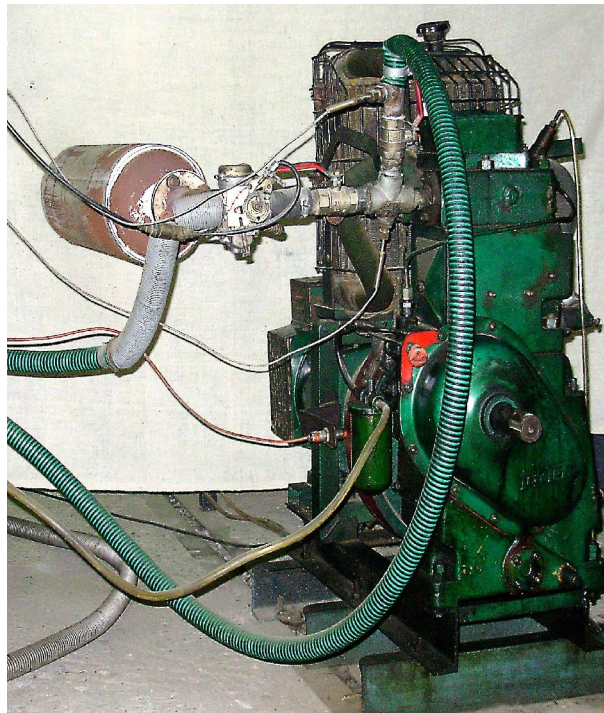


Fig. 4.3 Photographic view of test engine

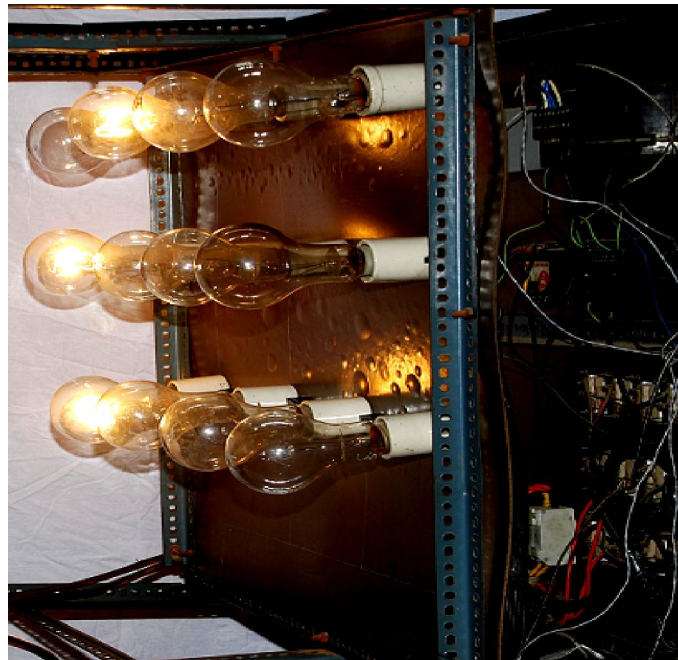


Fig. 4.4 Engine's loading system

Table 4.1 Technical specifications of test engine

S. No.	Features	Details
1.	Number of cylinder	1
2.	Number of stroke	4
3.	Cylinder orientation	Vertical
4.	Rated brake power, kW	7.4
5.	Rated speed, rpm	1500
6.	Bore x Stroke, mm <sup>2</sup>	102 x 116
7.	Displacement volume, cc	948
8.	Compression ratio	17.5:1
9.	Cooling system	Water cooled
10.	Lubrication system	Forced feed
11.	Fuel system	Gravity feed fuel system with efficient paper element filter
12.	SFC at rated HP/1500 rpm, g/kWh	251
13.	Lubricating oil consumption, %	1.0 (maximum) of SFC
14.	Lubricating oil sump capacity, liters	3.75
15.	Fuel tank capacity, liters	11.5
16.	Fuel tank re-filling time period	Every 5 hours engine running at rated speed
17.	Engine weight without flywheel, kg	127
18.	Weight of flywheel, kg	64
19.	Direction of crank rotation from side of flywheel	Clockwise
20.	Starting	Hand start with cranking handle

#### 4.4 Results and discussions

Physico-chemical properties of diesel and Jatropha based biodiesel (B100) have been measured in the laboratory well before the

commencement of the experiments. The instrument used have been shown in Appendix-1. These properties are listed in Table 4.2 as follows:

It is clear from the table 4.2 that the jatropha biodiesel (B100) has higher flash point and kinematic viscosity in comparison to neat diesel. The biodiesel has traces of sulphur whereas diesel has substantial content of sulphur. The cetane number of biodiesel is higher than diesel. The biodiesel contain around 11 percent of oxygen whereas diesel does not contain any oxygen.

Table 4.2 Properties of diesel and Jatropha based biodiesel

S. No.	Properties	Diesel	Jatropha based biodiesel (B100)
1.	Flash point, °C	76	162
2.	Kinematic viscosity, cSt at 40°C	3.21	4.12
3.	Sulfur, ppm	340	8
4.	Cetane number	47.2	49
5.	Carbon, % by wt	87	77
6.	Hydrogen, % by wt	13	12
7.	Oxygen by difference, % wt	Negligible	11

#### 4.4.1 Brake Thermal Efficiency

For comparative evaluations of the role of piston rings (standard face profile and three new face profile designs) and fuels (diesel and biodiesel); test engine performances in terms of brake thermal efficiency (BTE), brake specific fuel consumption (BSFC) and mass flow rate of fuel have been measured and reported herein. Marginal differences in BTE are recorded

with both the fuels when standard piston ring sets are used. Fig.4.5 shows variations of BTE with the engine loads for standard (conventional III) when diesel fuel is used to run the engine. Moreover, Fig.4.6 shows similar variations between BTE with load for biodiesel (B100). Highest thermal efficiencies of 25.48 percent and 25.56 percent are recorded at 80 percent of maximum load with diesel and biodiesel respectively. BTE decreases at higher loads (beyond 80 percent) due to poor combustion of fuels. This is a normal trend in compression ignition engines.

A significant improvement in BTE has been achieved when piston rings of new face profile design (III) is used in engine. The brake thermal efficiencies of engines fueled with diesel and biodiesel are relatively high on these rings.

The numerical values of these efficiencies reach to 27.16 percent and 28.29 percent with piston rings of new face profile design (III). Increase in BTE happens due to effective lubrication with new face profile design (III) of piston rings. Better lubrication reduces the mechanical losses at the interface of cylinder liner and piston rings, which enhances the efficiency of the engine.

The brake thermal efficiencies of the engine fueled with diesel and biodiesel increase 2 to 8 percent and 8 to 16 percent, respectively, with new face profile design (III) of piston rings in comparison to standard

(conventional) piston rings. Better BTE with biodiesel may be attributed to high cetane number resulting in better combustion of fuel.

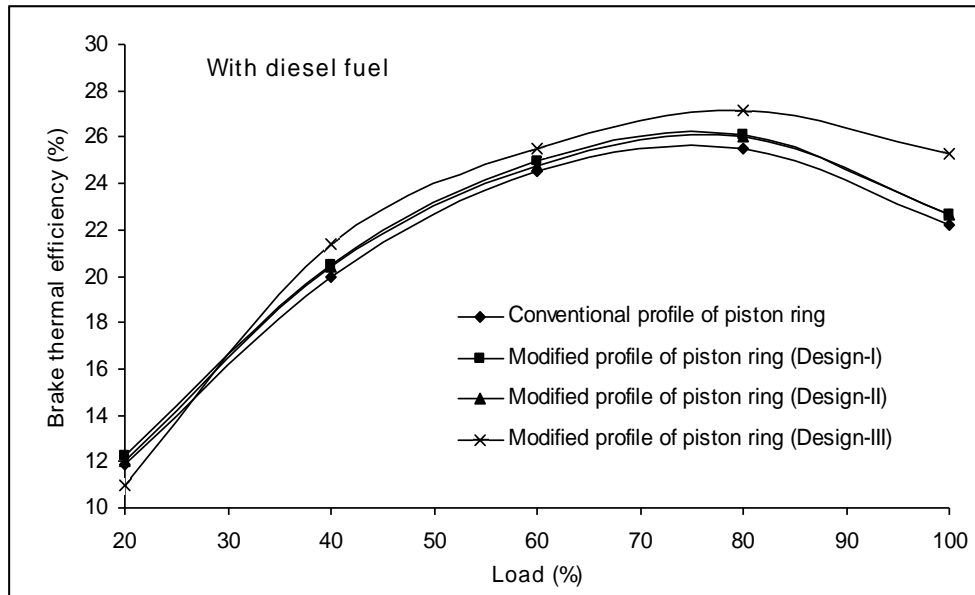


Fig. 4.5 Variation of brake thermal efficiency with load using diesel fuel

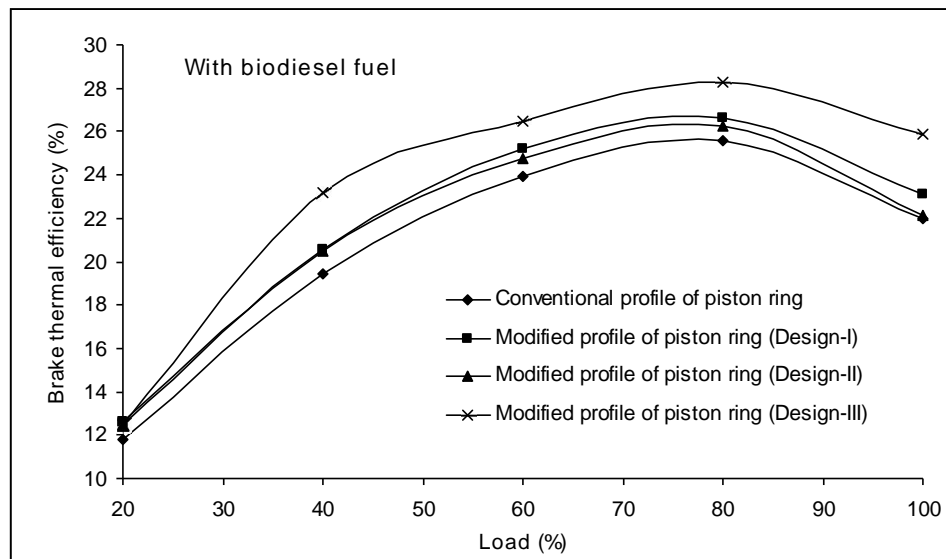


Fig. 4.6 Variation of brake thermal efficiency with load using biodiesel fuel

#### 4.4.2 Brake Specific Fuel Consumption

The variations of brake specific fuel consumption (BSFC) of the test engine run with diesel and biodiesel fuels with respect to loads are shown in Figs.7 & 8, respectively, for all profiles of piston rings under study. It can be seen from the plots that the BSFC reduces continuously with increase in applied load. However, it marginally increases at full load for both the fuels, which is the normal trend in IC engines. It is essential to mention here that the BSFC is considerably lower with the combination of biodiesel fuel and piston ring's face profile design (III) in comparison to the other cases. The BSFC reduces 28 to 34 percent for the combination of new face profile design (III) of piston ring and biodiesel. It is attributed to effective lubrication causing reduction of interface friction with modified face profile design (III) of the piston rings.

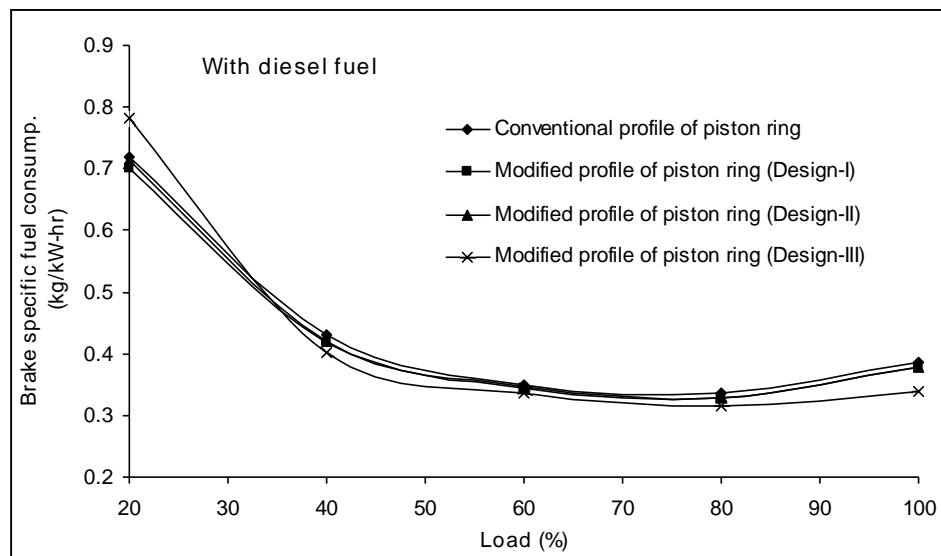


Fig. 4.7 Variation of brake specific fuel consumption with load

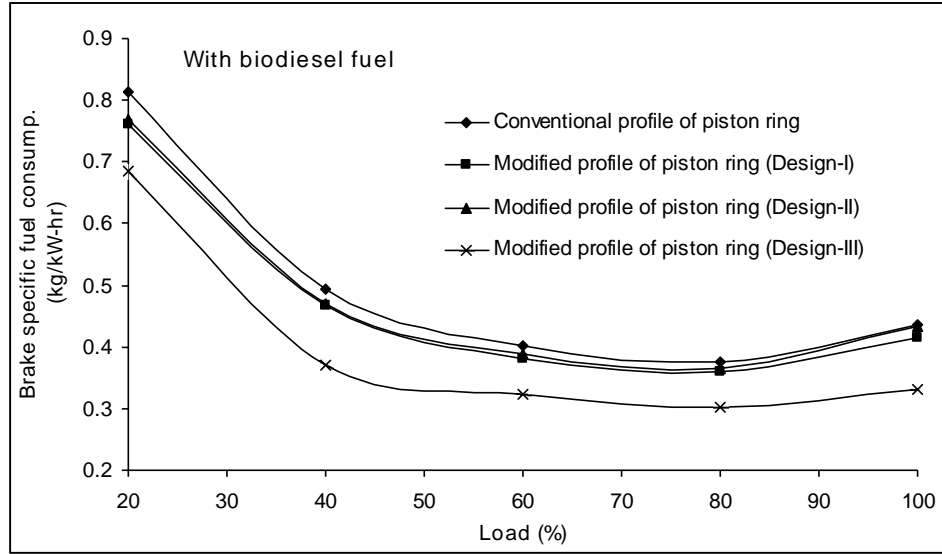


Fig. 4.8 Variation of brake specific fuel consumption with load

#### 4.4.3 Mass Flow Rate

The variations of mass flow rate of diesel and biodiesel fuels with load are illustrated in Figs. 9 & 10, respectively, for four sets of piston rings' face profiles. It can be seen from the graphs that mass flow rate increases continuously with increase in applied load. It is necessary to mention here that mass flow rate is significantly lower with the combination of biodiesel fuel and new face profile design (III) of piston ring in comparison to the other cases. The mass flow rate reduces 28 to 34 percent for the combination of new face profile design (III) of piston ring and biodiesel. Further, it is believed that this happens due to effective lubrication that causes reduction

in interfacial friction and better combustion of biodiesel due to high cetane number.

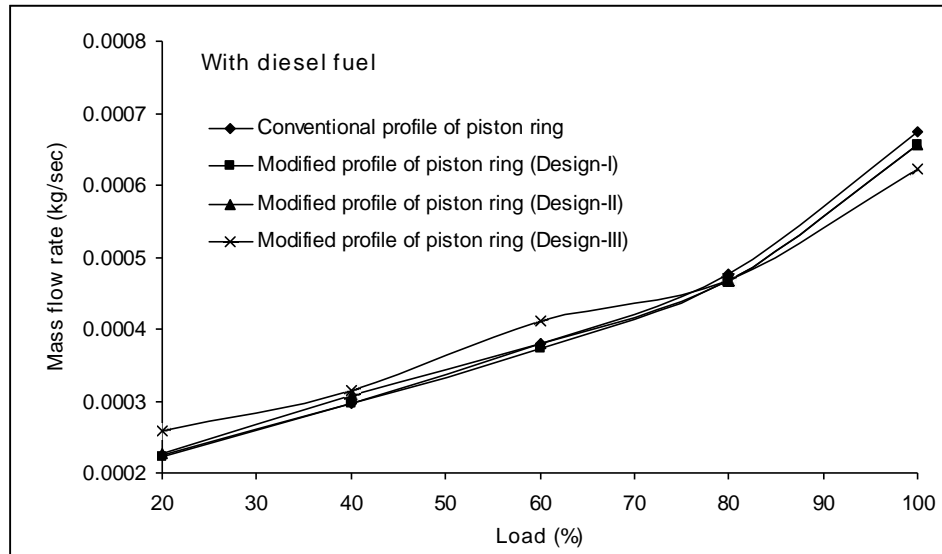


Fig. 4.9 Variation of mass flow rate of diesel with load

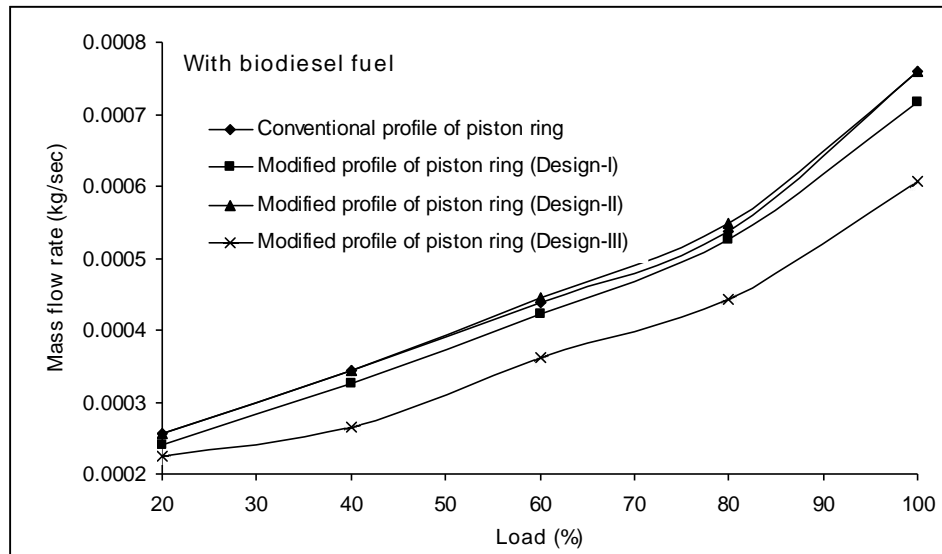


Fig. 4.10 Variation of mass flow rate of biodiesel with load



#### 4.4.4 Carbon Monoxide Emissions

Variations of carbon monoxide emissions with the variation of engine load using modified and conventional piston rings for commercial diesel fuel operation is shown in Fig 4.11 while these variations in biodiesel is shown in Fig. 4.12. As can be seen Figs. 11 & 12, the variation of CO emission up to 60% load is marginal and CO emission remained at very low level for both diesel as well as biodiesel.

In CI engine overall air-fuel ratio remains very lean up to 60% load. Typically the air-fuel ratio varies from 100:1 to about 40:1 during idling to about 60% load. However, it is found that CO emissions increased rapidly when engine has been operated at full load and at 80% load. During these conditions overall air-fuel ratio varies from 40:1 to about 22:1. In these conditions due to combustion mechanism of CI engine local air-fuel ratio may be either overrich or overlean.

In the overrich combustion zone the intermediate product of CO may not oxidized to CO<sub>2</sub> and will escapes to the exhaust when local temperature goes down. It is also found that CO emissions at higher loads in biodiesel operation is lower as compared to commercial diesel operation. This is attributed to oxygen 11% in itself in case of biodiesel Table 4.2.

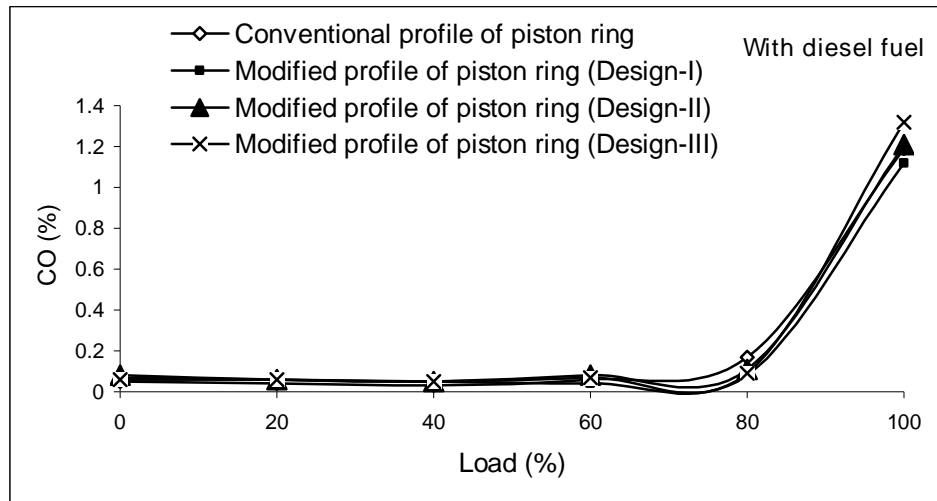


Fig. 4.11 Variation of carbon mono oxide with engine load using diesel fuel

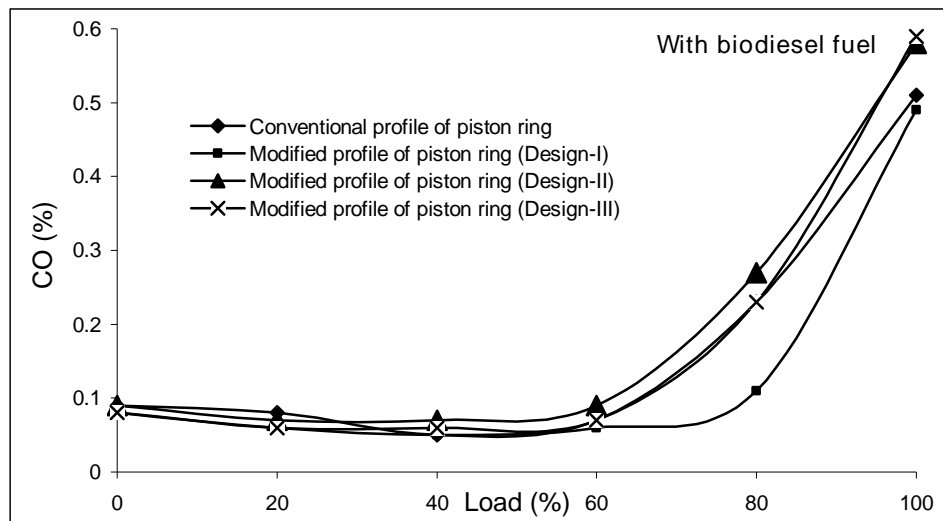


Fig. 4.12 Variation of carbon mono oxide with engine load using biodiesel fuel

#### 4.4.5 CO<sub>2</sub> Emissions

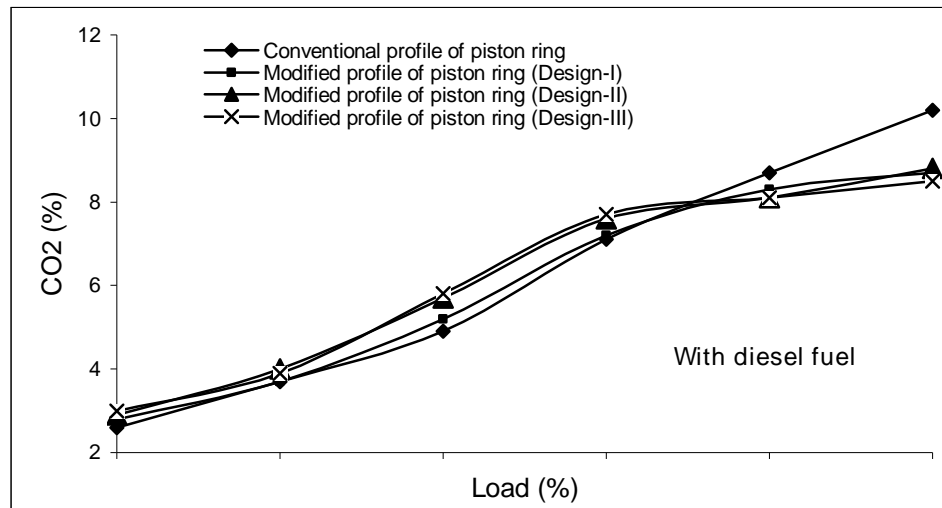


Fig. 4.13 Variation of CO<sub>2</sub> with engine load using diesel fuel

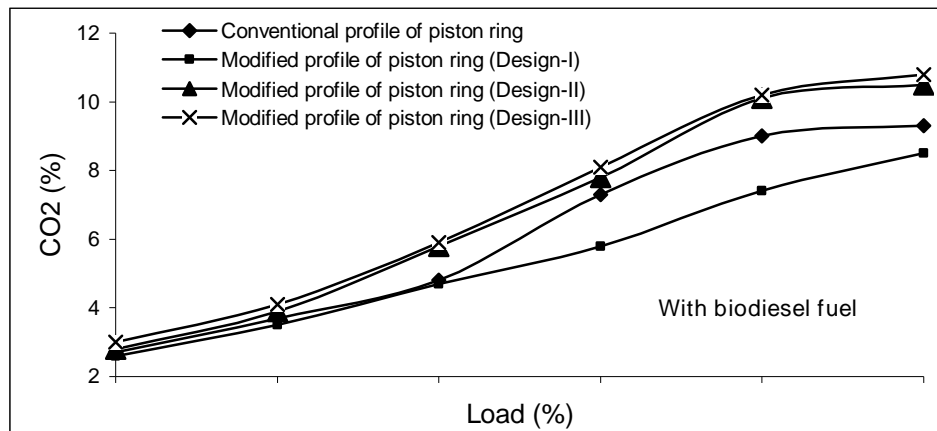


Fig. 4.14 Variation of CO<sub>2</sub> with engine load using biodiesel fuel

The variations of CO<sub>2</sub> emissions are shown in Figs.13 & 14 using diesel and biodiesel. During whole range of engine loading from idle condition to 100% loading in the interval of 20%, the CO<sub>2</sub> emissions for all ring sets are closed. Where as, it has been observed that during 60-100% loading of engine the curve for Design-III set has declined more than other

ring sets and with the diesel it has shown lesser among all sets. So at higher load with Design-III the green house effect is less in comparison to other profiles of piston rings.

#### 4.4.6 NO<sub>x</sub> Emissions

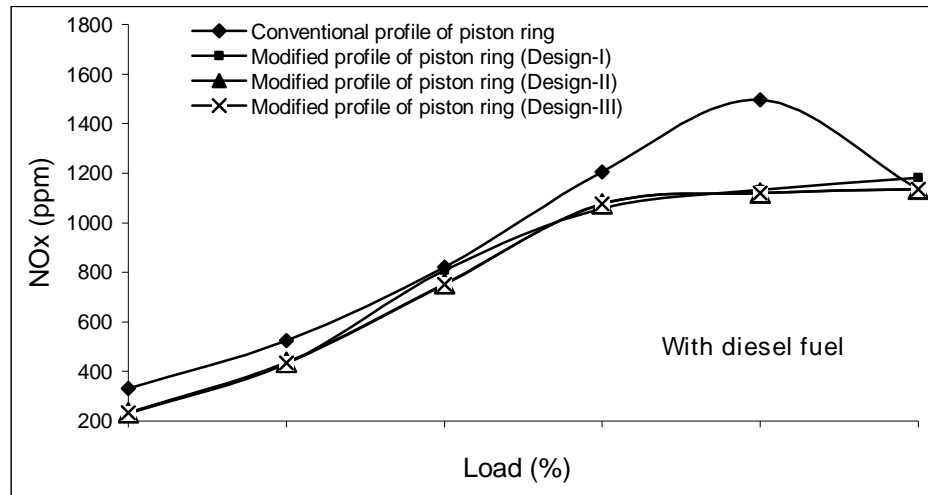


Fig. 4.15 Variation of NO<sub>x</sub> with engine load using diesel fuel

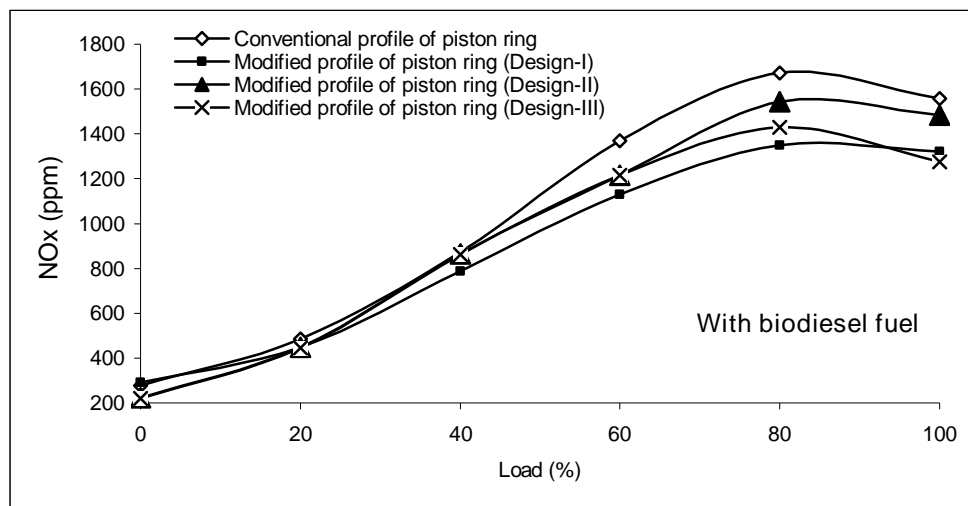


Fig. 4.16 Variation of NO<sub>x</sub> with engine load using biodiesel fuel

The variation of NO<sub>x</sub> emission with the variation to engine load using diesel fuel is shown in Figs 15 & 16. In CI engine temperature increases as load increases. It clearly evident from Figs.15 & 16 that the NO<sub>x</sub> emissions continuously go on increasing with increase of engine load and then decrease. The increase can be attributed to the fact that the chemical kinetics of the reaction leading to high heat release rate and thereby increasing the local temperature. This high temperature is translated into corresponding higher NO<sub>x</sub> emissions. The principal source of NO<sub>x</sub> emission is the oxidation of atmospheric N<sub>2</sub>. However, if the fuel contains significant amount of nitrogen, the oxidation of fuel nitrogen-containing compounds is an additional source of NO<sub>x</sub> emission. Diesel fuel may contain negligible amount of N<sub>2</sub>. However, biodiesel may have little more amount of N<sub>2</sub> in the fuel itself.

As it can be seen from Figs.15 & 16 amount of NO<sub>x</sub> emission increases as fuel increases in both diesel as well as biodiesel. A critical examination of these graphs shows that the level of NO<sub>x</sub> emission is about 7to10% higher in case of biodiesel as compared to commercial diesel. This is attributed to extra NO<sub>x</sub> formation due to higher level of N<sub>2</sub> in biodiesel. A marginal decrease of NO<sub>x</sub> emission at full load as compared to 80% load is also observed for both diesel and biodiesel with the all profiles of piston

rings. Marginal decrease of NO<sub>x</sub> at full load may be due to higher rate of fuel evaporation at the combustion zone at higher loads.

#### 4.4.7 Hydrocarbon Emissions

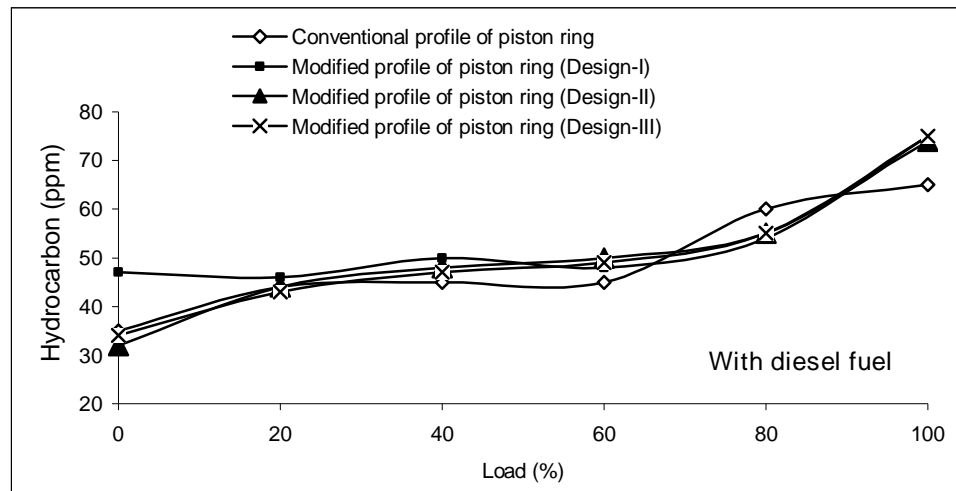


Fig. 4.17 Variation of Hydrocarbon with engine load using diesel fuel

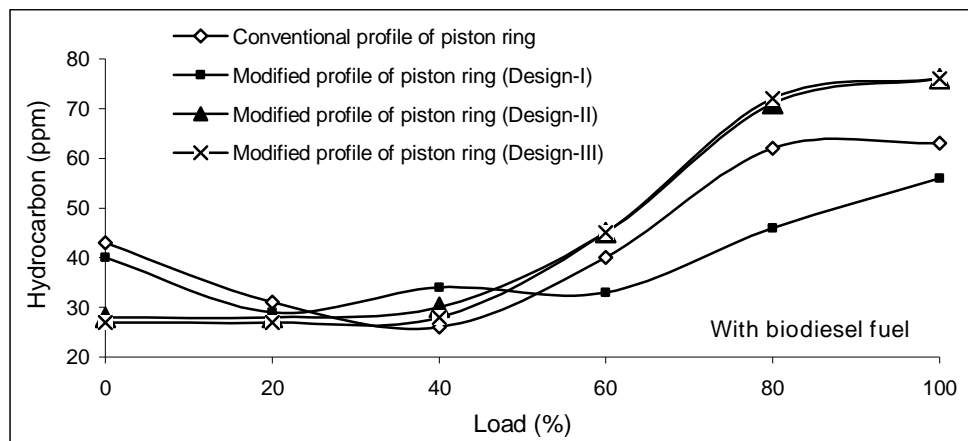


Fig. 4.18 Variation of Hydrocarbon with engine load using biodiesel fuel

In a CI engine the complex heterogeneous nature of combustion where fuel evaporation, fuel-air with burned-unburned gas mixing, and

combustion can occur simultaneously. Also the fuel used in this engine has higher molecular weight and less volatility. Also substantially paralysis of the fuel compounds occurs within the fuel sprays during the combustion process. During uncontrolled and controlled combustion phase there can be locally overlean mixture, locally overrich mixture and some combustible mixture. Therefore, the HC formation is very-very complex phenomena in such cases. However, it is found that HC remains similar in all profile of piston rings when diesel fuel is used as can be seen in Figs.17 & 18. Whereas, in case of biodiesel a large variation of HC emissions with different piston rings profile is observed. This is attributed to lack of evaporation and mixing of biodiesel and air

#### 4.4.8 Smoke Opacity

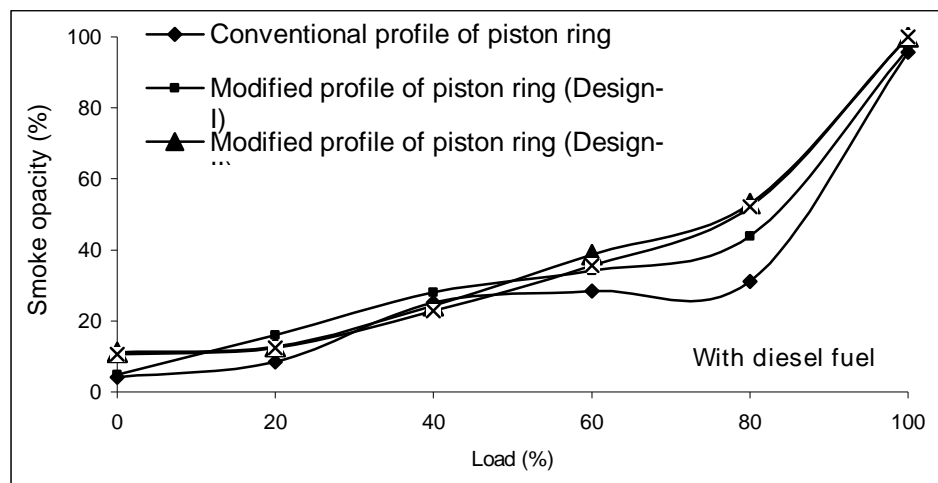


Fig. 4.19 Variation of smoke opacity with engine load using diesel fuel

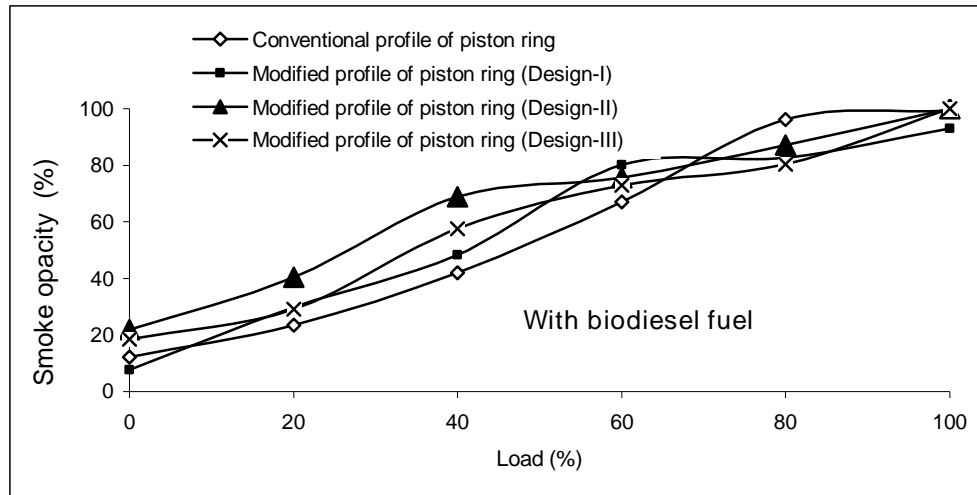


Fig. 4.20 Variation of smoke opacity with engine load using biodiesel fuel

The variation black smoke with different profiles of piston rings is shown in Figs.19 & 20 for commercial diesel and Jatropa based biodiesel respectively. Principally black smokes in CI engines consist of combustion generated carbonaceous material (soot). Sometimes some organic compounds are absorbed on an around soot particles. In most cases soot formation occurs in overrich zones due to lack of oxygen in these pockets. It has been found that the smoke density in case of diesel fuel up to 60% load is half of that of biodiesel fuel. This is attributed to lower viscosity of diesel hence better atomization, vaporization and mixing with hot air. However, smoke density increases at higher loads for both fuels. This is due to rich mixture causing partial combustion of fuel droplets.



## 4.5 Conclusions

The performance characteristics of a commercial diesel engine fueled with diesel and jatropha based biodiesel (B100) have been investigated experimentally using piston rings of new face profiles. Four sets of piston rings, a standard (conventional) and three new designs (I, II and III) have been used in the experiments. The main conclusions drawn from this investigation are:

- q The face profiles of piston rings have considerable impact on BTE and BSFC.
- q The BTE of engine fueled with diesel increases 2 to 8 percent with piston rings of new face profile design (III).
- q The BTE of engine fueled with bio-diesel (B100) enhances 8 to 16 percent with piston rings of new face profile design (III).
- q The BSFC reduces 28 to 34 percent for the combination of piston rings of new face profile design (III) and biodiesel.
- q The specific fuel consumption of biodiesel is lower than that diesel. It may be due to better combustion, high cetane number and inbuilt oxygen in biodiesel which result in better combustion.

- q The variation of CO emission up to 60% load is less and marginal for both diesel as well as biodiesel. CO emissions increased rapidly when engine is operated between 80% load and full load. In combustion zone the intermediate product of CO may not oxidized to CO<sub>2</sub>.
- q The CO emissions at higher loads in biodiesel operation is lower as compared to commercial diesel operation. This is attributed to oxygen 11% in itself in case of biodiesel
- q The CO<sub>2</sub> emissions for all ring sets are closed. Where as, it has been observed that during 60-100% loading of engine the curve for Design-III set has declined more than other ring sets and with the diesel it has shown lesser among all sets. So at higher load with Design-III the green house effect is less in comparison to other profiles of piston rings.
- q The rate of NO<sub>x</sub> emissions continuously go on increasing with increase of engine load and then decrease.
- q The HC remains about 50 ppm and 35 ppm when diesel and biodiesel is used as fuel respectively up to 60% loading of engine in all profile of piston rings. After that large variation i.e. rise have been observed. This is attributed to lack of evaporation and mixing of fuel and air.
- q The smoke density in case of diesel fuel up to 60% load is half of that of biodiesel fuel. This is attributed to lower viscosity of diesel hence better atomization, vaporization and mixing with hot air. However, smoke

density increases at higher loads for both fuels. This is due to rich mixture causing partial combustion of fuel droplets.

The findings of the study have been found very encouraging and it is envisaged that industrial application of results of present work may be useful in saving and conservation of the fuels.

\*\*\*\*\*

## Chapter 5

### Experimental Studies for Role of Surface Dimpling on the Performance of Lubricated Sliding Contact

---

This chapter incorporates the experimental studies carried out using a pin-on-disk tribometer for assessing the role of surface dimpling on the tribological performance of the lubricated sliding contacts. This study has been done in order to explore the role of surface dimpling/texturing on friction and wear behaviors of sliding contacts. Accordingly, to manufacture the texturing/dimpling in future (for future studies) on the face profile of piston rings for further improving the tribological performance of interfaces formed between piston ring and cylinder liner.

#### 5.1 Background

Surface texturing technology has recently been explored in the tribology field as a method for reducing the friction and improving the lubrication characteristics of various mechanical components. Several researchers [70-78] have demonstrated the potential benefits of modifying the topography of surfaces in the tribological contacts. The performance benefits of surface texturing/dimpling reported in the papers include: reduced friction, higher load bearing capacity, decreased surface damage, and increased service life. The mechanisms responsible for the improved performances of tribo-contacts are subjected to type of the applications and

operating conditions in which surface texturing are utilized. For conditions involving surface-to-surface contact, the presence of wear debris particles can be very detrimental to friction and wear behavior [79]. It was demonstrated that these particles can be removed from the contacting surfaces and trapped in surface depressions and undulations [80-81]. The presence of certain texture features may also benefit some lubricated systems by acting as reservoirs (storing valley) and supplying the lubricant directly at the interfaces [82-83]. Moreover, some well-designed texture features may also benefit the performance of the lubricant by boosting the hydrodynamic pressure [84-85]. The characteristic feature of textured surfaces for the purpose of improving tribological performance is that of micro sized depressions in the forms of grooves/dimples.

It is worth mentioning here that honing is one such surface texturing techniques, which is used as a finishing machining process for cylinder bores for IC engines. The micro grooved surface features that result from this process were shown to improve the lubrication action between the cylinder wall and piston rings. A more detailed study investigating the influence of micro grooved or dimpled surfaces, like those presented previously, reveals that the dimensions and layout of the features need to be precisely controlled in order to optimize the performance. Typical dimensions of the micro depression in these studies are 2–10  $\mu\text{m}$  depth, 50–

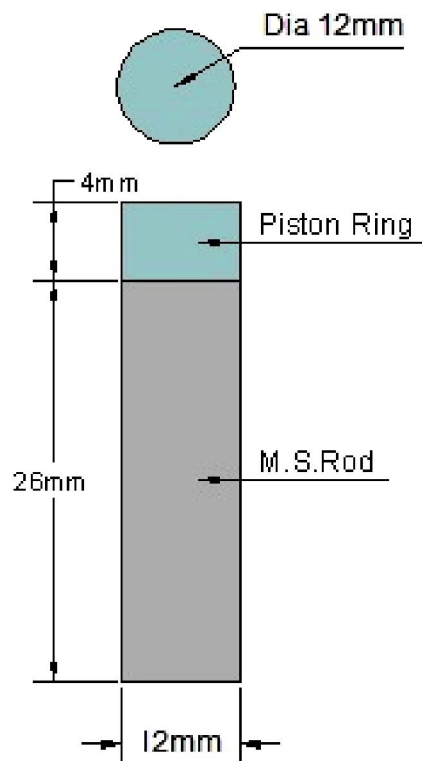
600  $\mu\text{m}$  width, and 2–50% area coverage ratio. To generate surface features with micrometer precision, several micro texturing techniques have been utilized [86, 87]. Literature reveals that chemical etching has been used economically to locally dissolve the surface material of tribo-elements for fabricating the micro /sub micro sized dimples.

Based on the literature review, it is observed that no work has been reported for the role of dimple sizes (varying 200-400  $\mu\text{m}$ ) on the tribological performances of the sliding contacts. It is essential to mention here that fabrications of such sizes of dimples will be economical if with these types of dimples improved tribological results are achieved.

## 5.2 Fabrication of pin and dimples on discs

Cylindrical mild steel pin (C-50) of diameter 12 mm has been chosen for conducting the experiments using a pin-on-disk tribometer. Geometrical features of the pin (sample material) and tribometer can be seen in Fig. 5.1 and Fig. 5.2, respectively. Dimples distributions on the discs' area have been prepared in CATIA commercial software as per the details explained in Figs. 3 and 4. Appendix-2 also provides the dimples related details on the disc. Print outs of the dimple models are used to prepare the templates for the chemical etching process. Dimpling has been done on disc plates made of steel (C-50) having approximately surface finish of the order of 0.2 $\mu\text{m}$ . Circular micro-dimples of 420  $\mu\text{m}$  diameter and depth of 200 - 250  $\mu\text{m}$  are

prepared. Total four pitches (1, 2, 3, 4 mm) have been used in fabrication of dimples on discs. The distributions of the dimples start from reference line for the first circumferential distance of the set of three consecutive dimples. For the second circumferential distance in the same set of three radial distances, dimpling starts from second angle. The third circumferential distance corresponding to third radial distance in the same set, dimple starts from third angle. In this way all the circumferential distance corresponding to set of three radial distances are formed by dimples. This forms the spiral pattern of dimpling on the discs (steel plate of 165 mm diameter and 8 mm thickness). Photographic view of a dimpled disc plate is shown in Fig. 5.5.



(a) Dimension of the pin



(b) Photographic view of pin

Fig.5.1 Details of pin used in the experiments

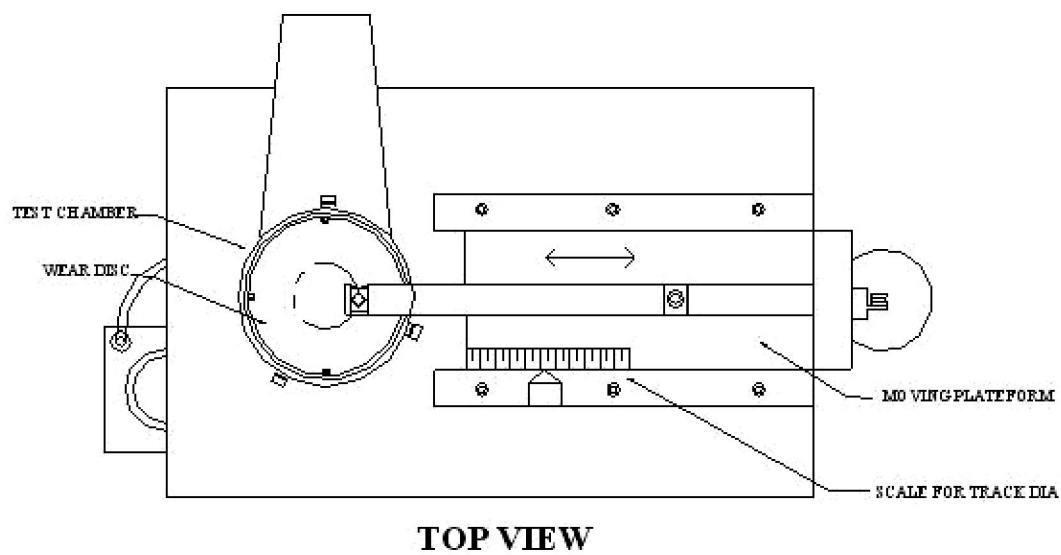
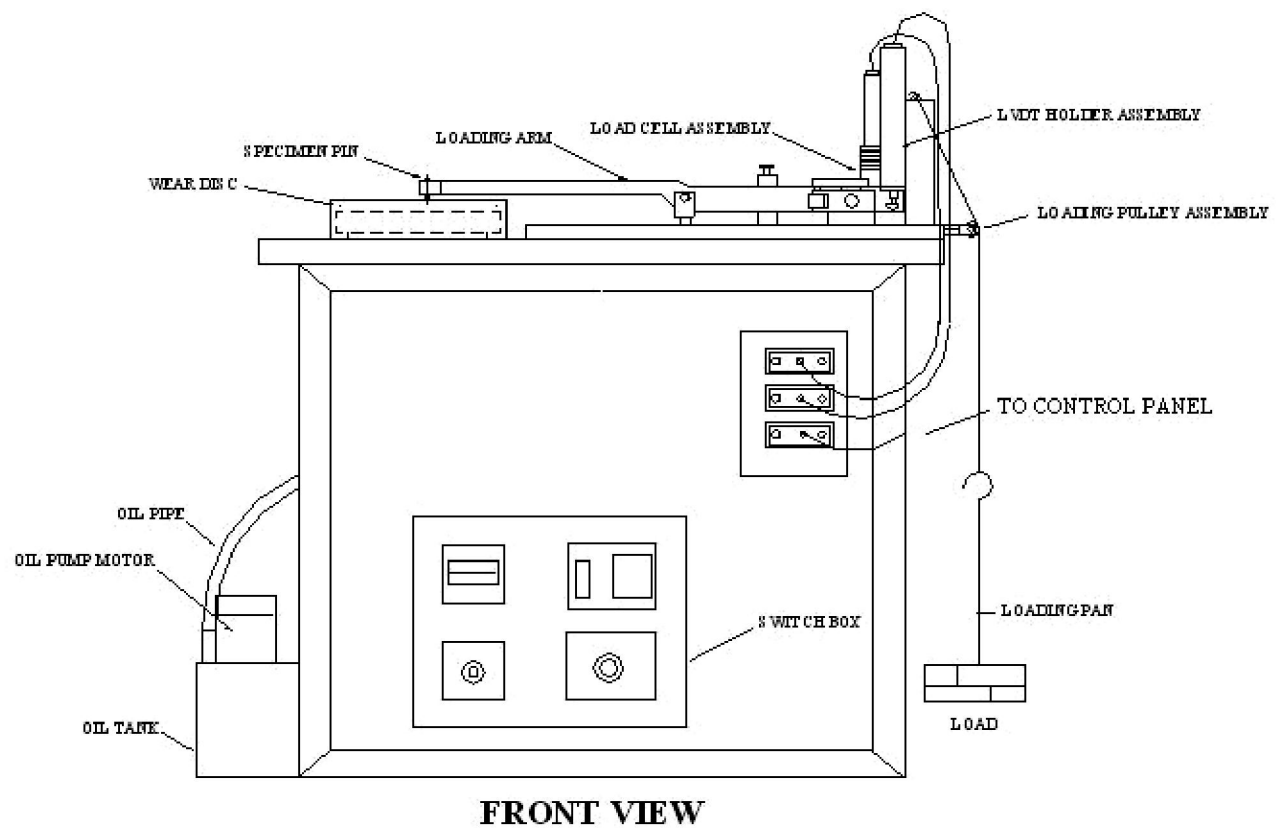


Fig. 5.2 Schematic diagram of pin-on disc tribometer



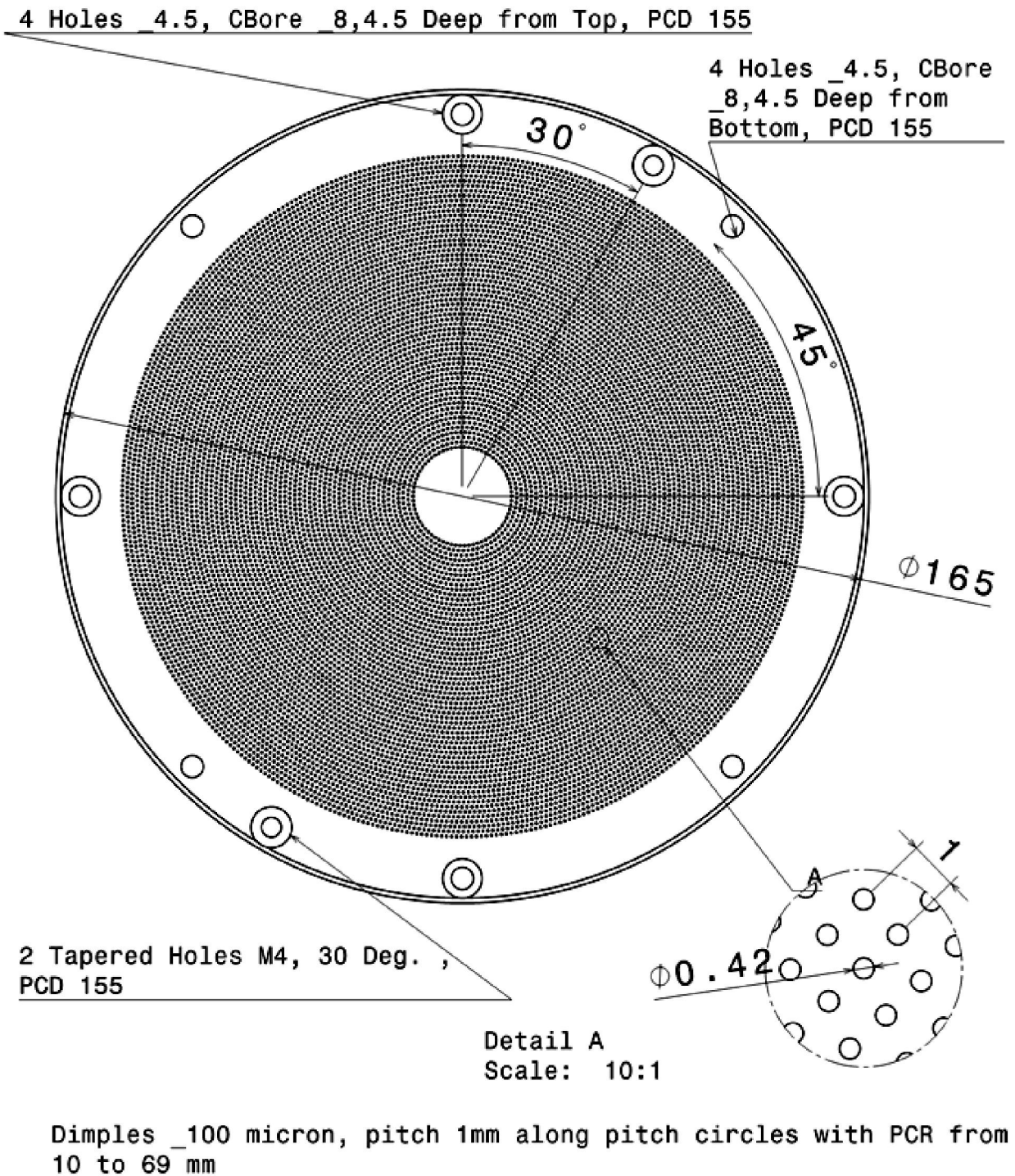
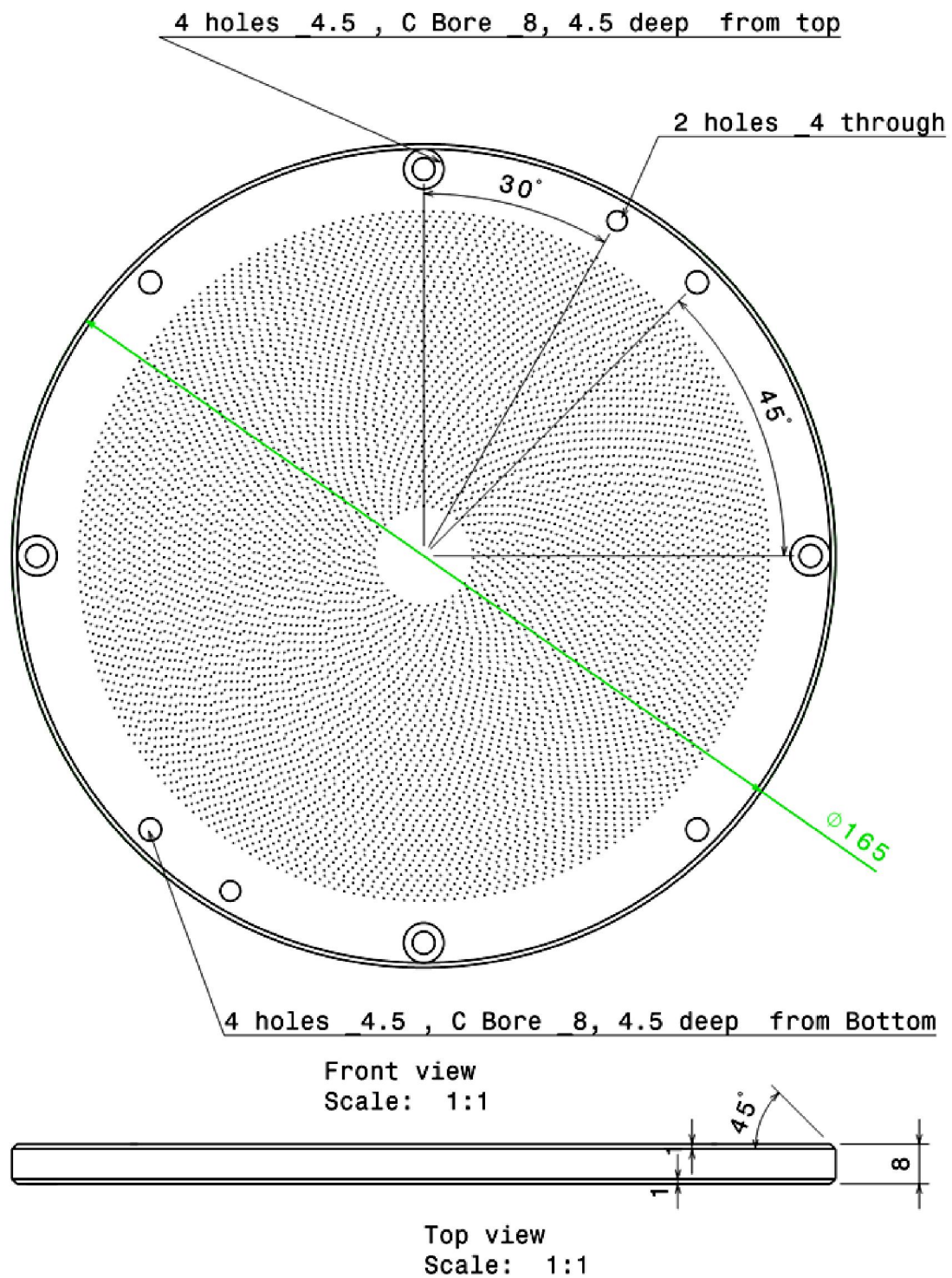


Fig. 5.3 Schematic diagrams of dimples on the disc



Dimples 100 micron , pitch 2mm along pitch circles with PCR from 10 to 69 mm.

Fig. 5.4 Orthographic views of the disc

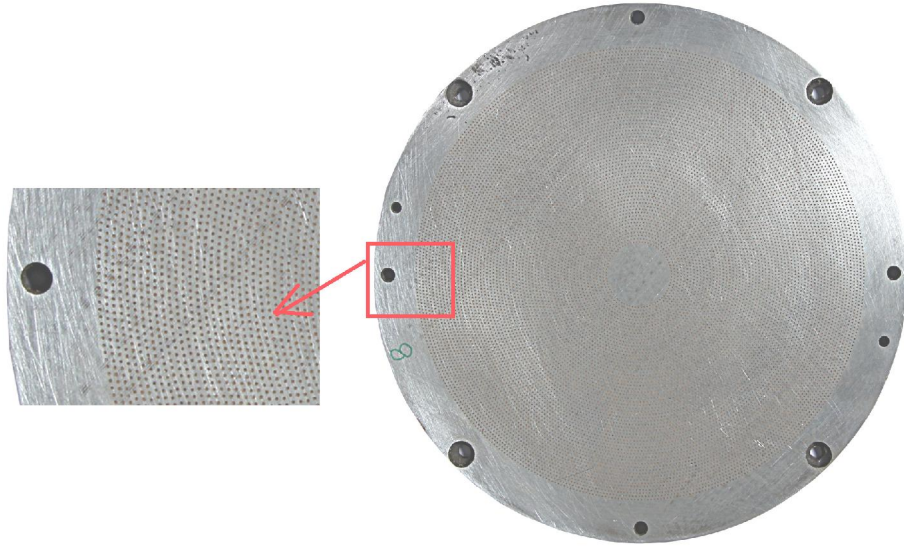


Fig. 5.5 Photographic view of a dimpled disc plate (C-50)

### 5.3 Experimentation

Experiments have been carried out on a pin-on-disc tribometer (refer Fig. 5.2). The ranges of parameters specified for the tribometer are provided in Table 5.1. Moreover, the some vital properties of the lubricating oil (used in the experiments) are listed in Table 5.2.

Table 5.1 Some specific parameters for tribometer

S. No.	Parameter	Numerical values
1	Pin diameter, mm	3,4,6,8,10 & 12
2.	Disc diameter, mm	165
3.	Thickness of disc, mm	8
4.	Speed, RPM	200 - 2000
5.	Friction force (tangential force), N	up to 200
6.	Applied normal load at the contact, N	up to 300

Table 5.2 Properties of lubricating oil (20W40)

S. No.	Property	Numerical value
1	Density, kg/m <sup>3</sup>	890
2	Specific gravity	0.8912
3	Dynamic viscosity, Pa-s	0.1075

It is essential to mention here that the tribological studies (friction and wear measurements) have been carried out for the loads characterized by the contact pressure varying in the range of 0.4 - 1.4 MPa at sliding speeds 0.5 - 10 m/s. Figure 5.6 illustrates the photographic views of dimpled discs after the experiments. It shows wear tracks.



Fig. 5.6 Photographic views of the dimpled discs after conducting the experiments

#### 5.4 Results and discussions

In order to access the role of dimples' pitches on the tribological behaviors of the sliding contacts, a set of experiments have been performed for studying the variation of coefficient of friction as function of dimple pitch. A plain and four dimpled discs (having pitches 1, 2, 3, and 4 mm) have been employed in the experiments. These studies have been performed by applying 120N load at 500 rpm. The track diameter on the disc has been kept 110 mm for the pin diameter of 12 mm. Variation of friction coefficient can be seen in Fig. 5.7. It can be noticed from this figure that friction coefficient reduces significantly at 1 mm value of dimple pitch in comparison to other cases. Thus, it was planned to perform the experiments with the disc having dimples of 1 mm pitch.

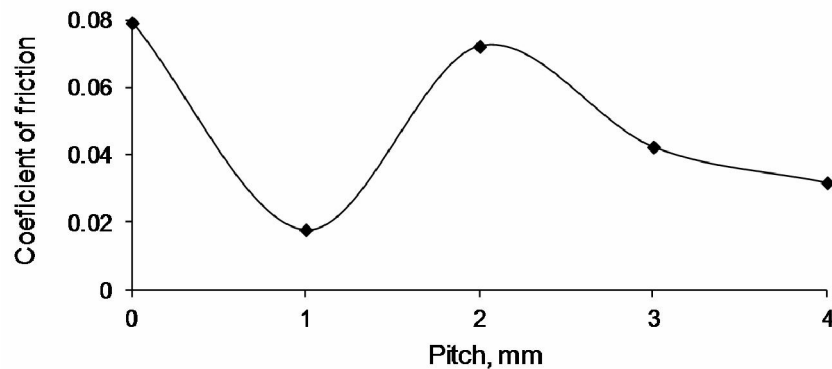


Fig. 5.7 Coefficient of friction variation with pitches of the dimples  
[Load= 118 N, Speed=500 rpm, Test duration = 40 minutes]

It is vital to mention here that while performing the experiments (results reported in Fig. 5.8) only in the beginning lubricant was spread over



the surface of the discs i.e. no lubricant was spread on the disc during the experiments. The experiments have been conducted for 40 minutes test duration at each speed by keeping the load constant i. e. 120N. For this case of experimental study, the variation of coefficient of friction with speed has been given in Fig. 5.8. It can be seen from this figure that coefficient of friction initially decreases and thereafter it increases linearly with speed. Corresponding to this study the wear (material loss from pin) has been plotted in Fig. 5.9. Negligible wear can be noticed from this curve. However, at the elevated speeds (after 1500 rpm), drastic increase in wear can be seen. It is believed that this happened due to metallic contact at high speeds due to large viscous heat dissipation in the interfacial lubricating film.

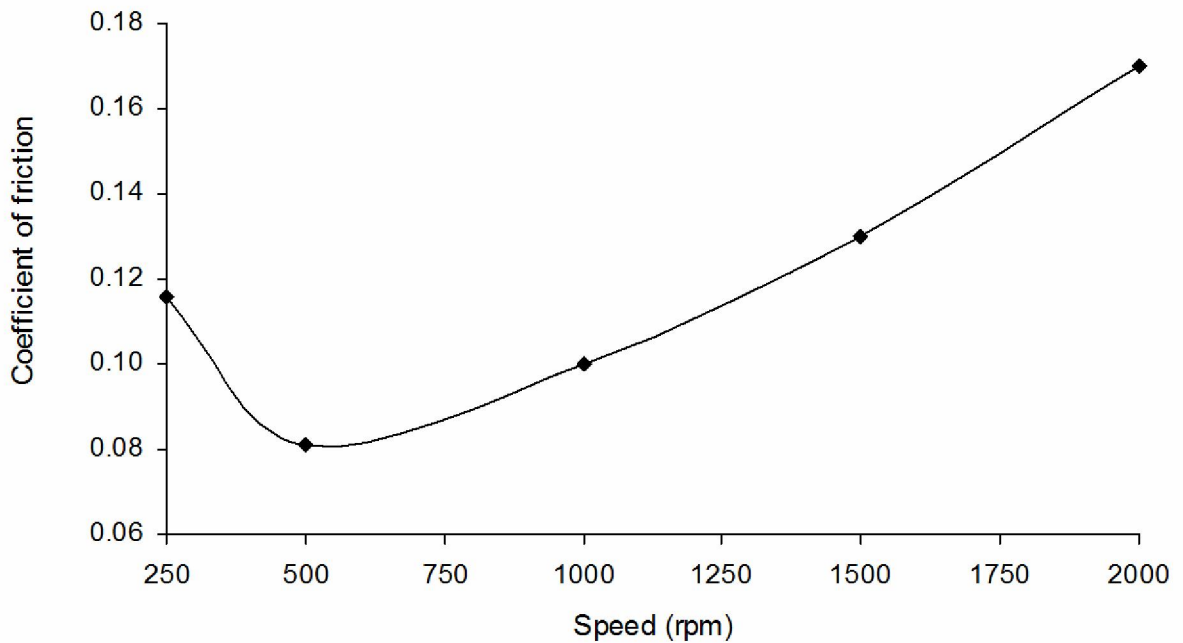


Fig. 5.8 Variation of coefficient of friction with speed (Mixed regime)  
[Load= 120 N, Test duration = 40 minutes, Pitch= 1mm]

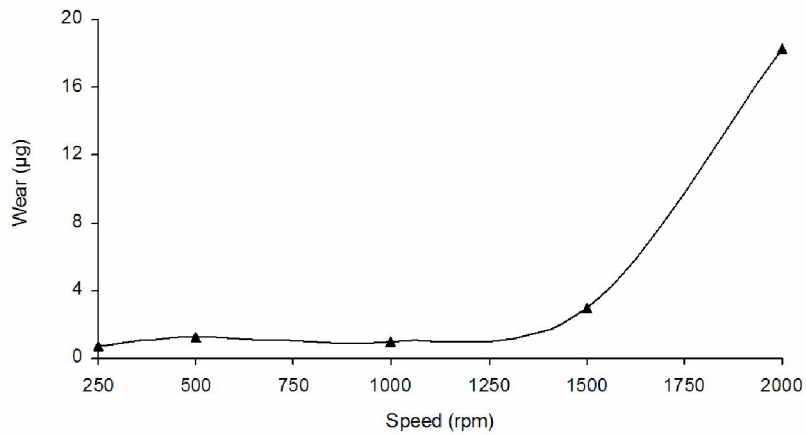


Fig. 5.9 Variation of wear (mass loss of pin) with speed (Mixed regime)  
[Load= 120 N, Test duration = 40 minutes, Pitch= 1mm]

A variation in coefficient of friction with respect to load is shown in Fig. 5.10 at the speed of 1000 rpm. Coefficient of friction decreases with increase in the load up to 135 N. Thereafter, friction enhances with increase in the load. Moreover, wear (mass loss of pin) continuously enhances up to 100 N, thereafter it starts reducing with increase in the load at the contact (refer Fig. 5.11). This trend does not provide a meaningful correlation between friction and wear.

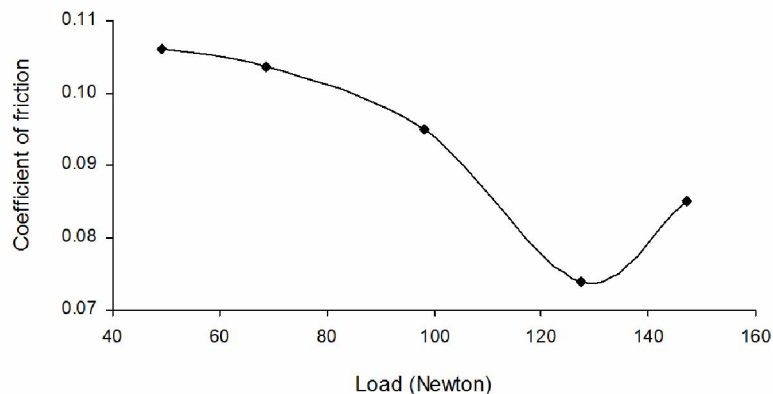


Fig. 5.10 Variation of coefficient of friction with load (Mixed regime)

[Speed=1000 rpm, Test duration = 40 minutes, Pitch= 1mm]

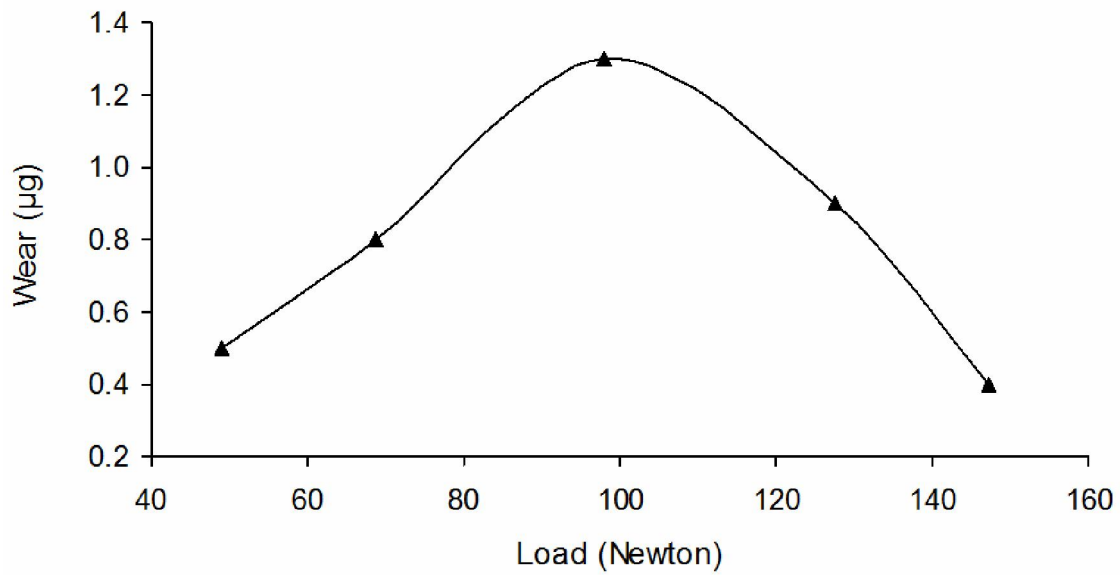


Fig. 5.11 Variation of wear with load (Mixed regime)

[Speed=1000 rpm, Test duration = 40 minutes, Pitch= 1mm]

The results of friction and wear variations reported in the Figs. 5.12 to 5.14 correspond to the continuous supply of lubricant (Fully flooded) at the interfaces of pin and disc. For this study also the load has been kept constant and the speed has been varied and vice-versa. It can be seen from the Fig. 5.12 that coefficient of friction continuously decreases with increase in the speed. Moreover, wear (weight loss of pin material) variation with increase in speed is presented in Fig.5.13. The wear of pin increases at low speed (up to 500 rpm), thereafter it decreases continuously. It is believed that this happens due to fully developed hydrodynamic lubrication at the elevated speeds.



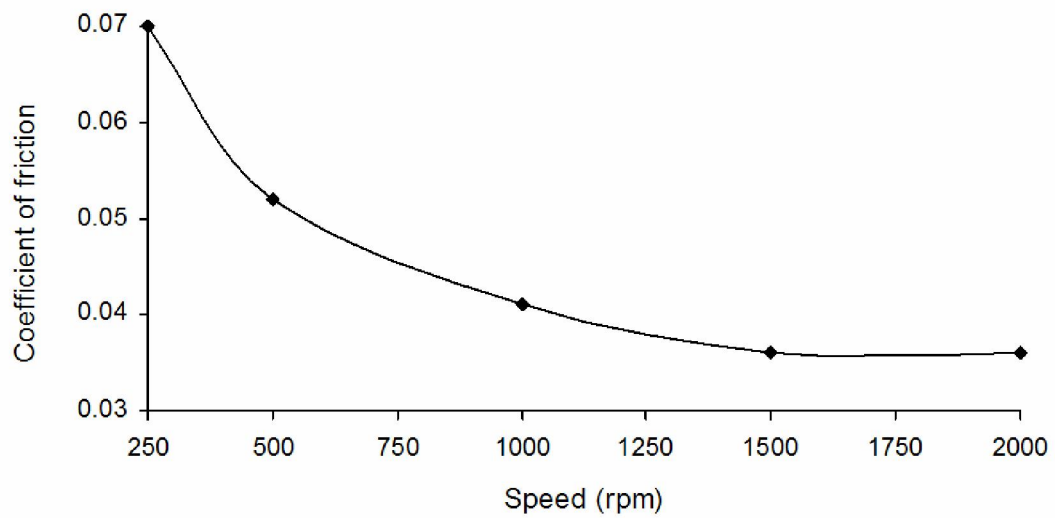


Fig. 5.12 Variation of coefficient of friction with speed (Fully flooded)  
[Load= 120 N, Test duration = 40 minutes, Pitch= 1mm]

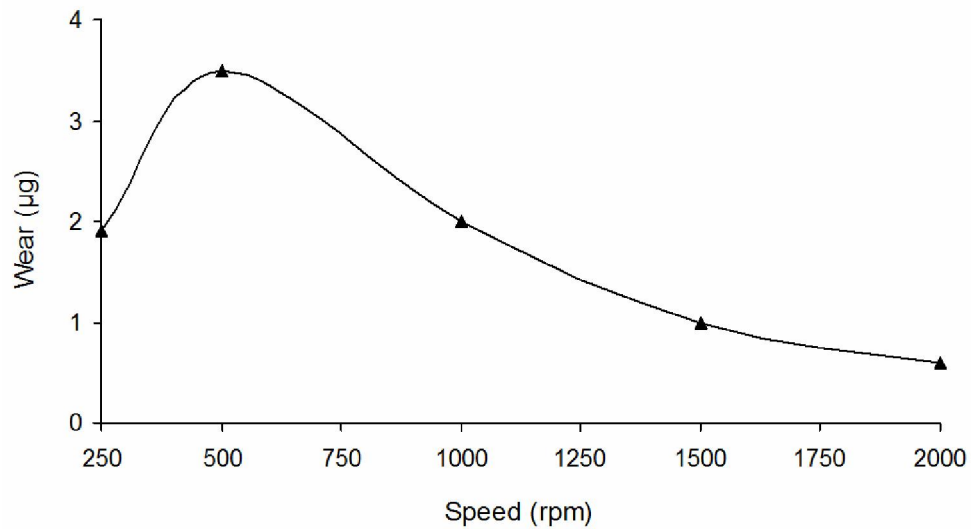


Fig. 5.13 Variation of wear with speed (Fully flooded)  
Load= 120 N, Test duration = 40 minutes, Pitch= 1mm]

Figures 5.14 and 5.15 present the results of friction and wear variations, respectively, as function of load. The experiments have been

carried out by keeping the speed constant 1000 rpm at 110 mm tract diameter on the disc. It has been observed that the coefficient of friction initially increases at low load but after that continuously decreases. Moreover, the trends of friction and wear variations appear similar. It is believed that this happens due to thick film formation leading to more frictional losses at light loads. However, with increase in the load, the reduction in film thickness takes place that might be yielding less coefficient of friction up to load of 130 N. Thereafter, friction increases due to commencement of metallic contacts at elevated loads.

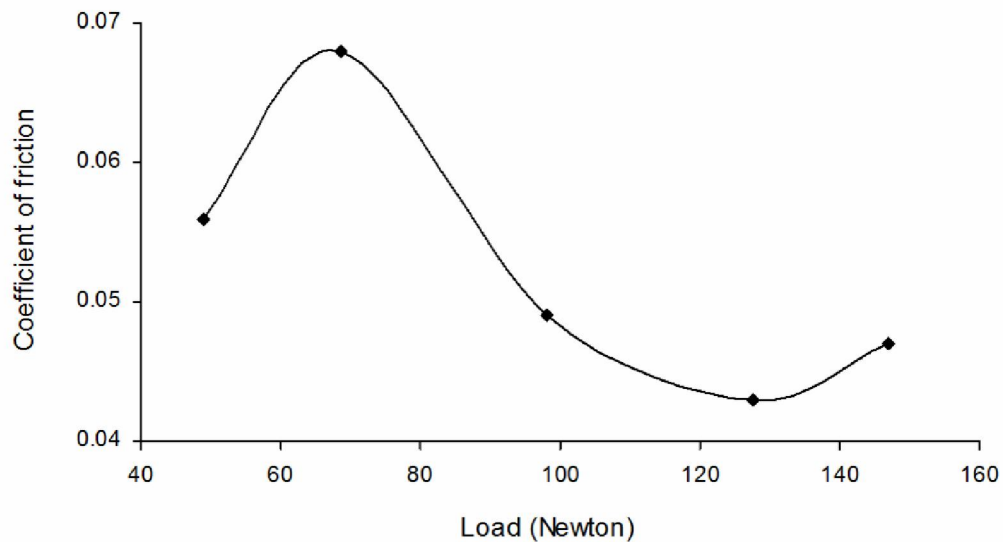


Fig. 5.14 Variation of coefficient of friction with load (Fully flooded)  
[Speed=1000 rpm, Test duration = 40 minutes, Pitch= 1mm]

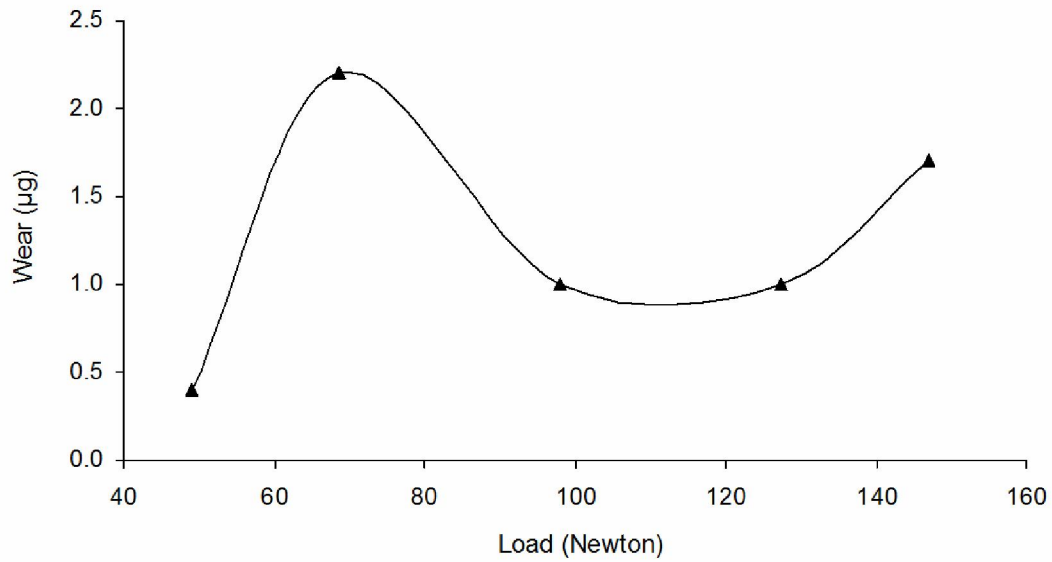


Fig. 5.15 Variation of wear with load (Fully flooded)  
[Speed=1000 rpm, Test duration = 40 minutes, Pitch= 1mm]

## 5.5 Conclusions

Based on the experimental studies reported in this chapter, it has been observed that micro-dimple area density play vital role in dictating the tribological behaviors of the sliding contacts. In presence of dimples, the coefficient of friction reduces significantly in comparison to plain surface disc plate. Thus, micro-dimples can be fabricated on the face of the piston rings for study of the performance of IC engines incorporating the vibration and noise of the engines.

\*\*\*\*\*

# Chapter 6

## Conclusions and Suggestions for Future Study

---

This thesis incorporates the works concerning the numerical modeling of the hydrodynamic lubrication at the interface formed between the piston ring and cylinder liner for assessing the energy efficient single continuous face profile of the piston rings. Moreover, fabricating the best face profile (exponential) on the piston rings of an IC engine, experiments have been carried out for the investigations of the fuel consumptions (diesel and Jatropha based biodiesel) and emissions. Significant results achieved from the mathematical model presented in chapters 3 and experimental results of chapters 4 and 5 are discussed herein. The conclusions of this thesis are grouped under three subtitles as described below.

### 6.1 Conclusions

The major conclusions of the studies reported in this thesis are as follows:

#### 6.1.1 Mathematical Model of Thermohydrodynamic Lubrication of Interface

- Four single continuous surface profiles (Catenoidal, Cubic, Exponential, and Parabolic) have been investigated for their suitability as energy efficient face profile of the piston ring for IC engines.
- Parabolic face profile of piston ring produces high frictional losses at the lubricated interface.

- Exponential face profile of the piston ring yields best result in terms of less power loss at the lubricated interface in comparison to other profiles under present investigation.
- Influence of viscous heat dissipation (thermal effects) on the performance parameters is generally low.

#### 6.1.2 Experiments with Exponential Face Profile of Piston Rings

- The performance characteristics of a commercial diesel engine fueled with diesel and jatropha based biodiesel (B100) have been investigated experimentally using piston rings of new face profiles.
- Four sets of piston rings, a standard (conventional) and three new designs (I, II and III) have been used in the experiments.
- The face profiles of piston rings have considerable impact on BTE and BSFC.
- The BTE of engine fueled with diesel increases 2 to 8 percent with piston rings of new face profile design (III).
- The BTE of engine fueled with biodiesel (B100) enhances 8 to 16 percent with piston rings of new face profile design (III).
- The BSFC reduces 28 to 34 percent for the combination of piston rings of new face profile design (III) and biodiesel.
- The specific fuel consumption of biodiesel is lower than that diesel. It may be due to better combustion, high cetane number and inbuilt oxygen in biodiesel which result in better combustion.
- Emissions are reducing considerably with exponential face profile of piston rings irrespective of the fuels used in the experiments on IC engine.

### 6.1.3 Tribological Studies with Dimpled Surface

- Pin-on-disc tribometer is employed to study the tribological role of surface dimpling.
- Micro-dimple area density play vital role in reducing the coefficient of friction at interface in boundary/mixed lubricating conditions.
- Coefficient of friction first decreases then increases with increase in sliding speed whereas wear remains constant.
- In hydrodynamic lubrication condition, the coefficient of friction continuously decreases with increase in the sliding speed.

### 6.2 Suggestions for Future Study

The study reported in this thesis may be extended in the following ways:

- By accurate manufacturing of the exponential face profile over the face of piston rings, rigorous experiments are required for assessing the performance parameters and wear of new face profile over long interval of time (500 – 1000 hours).
- Dynamic modeling of piston and piston ring (with new face profile) is needed.
- Theoretical and experimental studies with optimized surface dimpling on the face of the piston ring are required.

\*\*\*\*\*

## References

---

- [1] S. C. Tung, M. McMillan, "Automotive Tribology Overview of Current Advances and Challenges for the Future," *Tribology International*, Vol. 37, 2004, PP. 517-536.
- [2] <http://www.aalcar.com> dated 01/08/2012
- [3] <http://www.sacskyranch.com> dated 01/08/2012
- [4] K. Wannatong, S. Chanchaona, S. Sanitjai, "Simulation Algorithm for Piston Ring Dynamics," *Simulation Modeling Practice and Theory*, Vol. 16, 2008, PP. 127-146.
- [5] P. Jost, J. Schofield, "Energy Savings through Tribology: A Techno-economic Study," *Proceedings of Institution of Mechanical Engineers*, Vol. 195, 1981, PP. 151-173.
- [6] C. M. Taylor, "Automobile Engine Tribology – Design Considerations for Efficiency and Durability," *Wear*, Vol. 221, 1998, PP. 1-8.
- [7] D. E. Richardson, "Review of Power Cylinder Friction for Diesel Engines," *Transactions of the ASME, Journal of Engineering for Gas Turbines and Power*, Vol. 122, 2000, PP. 506-519.
- [8] R. L. Taylor, R. C. Coy, "Improved Fuel Efficiency by Lubricant Design: A Review," *Proceedings of the Institution of Mechanical Engineers, Journal of Engineering Tribology, Part-J*, Vol. 214, 2000, PP.1-15.
- [9] S. Korcek, R. K. Jensen, M. D. Johnson, J. Sorab, "Maximizing the Fuel Efficiency of Engine Oils: the Role of Tribology," *Tribotest*, Vol. 7, 2001, PP. 187-201.
- [10] E. P. Becker, "Trends in Tribological Materials and Engine Technology," *Tribology International*, Vol. 37, 2004, PP. 569-575.

- [11] K. Holmberg, P. Andersson, A. Erdemir, "Global Energy Consumption due to Friction in Passenger Cars," *Tribology International*, Vol. 47, 2012, PP. 221-234.
- [12] L. L. Ting, J. E. Mayer, "Piston Ring Lubrication and Cylinder Bore Wear Analysis: Part I – Theory," *Transactions of the ASME, Journal of Lubrication Technology*, Vol. 96, 1974, PP. 305-314.
- [13] P. C. Nautiyal, S. Singhal, J. P. Sharma, "Friction and Wear Processes in Piston Rings," *Tribology International*, Vol.16, 1983, PP. 43-49.
- [14] D. P. Hoult, "Lubrication and Support of a Single Piston Ring," *ASLE Transactions*, Vol. 28, 1984, PP. 139-149.
- [15] I. Sherrington, E. H. Smith, "Experimental Methods for Measuring the Oil Film Thickness between the Piston Rings and Cylinder wall of internal combustion Engines," *Tribology International*, Vol.18, 1985, PP. 315-320.
- [16] Y. Wakuri, T. Hamatake, M. Soejima, T. Kitahara, "Piston Ring Friction in Internal Combustion Engines," *Tribology International*, Vol. 25, 1992, PP. 299-308.
- [17] K. P. Oh, P. K. Goenka, "Elastohydrodynamic Lubrication of Piston Skirts," *Transactions of the ASME, Journal of Tribology*, Vol. 109, 1987, PP. 356-362.
- [18] G. K. Miltsios, D. J. Patterson, T. C. Papanastasiou, "Solution of the Lubrication Problem and Calculation of the Friction Force on the Piston Rings," *Transactions of the ASME, Journal of Tribology*, Vol. 111, 1989, PP. 635-642.
- [19] W. L. Blair, D. P. Hoult, V. W. Wong, "The Role of Piston Distortion on Lubrication in a Reciprocating Engine," *Transactions of the ASME, Journal of Engineering for Gas Turbines and Power*, Vol. 112, 1990, PP. 287-301.
- [20] D. C. Sun, "A Subroutine Package for Solving Slider Lubrication Problems," *Transactions of the ASME, Journal of Tribology*, Vol. 112, 1990, PP. 84-91.



- [21] R. S. Paranjpe, "Analysis of Non-Newtonian Effects in Dynamically Loaded Finite Mass Conserving Cavitation," Transactions of the ASME, Journal of Tribology, Vol. 114, 1992, PP. 736-746.
- [22] Y. -R. Jeng, "Theoretical Analysis of Piston-Ring Lubrication Part I – Fully Flooded Lubrication," Tribology Transaction, Vol. 35, 1992, PP. 696-706.
- [23] Y. -R. Jeng, "Theoretical Analysis of Piston-Ring Lubrication Part II – Starved Lubrication and Its Application to a Complete Ring Pack," Tribology Transaction, Vol. 35, 1992, 4, PP. 707-714.
- [24] D. Zhu, H. S. Cheng, T. Arai, K. Hamai, "A Numerical Analysis for Piston Skirts in Mixed Lubrication – Part I: Basic Modeling," Journal of Tribology, Vol. 114, 1992, PP. 553-562.
- [25] D. Zhu, H. S. Cheng, T. Arai, K. Hamai, "A Numerical Analysis for Piston Skirts in Mixed Lubrication – Part II: Deformation Considerations," Transactions of ASME, Journal of Tribology, Vol. 115, 1993, PP. 125-133.
- [26] Y. Hu, H. S. Cheng, T. Arai, Y. Kobayashi, S. Aoyama, "Numerical Simulation of Piston Ring in Mixed Lubrication – A Non-axisymmetrical Analysis," Transactions of the ASME, Journal of Tribology, Vol. 116, 1994, PP. 470-478.
- [27] Z. Dursunkaya, R. Keribar, V. Ganapathy, "A Model of Secondary Motion and Elastohydrodynamic Skirt Lubrication," Transactions of the ASME, Journal of Tribology, Vol. 116, 1994, PP. 777-785.
- [28] D. J. Radakovic, M. M. Khonsari, "Heat Transfer in Thin-Film Flow in the Presence of Squeeze and Shear Thinning: Application to Piston Rings," Transactions of the ASME, Journal of Heat Transfer, Vol. 119, 1997, PP. 249-257.
- [29] J. T. Sawicki, B. Yu, "Analytical Solution of Piston Ring Lubrication using Mass Conserving Cavitation Algorithm," Tribology Transactions, Vol. 43, 2000, PP. 419-426.
- [30] O. Akalin, G. M. Newaz, "Piston Ring-Cylinder Bore Friction Modeling in Mixed Lubrication Regime: Part I – Analytical Results,"

Transactions of the ASME, Journal of Tribology, Vol. 123, 2001, PP. 211-218.

- [31] O. Akalin, G. M. Newaz, "Piston Ring-Cylinder Bore Friction Modeling in Mixed Lubrication Regime: Part II – Correlation With Bench Test Data," Transactions of the ASME, Journal of Tribology, Vol. 123, 2001, PP. 219-223.
- [32] R. Rabute, T. Tian, "Challenges Involved in Piston Top Ring Designs for Modern SI Engines," Transactions of the ASME, Journal of Engineering for Gas Turbines and Power, Vol. 123, 2001, PP. 448-460.
- [33] Y. Harigaya, M. Suzuki, F. Toda, M. Takiguchi, "Analysis of Oil Film Thickness and Heat Transfer on a Piston Ring of a Diesel Engine: Effect of Lubricant Viscosity," Transactions of the ASME, Journal of Engineering for Gas Turbines and Power, Vol. 128, 2006, PP. 685-694.
- [34] F. M. Meng, Y. Y. Zhang, Y. Z. Hu, H. Wang, "Thermo-Elastohydrodynamic Lubrication Analysis of Piston Skirt Considering Oil Film Inertia Effect," Tribology International, Vol. 40, 2007, PP. 1089-1099.
- [35] E. A. Nada, I. A. Hinti, A. A. Sarkhi, B. Akash, "Effect of Piston Friction on the Performance of SI Engine: A New Thermodynamic Approach," Transactions of the ASME, Journal of Engineering for Gas Turbines and Power, Vol. 130, 2008, PP. 022802-022810.
- [36] P. Charles, M. Elfassi, A. A. Lubrecht, "Double Newtonian Rheology in a Model Piston Ring Cylinder Wall Contact," Tribology International, Vol. 43, 2010, PP. 1902-1907.
- [37] Z. Junhong, G. Hongge, N. I. Guangjian, "Piston-Ring and Cylinder-Liner Lubrication in Internal Combustion Engines Based on Thermo-Hydrodynamic," Chinese Journal of Mechanical Engineering, Vol. 24, 2011, PP. 1-5.
- [38] S. A. Qasim, M. A. Malik, M. A. Khan, R. Mufti, "Low Viscosity Shear Heating in Piston Skirts EHL in the Low Initial Engine Start Up Speeds," Tribology International, Vol. 44, 2011, PP. 1134-1143.

- [39] M. Pelosi, M. Ivantysynova, "A Geometric Multigrid Solver for the Piston-Cylinder Interface of Axial Piston Machines," *Tribology International*, Vol. 55, 2012, PP. 163-174.
- [40] W. J. Bartz, "Tribologically Caused Energy Losses," *Tribologia Finnish Journal of Tribology*, Vol. 7, 1988, PP. 2-27.
- [41] M. Takiguchi, K. Machida, S. Furuhashi, "Piston Friction Force of a Small High Speed Gasoline Engine," *Transactions of the ASME, Journal of Tribology*, Vol. 110, 1988, PP. 112-118.
- [42] P. C. Nautiyal, A. K. Gondal, D. Kumar, "Wear and Lubrication Characteristics of a Methanol-Fuelled Compression Ignition Engine – A Comparison with Pure Diesel and Biofuels Operation," *Wear*, Vol. 135, 1989, PP. 67-78.
- [43] M. F. Fox, J. D. Picken, Z. Pawlak, "The Effect of Water on the Acid-Base Properties of New and Used IC Engine Lubricating Oils," *Tribology International*, Vol. 23, 1990, PP. 183-188.
- [44] Y. Tateishi, "Tribological Issues in Reducing Piston Ring Friction Losses," *Tribology International*, Vol. 27, 1994, PP. 17-23.
- [45] S. W. Cho, S. M. Choi, C. S. Bae, "Frictional Modes of Barrel Shaped Piston Rings under Flooded Lubrication," *Tribology International*, Vol. 33, 2000, PP. 545-551.
- [46] R. M. Bata, A. C. Elrod, R. W. Rice, "Emissions from IC Engines Fueled with Alcohol – Gasoline Blends: A Literature Review," *Transactions of the ASME, Journal of Engineering for Gas Turbines and Power*, Vol. 111, 1989, PP. 424-432.
- [47] H. Aihara, "Tribology for Alternative Fuel Engines," *Tribology International*, Vol. 27, 1994, PP. 51-56.
- [48] J. M. Herdan, "Lubricating Oil Additives and the Environment- An Overview," *Lubrication Science*, Vol. 9, 1997, PP. 161-172.
- [49] W. J. Bartz, "Lubricants and the Environment," *Tribology International*, Vol. 31, 1998, PP. 35-47.

- [50] H. H. Masjuki, M. A. Maleque, A. Kubo, T. Nonaka, "Palm Oil and Mineral Oil based Lubricants – their Tribological and Emission Performance," *Tribology International*, Vol. 32, 1999, PP. 305-314.
- [51] W. D. Hsieh, R. H. Chen, T. L. Wu, T. H. Lin, "Engine Performance and Pollutant Emission of an SI Engine using Ethanol Gasoline Blended Fuels," *Atmospheric Environment*, Vol. 36, 2002, PP. 403-410.
- [52] A. S. Ramadhas, S. Jayaraj, C. Muraleedharan, "Use of Vegetable Oils as I.C. Engine Fuels – A Review," *Renewable Energy*, Vol. 29, 2004, PP. 727-742.
- [53] F. Yuksel, B. Yuksel, "The Use of Ethanol-Gasoline Blend as a Fuel in a SI Engine," *Renewable Energy*, Vol. 29, 2004, PP. 1181-1191.
- [54] E. Arcaklioglu, I. Celikten, "A Diesel Engine's Performance and Exhaust Emissions," *Applied Energy*, Vol. 80, 2005, PP. 11-22.
- [55] M. Pugazhvadivu, K. Jeyachandran, "Investigations on the Performance and Exhaust Emissions of a Diesel Engine Using Preheated Waste Frying Oil as Fuel," *Renewable Energy*, Vol. 30, 2005, PP. 2189-2202.
- [56] D. Agarwal, S. Sinha, A. K. Agarwal, "Experimental Investigation of Control of NO<sub>x</sub> Emissions in Biodiesel Fueled Compression Ignition Engine," *Renewable Energy*, Vol. 31, 2006, PP. 2356-2369.
- [57] J. N. Reddy, A. Ramesh, "Parametric Studies for Improving the Performance of a Jatropha Oil Fuelled Compression Ignition Engine," *Renewable Energy*, Vol. 31, 2006, PP. 1994-2016.
- [58] A. Neville, A. Morina, T. Haque, M. Voong, "Compatibility between Tribological Surfaces and Lubricant Additives – How Friction and Wear Reduction can be Controlled by Surface/Lube Synergies," *Tribology International*, Vol. 40, 2007, PP. 1680-1695.
- [59] V. Pradeep, R. P. Sharma, "Use of Hot EGR for NO<sub>x</sub> Control in a Compression Ignition Engine Fuelled With Bio-Diesel From Jatropha Oil," *Renewable Energy*, Vol. 32, 2007, PP. 1136-1154.

- [60] N. Saravanan, G. Nagarajan, S. Narayanasamy, "An Experimental Investigation on DI Diesel Engine with Hydrogen Fuel," *Renewable Energy*, Vol. 33, 2008, PP. 415-421.
- [61] E. M. Shahid, Y. Jamal, "A Review of Biodiesel as Vehicular Fuel," *Renewable & Sustainable Energy Reviews*, Vol. 12, 2008, PP. 2484-2494.
- [62] J. Janaun, N. Ellis, "Perspective on Biodiesel as a Sustainable Fuel," *Renewable and Sustainable Energy Reviews*, Vol. 14, 2010, PP.1312-1320.
- [63] M. Koc, Y. Sekmen, T. Topgul, H. S. Yucesu, "The Effects of Ethanol Unleaded Gasoline Blends on Engine Performance and Exhaust Emissions in Spark Ignition Engine," *Renewable Energy*, Vol. 34, 2009, PP. 2101-2106.
- [64] H. Rahimi, B. Ghobadian, T. Yusuf, G. Najafi, M. Khatamifar, "Diesterol: An Environment – Friendly IC Engine Fuel," *Renewable Energy*, Vol. 34, 2009, PP. 335-342.
- [65] S. A. Basha, K. R. Gopal, S. Jebaraj, "A Review on Biodiesel Production, Combustion, Emissions and Performance," *Renewable and Sustainable Energy Reviews*, Vol. 13, 2009, PP. 1628-1634.
- [66] G. Knothe, "Biodiesel and Renewable Diesel: A Comparison," *Progress in Energy and Combustion Science*, Vol.36, 2010, PP. 364-373.
- [67] S. Jain, M. P. Sharma, "Prospects of Biodiesel from Jatropha in India: A Review," *Renewable and Sustainable Energy Reviews*, Vol. 14, 2010, PP. 763-771.
- [68] A. Igartua, R. Nevshupa, X. Fernandez, M. Conte, R. Zabala, J. Bernaola, P. Zabala, R. Luther, J. Rausch, "Alternative Eco-friendly Lubes for Clean Two-stroke Engines," *Tribology International*, Vol. 44, 2011, PP. 727-736.

- [69] J. Xue, T. E. Grift, A. C. Hansen, "Effect of Biodiesel on Engine Performances and Emissions," *Renewable and Sustainable Energy Reviews*, Vol. 15, 2011, PP. 1098-1116.
- [70] I. Etsion, G. Halperin, "A Laser Surface Textured Hydrostatic Mechanical Seal," *Tribology Transactions*, Vol. 45, 2002, PP. 430-434.
- [71] I. Etsion, L. Burstein, "Model for Mechanical Seals with Regular Micro Surface Structure," *Tribology Transactions*, Vol. 39, 1996, PP. 677-683.
- [72] I. Etsion, Y. Kligerman, G. Halperin, "Analytical and Experimental Investigation of Laser Textured Mechanical Seal Faces," *Tribology Transactions*, Vol. 42, 1999, PP. 511-516.
- [73] X. Q. Yu, S. He, R. L. Cai, "Frictional Characteristics of Mechanical Seals with a Laser-Textured Seal Face," *Journal of Materials Processing Technology*, Vol. 129, 2002, PP. 463-466.
- [74] X. Wang, K. Kato, K. Adachi, K. Aizawa, "The Effect of Laser Texturing of SiC Surface on the Critical Load for the Transition of Water Lubrication Mode from Hydrodynamic to Mixed," *Tribology International*, Vol. 34, 2001, PP. 703-711.
- [75] X. Wang, K. Kato, K. Adachi, K. Aizawa, "Loads Carrying Capacity Map for the Surface Texture Design of SiC Thrust Bearing Sliding in Water," *Tribology International*, Vol. 36, 2003, PP. 189-197.
- [76] Y. Kligerman, I. Etsion, A. Shinkarenko, "Improving Tribological Performance of Piston Rings by Partial Surface Texturing," *Transactions of the ASME, Journal of Tribology*, Vol. 127, 2005, PP. 632-638.
- [77] G. Ryk, Y. Kligerman, I. Etsion, "Experimental Investigation of Laser Surface Texturing for Reciprocating Automotive Components," *Tribology Transactions*, Vol. 45, 2002, PP. 444-449.
- [78] G. Ryk, I. Etsion, "Testing Piston Rings with Partial Laser Surface Texturing for Friction Reduction," *Wear*, Vol. 261, 2006, PP. 792-796.

- [79] N. P. Suh, M. Mosleh, P. S. Howard, "Control of Friction," *Wear*, Vol. 175, 1994, PP. 151-158.
- [80] H. Tian, N. Saka, N. P. Suh, "Boundary Lubrication Studies on Undulated Titanium Surfaces," *Tribology Transactions*, Vol. 32, 1989, PP. 289-296.
- [81] U. Pettersson, S. Jacobson, "Influence of Surface Texture on Boundary Lubricated Sliding Contacts," *Tribology International*, Vol. 36, 2003, PP. 857-864.
- [82] M. Wakuda, Y. Yamauchi, S. Kanzaki, Y. Yasuda, "Effect of Surface Texturing on Friction Reduction between Ceramic and Steel Materials under Lubricated Sliding Contact," *Wear*, Vol. 254, 2003, PP. 356-363.
- [83] I. Krupka, D. Koutný, M. Hartl, "Behavior of Real Roughness Features within Mixed Lubricated Non-Conformal Contacts," *Tribology International*, Vol. 41, 2008, PP. 1153-1160.
- [84] T. Nanbu, N. Ren, Y. Yasuda, D. Zhu, Q. J. Wang, "Micro-Textures in Concentrated Conformal-Contact Lubrication: Effects of Texture Bottom Shape and Surface Relative Motion," *Tribology Letters*, Vol. 29, 2008, PP. 241-252.
- [85] A. Erdemir, "Review of Engineered Tribological Interfaces for Improved Boundary Lubrication," *Tribology International*, Vol. 38, 2005, PP. 249-256.
- [86] L. Mourier, D. Mazuyer, A. A. Lubrecht, C. Donnet, "Transient Increase of Film Thickness in Micro-Textured EHL Contacts," *Tribology International*, Vol. 39, 2006, PP. 1745-1756.
- [87] I. Etsion, "State of the Art in Laser Surface Texturing," *Transactions of the ASME, Journal of Tribology*, Vol. 127, 2005, PP. 248-253.

## Appendix-I

### Instruments for measurement of properties of fuels

Density of fuel is the mass of the matter per unit volume of the space covered by it. The measurement has been performed at room temperature. The density of diesel and jatropha based biodiesel have been measured with the help of a U-Tube Oscillating True Density meter as shown in Fig. A1.



Fig. A1. U-Tube Oscillating True Density meter

Viscosity is measurement of shear stress exerted as internal friction with respect to velocity gradient of fluid. Moreover, viscosity is a measure of internal resistance developed due to molecular friction having relative velocity between the elements of fluid or fluid with respect to other material. Viscosity of fuel has major affects on fuel delivery rates, atomization, mixing of air and fuel in combustion chamber of an IC engine. Kinematic viscosity of the fuel samples has been measured using kinematic viscometer shown in Fig. A2. at 40°C as per the specification given in ASTM D445. A capillary tube has been selected and filled with fuel up to the mark in made on it. The temperature of the water in the bath has been maintained at 40°C and then sample has been allowed to flow through the capillary. The



required time has measured for calculating kinematic viscosity using the expression given below:

$$= c * t$$

Where,  $\nu$  = Kinematic viscosity, cSt or mm<sup>2</sup>/sec

c = constant; mm<sup>2</sup>/sec<sup>2</sup> and t=time, second.



Fig. A2. Kinematic viscometer

### Flash point

Flash point of fuel is the minimum temperature at which the fuel vapors mixed with air forms an ignitable mixture on application of a small pilot flame and shows a momentary flash. The flash point of the test fuels has been measured as per the standard of ASTM D 93. The sample of required quantity has been uniformly and properly heated in a test cup at a slow and constant rate of stirring. A small pilot flame has directed into the cup through the opening provided at the top cover at the regular intervals as shown in Fig. A3. The minimum temperature at which these vapor just catches flash is recorded the flash point of that fuel.



Fig. A3. A Pensky Martens apparatus used for determination of flash point  
Calorific Value

The calorific value (CV) is the heat liberated when unit mass of fuel is completely burnt in a calorimeter under specified conditions. Higher CV of fuel is the heat liberated in kJ per kg or  $\text{m}^3$ . The CV of the fuel has been measured in the laboratory with the calorimeter as per the specification mentioned in ASTM D240. The combustion of fuel takes place in a fully enclosed vessel at constant volume in the presence of oxygen supplied from oxygen cylinder which ignites electrically.



Fig. A4. Calorimeter

#### 4.4 The exhaust emissions

The exhaust emissions have been measured with the help of smoke meters and gas analyzer as shown in Fig. A5(a) and Fig. A5(b). as per ASTM and respectively. With the help of both the instrument CO<sub>2</sub>, NO<sub>x</sub>, hydrocarbon, carbon mono oxide and smoke opacity have been measured.



Fig. A5(a). Smoke meter

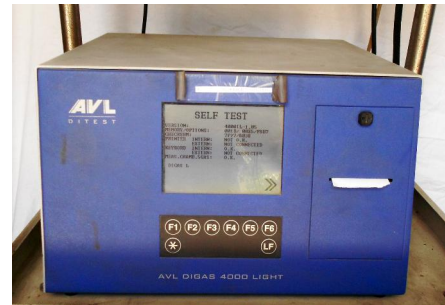
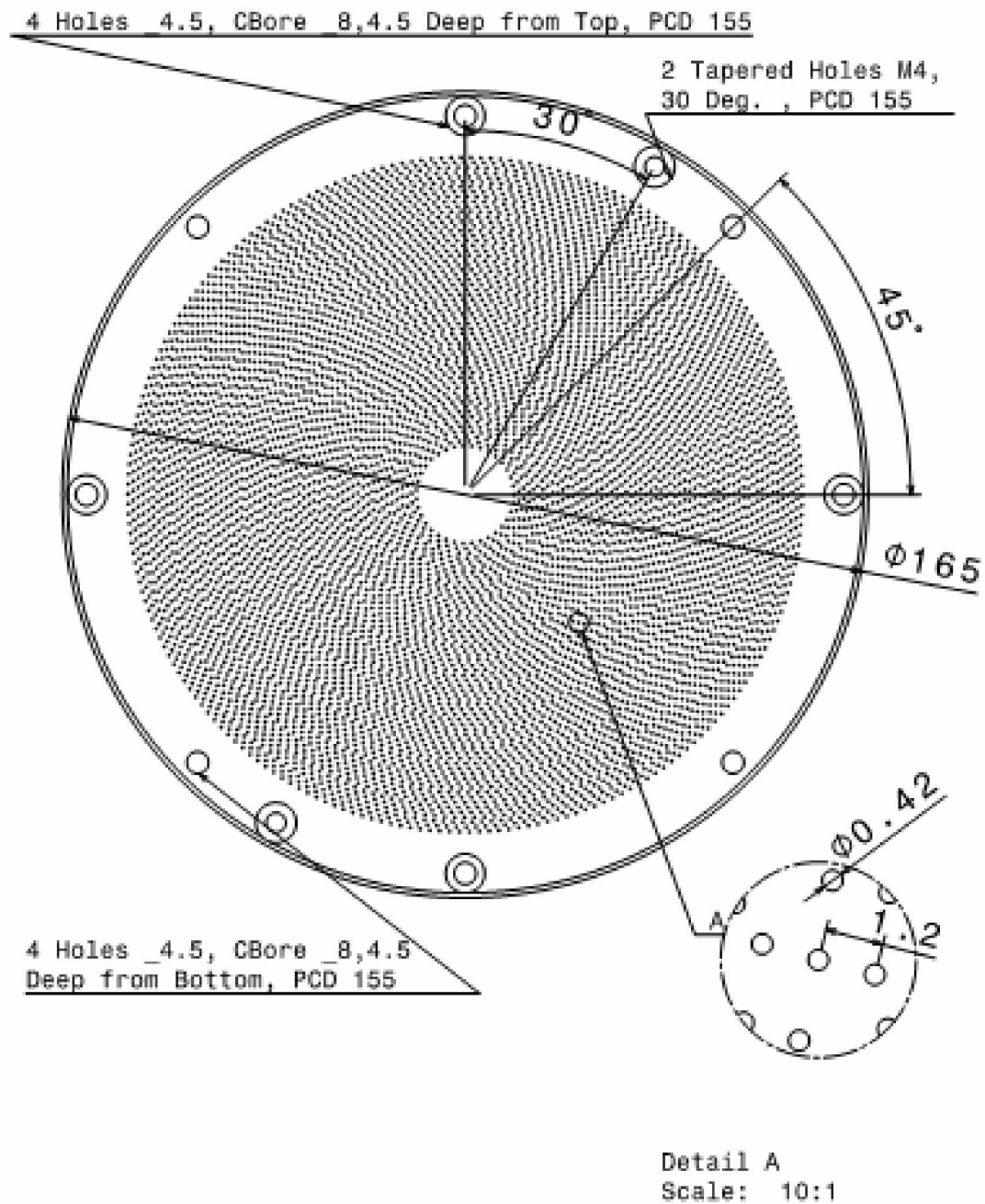


Fig. A5(b). Gas analyzer

## Appendix-II

### Drawings of discs having different pitches



Dimples 100 micron, pitch 1mm along pitch circles with PCR from 10 to 69 mm

Fig. B1. Dimpled disc with pitch=1 mm, 420 micron

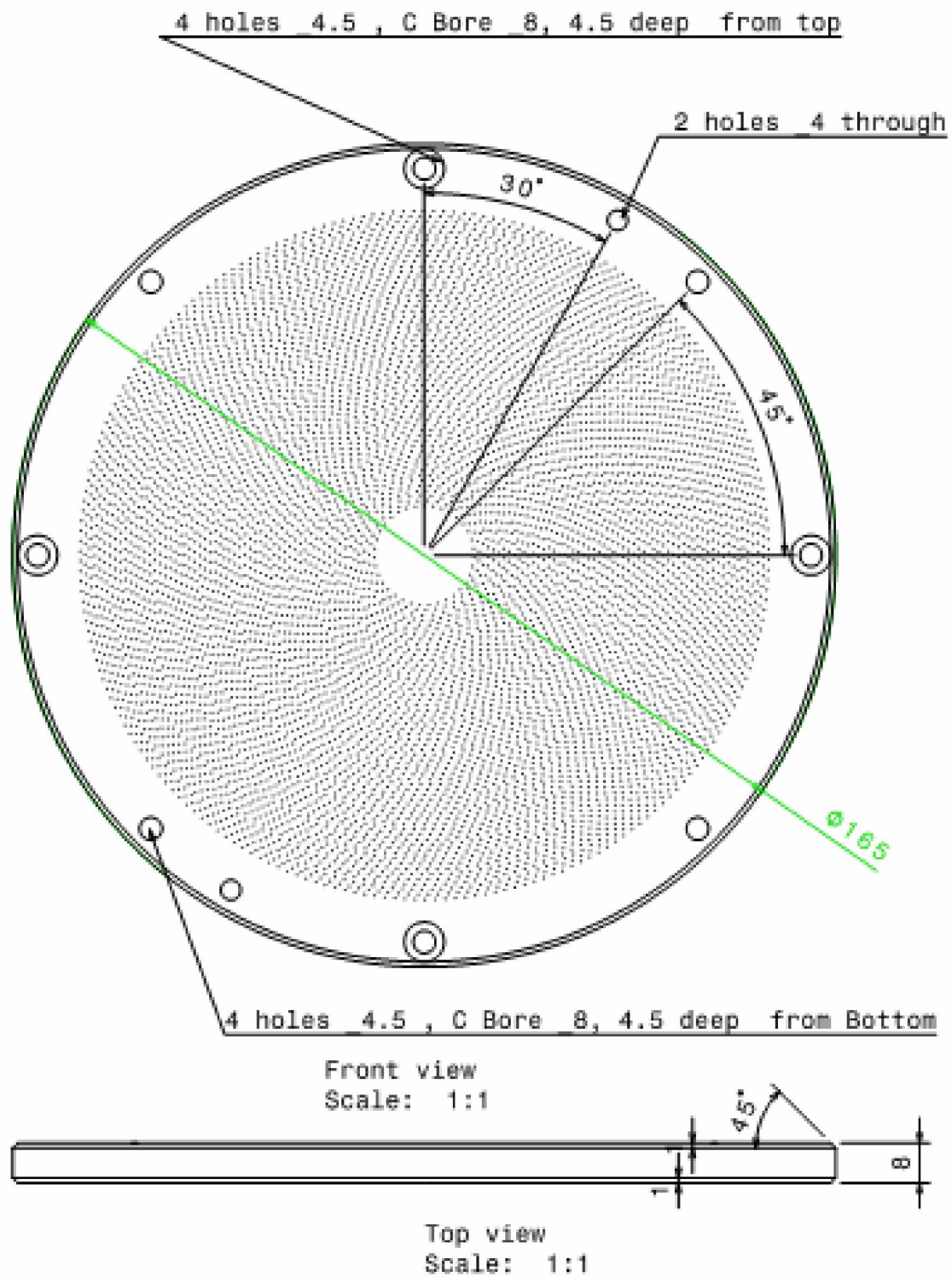
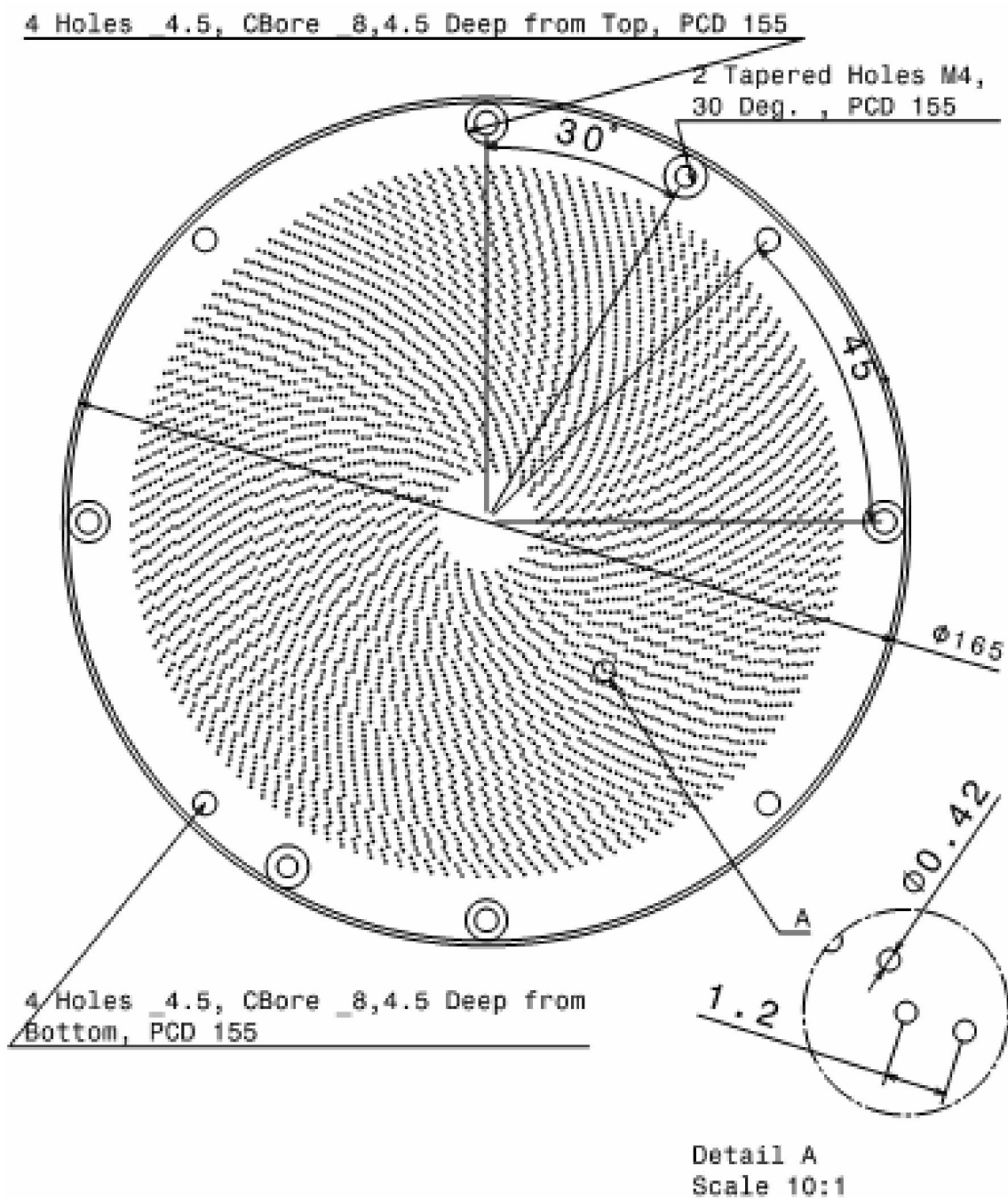


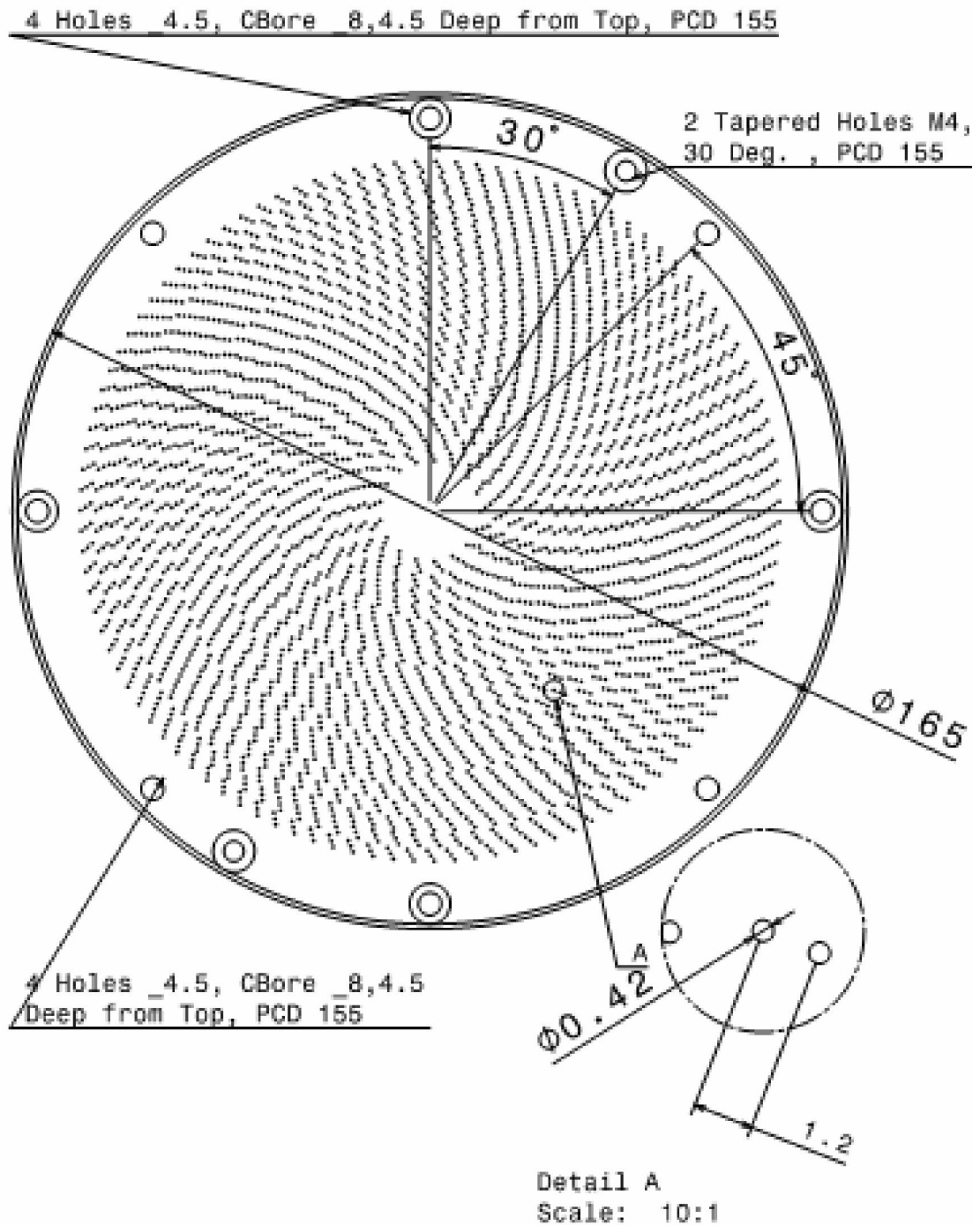
Fig. B2. Dimpled disc with pitch=2 mm, 420 micron



Dimples 100 micron, pitch 1mm along pitch circles with  
PCR from 10 to 69 mm

Fig. B3. Dimpled disc with pitch=3 mm , 420 micron





Dimples 100 micron, pitch 1mm along pitch circles with PCR from 10 to 69 mm

Fig. B4.Dimpled disc with pitch=4 mm, 420 micron

# “Thermohydrodynamic Analysis of Lubricated Piston Rings of Internal Combustion Engine”

## Abstract

Petroleum and automotive industries are facing tough time across the globe due to steep rise in petroleum based fuels' prices and ever increasing governments regulations related to improving the fuel economy and lower emissions from the fuel and lubricant system of IC engines. Therefore, worldwide substantial efforts in the design of reciprocating internal combustion (IC) engines are being made by the researchers for improving the fuel economy and reducing the exhaust emissions. Nowadays, great attention is being given on the reduction of friction at the various interfaces formed between the mating components of the IC engines. Effective lubrication at the interfaces of cylinder liner/piston rings, piston/piston rings, and piston skirt/cylinder liner play vital role in achieving high power efficiency, ensuring long operational life of the interfaces, limiting the consumptions of lubricating oil and fuel, providing a good dynamic sealing at various interfaces. Thus, efficient design of contacts formed between piston rings and counter surfaces in piston assembly is a great desirable task in the emerging scenario. It is worth mentioning here that dearth of studies can be seen in literature on the design and development of smart piston rings. Therefore, the main objective of this thesis is to study mathematically hydrodynamic lubrication of the interfaces formed between the cylinder liner and various surface profiles of the piston rings for reducing the frictional losses at the interfacial contacts. In the investigation reported herein, four single continuous surface profiles (Catenoidal, Cubic, Exponential, and Parabolic) on the face (surface in contact with cylinder liner) of piston rings have been considered for arriving on the



best efficient face profile among these. These surface profiles for face of piston rings have been chosen in this investigation looking their potential performance as faces of pads in thrust bearing. The additional objective of this thesis is to perform the experiments on a commercial IC engine by manufacturing the best face profile (arrived based on mathematical modeling) on all the compression piston rings for accessing the fuel saving and exhaust emissions.

Coupled solution of governing equations (Reynolds equation, Energy equation, Film thickness relation, and Rheological relation) has been achieved using finite difference method. Gauss-Seidel iterative method is employed in the solution of discretized equations. Using appropriate boundary conditions and convergence criterion, performance parameters of a single interface (cylinder liner and face of piston ring) have been thoroughly investigated. Based on the numerical study, it has been observed that exponential face profile of the piston ring yields lesser friction than other three profiles (Catenoidal, Cubic, and Polynomial). Thus, exponential face profile has been tried to fabricate on the faces of compression piston rings. However, due to manufacturing constraint an approximate exponential face profile only could be realized. Using approximate exponential face profile on compression piston rings, experiments have been carried out on a commercial diesel engine fueled with diesel and Jatropha based biodiesel (B100) at various loads. This exponential face profile of piston ring has considerable impact on engine's brake thermal efficiency (BTE), brake specific fuel consumption (BSFC), and mass flow rate, irrespective of fuels used. BTE of engine fueled with diesel increases 2 - 8% with exponential face profile design (III) of piston ring in comparison to standard (conventional) piston ring. BTE enhances 8 - 16%

when engine is fueled with biodiesel using exponential face profile design (III) on piston rings. Corresponding to increase in BTE, the reduction in BSFC (biodiesel) is about 28 - 34%. Moreover, significant reductions in exhaust emissions are also recorded with exponential face profile on compression piston rings.

Moreover, friction reduction due to dimpling has been also explored. In this direction, some experiments have been conducted using a pin-on-disc machine. The investigations carried out with micro-dimpling on generic tribo-contact give very significant reduction at interfacial friction. Thus, in future dimpling may be tried on face of piston rings for development of smart piston rings.

\*\*\*\*\*